

On the loss of orthogonality in low-synchronization variants of reorthogonalized block classical Gram-Schmidt

Erin Carson* Kathryn Lund^{†,‡} Yuxin Ma* Eda Oktay^{*,§}

**Department of Numerical Mathematics, Faculty of Mathematics and Physics, Charles University, Sokolovská 49/83, 186 75 Praha 8, Czechia*

Email: {carson, oktay}@karlin.mff.cuni.cz, Email: yuxin.ma@matfyz.cuni.cz,

ORCID: 0000-0001-9469-7467, ORCID: 0000-0003-0761-2184, ORCID: 0000-0002-2860-0134

[†]*Computational Mathematics Theme, Building R71, STFC Rutherford Appleton Laboratory, Harwell Oxford, Didcot, Oxfordshire, OX11 0QX, United Kingdom*

Email: kathryn.lund@stfc.ac.uk, ORCID: 0000-0001-9851-6061

[‡]*Computational Methods in Systems and Control Theory, Max Planck Institute for Dynamics of Complex Technical Systems, Sandtorstr. 1, 39106 Magdeburg, Germany*

[§]*Department of Mathematics, Chemnitz University of Technology, Reichenhainer Str. 41, 09126 Chemnitz, Germany*

Abstract: Interest in communication-avoiding orthogonalization schemes for high-performance computing has been growing recently. This manuscript addresses open questions about the numerical stability of various block classical Gram-Schmidt variants that have been proposed in the past few years. An abstract framework is employed, the flexibility of which allows for new rigorous bounds on the loss of orthogonality in these variants. We first analyze a generalization of (reorthogonalized) block classical Gram-Schmidt and show that a “strong” intrablock orthogonalization routine is only needed for the very first block in order to maintain orthogonality on the level of the unit roundoff. In particular, this “strong” first step does not have to be a reorthogonalized QR itself and subsequent steps can use less stable QR variants, thus keeping the overall communication costs low.

Then, using this variant, which has four synchronization points per block column, we remove the synchronization points one at a time and analyze how each alteration affects the stability of the resulting method. Our analysis shows that the variant requiring only one synchronization per block column, equivalent to a variant previously proposed in the literature, cannot be guaranteed to be stable in practice, as stability begins to degrade with the first reduction of synchronization points. As a negative result, we conclude that this particular block algorithm should be avoided in practice.

Our analysis of block methods also provides new, more positive theoretical results for the single-column case. In particular, it is proven that DCGS2 from [Bielich, D. et al. *Par. Comput.* 112 (2022)] and CGS-2 from [Świrydowicz, K. et al, *Num. Lin. Alg. Appl.* 28 (2021)] are as stable as Householder QR. Numerical examples from the `BlockStab` toolbox are included throughout, to help compare variants and illustrate the effects of different choices of intraorthogonalization subroutines.

Keywords: backward stability, Gram-Schmidt, low-synchronization, communication-avoiding, Arnoldi method, Krylov subspaces, loss of orthogonality

Mathematics subject classification: 65-04, 65F10, 65F25, 65F50, 65G50, 65Y05

Novelty statement: Bounds on the loss of orthogonality are proven for a block Gram-Schmidt variant with one synchronization point. As a by-product, bounds on the order of unit roundoff are obtained for the single-column variant, which was until now an open problem. New bounds are also proven for block classical Gram-Schmidt, and a variety of numerical examples are provided to confirm the theoretical results.

1 Introduction

With the advent of exascale computing, there is a pressing need for highly parallelizable algorithms that also reduce *communication*, i.e., data movement and synchronization. An underlying kernel in diverse numerical linear applications is the orthogonalization of a matrix, whose efficiency is limited by inner products and vector normalizations involving *synchronization points* (*sync points*), which dominate communication costs. In the case of an inner product or norm, a sync point arises when a vector is stored in a distributed fashion across nodes: each node locally computes part of the inner product and then must transmit its result to all other nodes so that each can assemble the full inner product. Communication-avoiding methods such as s -step Krylov subspace methods have proven to be effective adaptations in practice; see, e.g., [1, 10, 17, 25]. Such methods implicitly rely on a stable block Gram-Schmidt (BGS) routine that should itself be communication-avoiding. Blocking alone reduces the number of sync points, as previously vector-wise operations can instead be performed on tall-skinny matrices or *block vectors*, thus replacing single inner products with block inner products and normalizations with low-sync QR factorizations. Low-sync variants of BGS have attracted much recent attention [4, 6–8, 21, 22, 24–26], but their stability, in particular how well they preserve orthogonality between basis vectors, is often poor, which can lead to issues in downstream applications like Krylov subspace methods, least-squares, or eigenvalue solvers. Understanding the floating-point stability of low-sync BGS methods is thus imperative for their reliable deployment in exascale environments.

To be more precise, we define a *block vector* $\mathbf{X} \in \mathbb{R}^{m \times s}$ as a concatenation of s column vectors. We are interested in computing an economic QR decomposition for the concatenation of p block vectors

$$\mathbf{X} = [\mathbf{X}_1 \quad \mathbf{X}_2 \quad \cdots \quad \mathbf{X}_p] \in \mathbb{R}^{m \times ps}$$

with $m \geq ps$. We achieve this via a BGS procedure that takes \mathbf{X} and a block size s as arguments and returns an orthogonal basis $\mathbf{Q} \in \mathbb{R}^{m \times ps}$, along with an upper triangular $\mathbf{R} \in \mathbb{R}^{ps \times ps}$ such that $\mathbf{X} = \mathbf{Q}\mathbf{R}$. Both \mathbf{Q} and \mathbf{R} are computed block-wise, meaning that s new columns of \mathbf{Q} are generated per iteration, as opposed to just one column at a time.

In addition to sync points, we are also concerned with the stability of BGS, which we measure here in terms of the *loss of orthogonality* (*LOO*),

$$\left\| I - \bar{\mathbf{Q}}^T \bar{\mathbf{Q}} \right\|, \quad (1)$$

where I is the $ps \times ps$ identity matrix and $\bar{\mathbf{Q}} \in \mathbb{R}^{m \times ps}$ denotes a computed basis with floating-point error. We will also consider the relative residual

$$\frac{\|\mathbf{X} - \bar{\mathbf{Q}}\bar{\mathbf{R}}\|}{\|\mathbf{X}\|} \quad (2)$$

and relative Cholesky residual,

$$\frac{\|\mathbf{X}^T \mathbf{X} - \bar{\mathbf{R}}^T \bar{\mathbf{R}}\|}{\|\mathbf{X}\|^2}, \quad (3)$$

where $\bar{\mathbf{R}}$ is the computed version of \mathbf{R} with floating-point error and $\|\cdot\|$ denotes the induced 2-norm. The residual (3) measures how close a BGS method is to correctly computing a Cholesky decomposition of $\mathbf{X}^T \mathbf{X}$, which can provide insight into the stability pitfalls of a method; see, e.g., [7, 13].

The ideal BGS would require one sync point per block vector and return $\bar{\mathbf{Q}}$ and $\bar{\mathbf{R}}$ such that (1)-(3) are $\mathcal{O}(\varepsilon)$, where ε denotes the *unit roundoff*, without any conditions on \mathbf{X} , except perhaps

that the 2-norm condition number $\kappa(\mathcal{X})$ is no larger than $\mathcal{O}(\varepsilon^{-1})$. To the best of our knowledge, no such BGS method exists, and one must make trade-offs regarding the number of sync points and stability. In practice, the acceptable level of the LOO is often well above machine precision; e.g., the Generalized Minimal Residual (GMRES) method is known to be backward stable with Arnoldi based on modified Gram-Schmidt (MGS), whose LOO depends linearly on the condition number of \mathcal{X} [15]. A similar result for block GMRES remains open, however [5].

A key issue affecting the stability of a BGS method is the choice of *intraorthogonalization* routine, or the so-called “local” QR factorization of a single block column; in the pseudocode throughout this manuscript, we denote this routine as “intraortho” or simply IO. Traditional Householder QR (HouseQR) or Givens QR (GivensQR) are common choices due to their unconditional $\mathcal{O}(\varepsilon)$ LOO, but they introduce additional sync points [14, 16]. One-sync variants include, e.g., Tall-Skinny QR (TSQR [11, 12]), also known as AllReduceQR [20], and CholQR [23]. TSQR/AllReduceQR is known to have $\mathcal{O}(\varepsilon)$ LOO, while that of CholQR is bounded by $\mathcal{O}(\varepsilon)\kappa^2(\mathbf{X})$, where $\kappa^2(\mathbf{X})$ itself should be bounded by $\mathcal{O}(\varepsilon^{-1/2})$.

In this manuscript, we focus on reorthogonalized variants of block classical Gram-Schmidt (BCGS). We begin by proving LOO bounds on BCGS, which has not been done rigorously before to the best of our knowledge (Section 2). A key feature of our analysis is an abstract framework that highlights the effects of the projection and intraortho stages. Furthermore, we consider a variant of BCGS that only requires a “strong” first step (BCGS-A). Although this modification does not improve the numerical behavior of BCGS, its reorthogonalized variant BCGSI+A enjoys $\mathcal{O}(\varepsilon)$ LOO with more relaxed assumptions on the subsequent IOs than those of Barlow and Smoktunowicz [3] and Barlow [2](BCGSI+), and lower communication cost. In Section 3, we derive a BGS method with one sync point from BCGSI+A, which is similar to the one-sync variant BCGSI+LS ([8, Algorithm 7] and [25, Figure 3]), and is a block analogue of DCGS2 and CGS-2 with Normalization and Reorthogonalization Lags ([4, Algorithm 2] and [22, Algorithm 3], respectively). Unlike [4, 22], we do not use the notion of lags or delays; instead, we view things in terms of shifting the window of the for-loop, which simplifies the mathematical analysis. We derive the one-sync algorithm in three stages—BCGSI+A-3S, BCGSI+A-2S, and BCGSI+A-1S—in order to systematically demonstrate how new floating-point error is introduced with the successive removal of sync points. We then prove stability bounds for these algorithms in Section 4. A summary and discussion of all the bounds is provided in Section 5, along with an important corollary: BCGSI+A-1S achieves $\mathcal{O}(\varepsilon)$ LOO for $s = 1$. In other words, [4, Algorithm 2] and [22, Algorithm 3] are effectively as stable as HouseQR, which thus far has not been rigorously proven. Section 6 concludes our work with an outlook for future directions.

A few remarks regarding notation are necessary before proceeding. Generally, uppercase Roman letters (R_{ij}, S_{ij}, T_{ij}) denote $s \times s$ block entries of a $ps \times ps$ matrix, which itself is usually denoted by uppercase Roman script ($\mathcal{R}, \mathcal{S}, \mathcal{T}$). A block column of such matrices is denoted with MATLAB indexing:

$$\mathcal{R}_{1:k-1,k} = \begin{bmatrix} R_{1,k} \\ R_{2,k} \\ \vdots \\ R_{k-1,k} \end{bmatrix}.$$

For simplicity, we also abbreviate standard $ks \times ks$ submatrices as $\mathcal{R}_k := \mathcal{R}_{1:k,1:k}$.

Bold uppercase Roman letters ($\mathbf{Q}_k, \mathbf{X}_k, \mathbf{U}_k$) denote $m \times s$ block vectors, and bold, uppercase Roman script ($\mathcal{Q}, \mathcal{X}, \mathcal{U}$) denotes an indexed concatenation of p such vectors. Standard $m \times p$ submatrices are abbreviated as

$$\mathcal{Q}_k := \mathcal{Q}_{1:k} = [\mathbf{Q}_1 \quad \mathbf{Q}_2 \quad \cdots \quad \mathbf{Q}_k].$$

We will aim for bounds in terms of the induced 2-norm $\|\cdot\|$, but we will also make use of the Frobenius norm in the analysis, denoted as $\|\cdot\|_F$. By $\text{tr}(A)$ we denote the trace of a square matrix A . Furthermore, we always take $\kappa(A)$ to mean the 2-norm condition number defined as the ratio between the largest and smallest singular values of A .

2 Improved stability of BCGS with inner reorthogonalization

It is well known that **BCGS** is itself low-sync, in the sense that only 2 sync points are required per block vector, assuming that we only employ IOs that themselves require just one sync point (e.g., **TSQR** or **CholQR**). In comparison to block modified Gram-Schmidt (**BMGS**), which requires $k + 1$ sync points for the k th iteration, a fixed number of sync points per iteration can have clear performance benefits; see, e.g., [4, 19, 22, 25].

We will consider a slight modification to **BCGS** in the first step. We call this variant **BCGS-A**, as in Algorithm 1, where “A” here stands for “alpha” or the German “Anfang”, as the key change is made at the beginning of the algorithm. The idea is to require that IO_A be strongly stable like **HouseQR** and then allow for more flexibility in the IO used in the for-loop.

Algorithm 1 $[\mathcal{Q}, \mathcal{R}] = \text{BCGS-A}(\mathcal{X}, \text{IO}_A, \text{IO})$

```

1:  $[\mathbf{Q}_1, R_{11}] = \text{IO}_A(\mathbf{X}_1)$ 
2: for  $k = 2, \dots, p$  do
3:    $\mathcal{R}_{1:k-1,k} = \mathbf{Q}_{k-1}^T \mathbf{X}_k$ 
4:    $[\mathbf{Q}_k, R_{kk}] = \text{IO}(\mathbf{X}_k - \mathbf{Q}_{k-1} \mathcal{R}_{1:k-1,k})$ 
5: end for
6: return  $\mathcal{Q} = [\mathbf{Q}_1, \dots, \mathbf{Q}_p]$ ,  $\mathcal{R} = (R_{ij})$ 

```

Unfortunately, **BCGS** (i.e., **BCGS-A** with $\text{IO}_A = \text{IO}$) can exhibit an LOO worse than $\mathcal{O}(\varepsilon) \kappa^2(\mathcal{X})$, and the situation is no better for **BCGS-A**. A natural solution often seen in practice is to run **BCGS** twice and combine the for-loops, leading to what we call **BCGSI+**, with I+ standing for “inner reorthogonalization”; see Algorithm 2 but assume $\text{IO}_A = \text{IO}_1 = \text{IO}_2$. **BCGSI+** has 4 sync points per iteration and has been analyzed by Barlow and Smoktunowicz [3], who show that as long as the IO has $\mathcal{O}(\varepsilon)$ LOO, then the overall method also has $\mathcal{O}(\varepsilon)$ LOO.

Figure 1 provides a comparison among **BCGS**, **BCGS-A** and **BCGSI+** for different choices of IOs. All plots in this section are generated by the MATLAB toolbox **BlockStab**¹ in double precision ($\varepsilon \approx 10^{-16}$) on what are called **monomial**² matrices; see the script `test_roadmap.m`. We have used MATLAB 2024a on a Dell laptop running Windows 10 with an 12th Gen Intel Core i7-1270P processor and 32GB of RAM. We use notation like $\text{BGS} \circ \text{IO}$ to denote the composition of the outer block “skeleton” and intraorthogonalizing “muscle”. We have fixed $\text{IO}_A = \text{HouseQR}$ for all “A” methods, and only the choice of $\text{IO} = \text{IO}_1 = \text{IO}_2$ is reported in the legends. Note that **CholQR** is implemented without a fail-safe for violating positive definiteness.³

It is clear from Figure 1 that **BCGSI+** does not exhibit $\mathcal{O}(\varepsilon)$ LOO for $\text{IO} = \text{CholQR}$. However, by requiring the first block vector to be orthogonalized by something as stable as **HouseQR**, we can relax the requirement for subsequent IOs and prove a stronger result than in [3]. We denote this modified algorithm **BCGSI+A**, given as Algorithm 2. **BCGSI+A** can also be interpreted as a generalization of the **BCGSI+F** approach introduced in [26].

The way Algorithm 2 is written, it would appear that we store three auxiliary matrices $\mathcal{S}, \mathcal{T} \in \mathbb{R}^{ps \times ps}$ and $\mathcal{U} \in \mathbb{R}^{m \times ps}$, where $\mathcal{S}_{ij} = (S_{ij})$, $\mathcal{T}_{ij} = (T_{ij})$, and $\mathcal{U} = [\mathbf{U}_1 \ \mathbf{U}_2 \ \dots \ \mathbf{U}_p]$. In practice, the entire matrices need not be stored and built, but their theoretical construction is helpful for proving stability bounds. Further note the three different colors used for different sections of the algorithm: **blue** for the first BGS step, **red** for the second, and **purple** for combining quantities from each step to finalize entries of \mathcal{R} . These colors may help some readers in Section 3 when we derive variants with fewer sync points.

Figure 2 demonstrates the improved behavior of **BCGSI+A** relative to **BCGSI+**. In particular, note that the relative Cholesky residual is restored to $\mathcal{O}(\varepsilon)$ for $\text{IO} = \text{CholQR}$, indicating that **BCGSI+A** returns a reliable Cholesky factor \mathcal{R} for a wider range of IOs than **BCGSI+**. Practically speaking,

¹<https://github.com/katlund/BlockStab/releases/tag/v2.1.2024>

²Each such matrix is a concatenation of r block vectors $\mathbf{X}_k = [\mathbf{v}_k \ A\mathbf{v}_k \ \dots \ A^{t-1}\mathbf{v}_k]$, $k \in \{1, \dots, r\}$, where each \mathbf{v}_k is randomly generated from the uniform distribution with norm 1, while A is an $m \times m$ diagonal operator having evenly distributed eigenvalues in $(0.1, 10)$. A sequence of such matrices with growing condition number is generated by varying r and t ; in particular, $rt = ps$, but it is not necessary that $r = p$ or $t = s$.

³See the `chol_free` subroutine in **BlockStab**, based on [16, Algorithm 10.2].

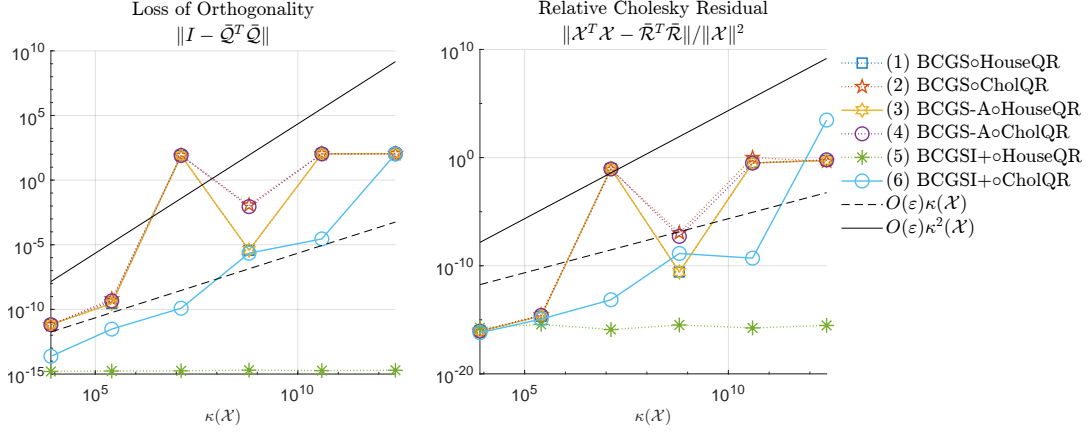


Figure 1: Comparison among **BCGS**, **BCGS-A**, and **BCGSI+** on a class of monomial matrices from **BlockStab**.

Algorithm 2 $[\mathcal{Q}, \mathcal{R}] = \text{BCGSI+A}(\mathcal{X}, \text{IO}_A, \text{IO}_1, \text{IO}_2)$

- 1: $[\mathcal{Q}_1, R_{11}] = \text{IO}_A(\mathbf{X}_1)$
 - 2: **for** $k = 2, \dots, p$ **do**
 - 3: $\mathcal{S}_{1:k-1,k} = \mathcal{Q}_{k-1}^T \mathbf{X}_k$ ▷ step k.1.1 – first projection
 - 4: $[\mathbf{U}_k, S_{kk}] = \text{IO}_1(\mathbf{X}_k - \mathcal{Q}_{k-1} \mathcal{S}_{1:k-1,k})$ ▷ step k.1.2 – first intraortho
 - 5: $\mathcal{T}_{1:k-1,k} = \mathcal{Q}_{k-1}^T \mathbf{U}_k$ ▷ step k.2.1 – second projection
 - 6: $[\mathcal{Q}_k, T_{kk}] = \text{IO}_2(\mathbf{U}_k - \mathcal{Q}_{k-1} \mathcal{T}_{1:k-1,k})$ ▷ step k.2.2 – second intraortho
 - 7: $\mathcal{R}_{1:k-1,k} = \mathcal{S}_{1:k-1,k} + \mathcal{T}_{1:k-1,k} S_{kk}$ ▷ step k.3.1 – form upper \mathcal{R} column
 - 8: $R_{kk} = T_{kk} S_{kk}$ ▷ step k.3.2 – form \mathcal{R} diagonal entry
 - 9: **end for**
 - 10: **return** $\mathcal{Q} = [\mathcal{Q}_1, \dots, \mathcal{Q}_p]$, $\mathcal{R} = (R_{ij})$
-

BCGSI+A only needs an expensive (but stable) **IO** once at the beginning, and less expensive (and even less stable) **IOs** for the remaining iterations.

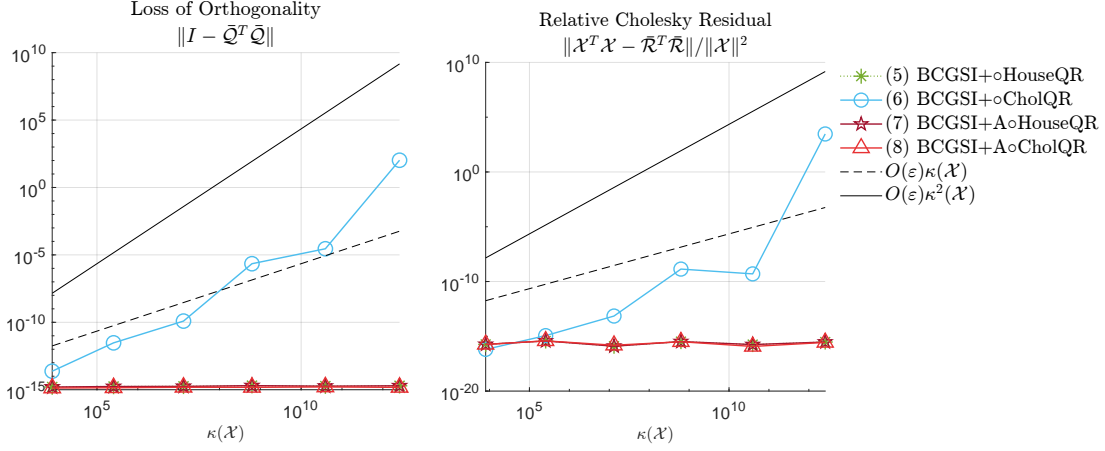


Figure 2: Comparison between **BCGSI+** (i.e., Algorithm 2 with all **IOs** equal) and **BCGSI+A** ($\text{IO}_A = \text{HouseQR}$ and $\text{IO}_1 = \text{IO}_2$) on a class of monomial matrices.

In the following subsections, we introduce an abstract framework for handling the stability analysis of a general BGS routine by splitting it into projection and intraortho stages. We then prove bounds for **BCGS-A** and **BCGSI+A** encompassing a wide variety of configurations.

2.1 An abstract framework for block Gram-Schmidt

For a general BGS procedure, given \mathcal{Q}_{prev} satisfying $\mathcal{Q}_{prev}^T \mathcal{Q}_{prev} = I$ and \mathbf{X} , each iteration aims to compute an orthogonal basis \mathbf{Q} of the next block vector \mathbf{X} that satisfies $\mathcal{Q}_{new}^T \mathcal{Q}_{new} = I$ with $\mathcal{Q}_{new} = [\mathcal{Q}_{prev}, \mathbf{Q}]$. Furthermore, the iteration can be divided into two stages:

$$\begin{aligned} \text{projection stage: } & \mathbf{G} = \text{Proj}(\mathbf{X}, \mathcal{Q}_{prev}); \text{ and} \\ \text{intraortho stage: } & [\mathbf{Q}, \mathbf{R}] = \text{QR}(\mathbf{G}). \end{aligned} \quad (4)$$

In practice, $\text{Proj}(\cdot)$ represents an algorithmic choice that has different rounding error consequences. Generally, the intraortho stage will be identical to the choice(s) of **IO**⁴.

Let $\tilde{\mathbf{G}}$ denote the exact result of $\text{Proj}(\mathbf{X}, \mathcal{Q}_{prev})$, where \mathcal{Q}_{prev} is the computed version of \mathcal{Q}_{prev} from a given algorithm. Taking rounding errors into account, the computed quantity of the projection stage would then satisfy

$$\bar{\mathbf{G}} = \tilde{\mathbf{G}} + \Delta \mathbf{E}_{\text{proj}}, \quad \|\Delta \mathbf{E}_{\text{proj}}\| \leq \psi, \quad (5)$$

where $\psi > 0$ is related to the unit roundoff ε , the condition number $\kappa(\mathbf{X})$, and the definition of Proj itself. Meanwhile, the computed quantities of the intraortho stage satisfy

$$\begin{aligned} \bar{\mathbf{G}} + \Delta \mathbf{G} &= \bar{\mathbf{Q}} \bar{\mathbf{R}}, \quad \|\Delta \mathbf{G}\| \leq \rho_{\text{qr}} \|\bar{\mathbf{G}}\|, \\ \|I - \bar{\mathbf{Q}}^T \bar{\mathbf{Q}}\| &\leq \omega_{\text{qr}}, \end{aligned} \quad (6)$$

where $\rho_{\text{qr}} \in (0, 1]$ and $\omega_{\text{qr}} < 1$ depend on the **IO**. For example, (6) holds for **HouseQR** and **GivensQR**, which satisfy

$$\begin{aligned} \bar{\mathbf{G}} + \Delta \tilde{\mathbf{G}} &= \tilde{\mathbf{Q}} \tilde{\mathbf{R}}, \quad \|\Delta \tilde{\mathbf{G}}\| \leq \mathcal{O}(\varepsilon) \|\bar{\mathbf{G}}\|, \\ \bar{\mathbf{Q}} &= \tilde{\mathbf{Q}} + \Delta \mathbf{Q}, \quad \|\Delta \mathbf{Q}\| \leq \mathcal{O}(\varepsilon), \end{aligned} \quad (7)$$

⁴Indeed, the intraortho stage could be replaced by a more general factorization than one that returns an orthogonal basis; see, e.g., [26].

Methods	ρ_{qr}	ω_{qr}
HouseQR	$\mathcal{O}(\varepsilon)$	$\mathcal{O}(\varepsilon)$
GivensQR	$\mathcal{O}(\varepsilon)$	$\mathcal{O}(\varepsilon)$
MGS	$\mathcal{O}(\varepsilon)$	$\mathcal{O}(\varepsilon) \kappa$
CholQR	$\mathcal{O}(\varepsilon)$	$\mathcal{O}(\varepsilon) \kappa^2$

Table 1: Values of ρ_{qr} and ω_{qr} for common IO choices.

with $\tilde{\mathbf{Q}}$ exactly satisfying $\tilde{\mathbf{Q}}^T \tilde{\mathbf{Q}} = I$, because from (7) we have

$$\begin{aligned} \bar{\mathbf{G}} + \Delta \tilde{\mathbf{G}} + \Delta \mathbf{Q} \bar{\mathbf{R}} &= \bar{\mathbf{Q}} \bar{\mathbf{R}}, \\ \|\bar{\mathbf{R}}\| &\leq (1 + \mathcal{O}(\varepsilon)) \|\bar{\mathbf{G}}\| + \mathcal{O}(\varepsilon) \|\bar{\mathbf{R}}\| \Rightarrow \|\bar{\mathbf{R}}\| \leq \frac{1 + \mathcal{O}(\varepsilon)}{1 - \mathcal{O}(\varepsilon)} \|\bar{\mathbf{G}}\|. \end{aligned} \quad (8)$$

Furthermore, HouseQR and GivensQR satisfy

$$\begin{aligned} \bar{\mathbf{G}} + \Delta \mathbf{G} &= \bar{\mathbf{Q}} \bar{\mathbf{R}}, \quad \|\Delta \mathbf{G}\| \leq \mathcal{O}(\varepsilon) \|\bar{\mathbf{G}}\|, \\ \|I - \bar{\mathbf{Q}}^T \bar{\mathbf{Q}}\| &\leq \mathcal{O}(\varepsilon). \end{aligned} \quad (9)$$

From [16, Theorems 19.4, 19.10, 19.13] and the discussion above, we show example values of ρ_{qr} and ω_{qr} for different methods in Table 1.

In the remainder of this section, we abstract the induction process appearing in a typical BGS analysis through a series of lemmas. Given $\bar{\mathbf{Q}}_{\text{prev}}$ satisfying

$$\|I - \bar{\mathbf{Q}}_{\text{prev}}^T \bar{\mathbf{Q}}_{\text{prev}}\| \leq \omega_{\text{prev}}, \quad (10)$$

for some $0 < \omega_{\text{prev}} \leq 1$, it follows that

$$\|\bar{\mathbf{Q}}_{\text{prev}}\| \leq 1 + \omega_{\text{prev}} \leq \mathcal{O}(1). \quad (11)$$

We aim to derive a ω_{new} in relation to ω_{prev} , ψ , ρ_{qr} , and ω_{qr} such that

$$\|I - \bar{\mathbf{Q}}_{\text{new}}^T \bar{\mathbf{Q}}_{\text{new}}\| \leq \omega_{\text{new}},$$

and then bound the LOO of the final result of the iteration by induction. The following lemma addresses the impact of ω_{prev} , ψ , ρ_{qr} , and ω_{qr} on ω_{new} .

Lemma 1. *Assume that $\bar{\mathbf{G}}$, $\tilde{\mathbf{G}}$, $\bar{\mathbf{Q}}$, $\bar{\mathbf{R}}$, and $\bar{\mathbf{Q}}_{\text{prev}}$ satisfy (5), (6), and (10), and that*

$$\frac{(1 + \rho_{\text{qr}})\psi}{\sigma_{\min}(\tilde{\mathbf{G}})} + \rho_{\text{qr}}\kappa(\tilde{\mathbf{G}}) < 1$$

is satisfied. Furthermore, assume that $\bar{\mathbf{R}}$ is nonsingular. Then

$$\|\bar{\mathbf{R}}^{-1}\| \leq \frac{1 + \omega_{\text{qr}}}{\sigma_{\min}(\tilde{\mathbf{G}}) - (1 + \rho_{\text{qr}})\psi - \rho_{\text{qr}}\kappa(\tilde{\mathbf{G}})} \|\tilde{\mathbf{G}}\| \quad (12)$$

and $\bar{\mathbf{Q}}_{\text{new}} = [\bar{\mathbf{Q}}_{\text{prev}}, \bar{\mathbf{Q}}]$ satisfies

$$\begin{aligned} &\|I - \bar{\mathbf{Q}}_{\text{new}}^T \bar{\mathbf{Q}}_{\text{new}}\| \\ &\leq \omega_{\text{prev}} + 2 \|\bar{\mathbf{Q}}_{\text{prev}}^T \tilde{\mathbf{G}} \bar{\mathbf{R}}^{-1}\| + \omega_{\text{qr}} \\ &\quad + \frac{2(1 + \omega_{\text{prev}})(1 + \omega_{\text{qr}}) \left(\rho_{\text{qr}}\kappa(\tilde{\mathbf{G}}) + (1 + \rho_{\text{qr}})\psi / \sigma_{\min}(\tilde{\mathbf{G}}) \right)}{1 - (1 + \rho_{\text{qr}})\psi / \sigma_{\min}(\tilde{\mathbf{G}}) - \rho_{\text{qr}}\kappa(\tilde{\mathbf{G}})}. \end{aligned} \quad (13)$$

Lemma 1 illustrates how Proj and QR influence the LOO of $\bar{\mathbf{Q}}_{new}$. It also implies that we only need to estimate $\left\| \bar{\mathbf{Q}}_{prev}^T \tilde{\mathbf{G}} \bar{\mathbf{R}}^{-1} \right\|$, ψ , ρ_{qr} , and ω_{qr} to assess the LOO of $\bar{\mathbf{Q}}_{new}$.

Before proving Lemma 1, we first give the following lemma to be used in its proof.

Lemma 2. Assume that for \mathbf{W} , \mathbf{U} , $\Delta\mathbf{W} \in \mathbb{R}^{m \times s}$ and $R \in \mathbb{R}^{s \times s}$ nonsingular,

$$\mathbf{W} + \Delta\mathbf{W} = \mathbf{U}R.$$

Then

$$\|R^{-1}\| \leq \frac{\|\mathbf{U}\|}{\sigma_{\min}(\mathbf{W}) - \|\Delta\mathbf{W}\|}. \quad (14)$$

Proof. By the perturbation theory of singular values [14, Corollary 8.6.2], we have

$$\sigma_{\min}(\mathbf{W}) - \|\Delta\mathbf{W}\| \leq \sigma_{\min}(\mathbf{U}R).$$

Together with

$$\sigma_{\min}^2(\mathbf{U}R) = \min_{\mathbf{y}} \left(\frac{\|\mathbf{U}R\mathbf{y}\|^2}{\|\mathbf{y}\|^2} \right) \leq \min_{\mathbf{y}} \left(\frac{\|\mathbf{U}\|^2 \|\mathbf{R}\mathbf{y}\|^2}{\|\mathbf{y}\|^2} \right) \leq \|\mathbf{U}\|^2 \sigma_{\min}^2(R),$$

we can bound $\|R^{-1}\|$ as

$$\|R^{-1}\| = \frac{1}{\sigma_{\min}(R)} \leq \frac{\|\mathbf{U}\|}{\sigma_{\min}(\mathbf{W}) - \|\Delta\mathbf{W}\|}.$$

□

Note that we do not assume that \mathbf{U} in Lemma 2 is orthogonal.

Proof of Lemma 1. Notice that

$$\left\| I - \bar{\mathbf{Q}}_{new}^T \bar{\mathbf{Q}}_{new} \right\| \leq \left\| I - \bar{\mathbf{Q}}_{prev}^T \bar{\mathbf{Q}}_{prev} \right\| + 2 \left\| \bar{\mathbf{Q}}_{prev}^T \bar{\mathbf{Q}} \right\| + \left\| I - \bar{\mathbf{Q}}^T \bar{\mathbf{Q}} \right\|.$$

Together with (5), (6), (10) and (11), we obtain

$$\begin{aligned} \left\| \bar{\mathbf{Q}}_{prev}^T \bar{\mathbf{Q}} \right\| &= \left\| \bar{\mathbf{Q}}_{prev}^T (\tilde{\mathbf{G}} + \Delta\mathbf{E}_{proj} + \Delta\mathbf{G}) \bar{\mathbf{R}}^{-1} \right\| \\ &\leq \left\| \bar{\mathbf{Q}}_{prev}^T \tilde{\mathbf{G}} \bar{\mathbf{R}}^{-1} \right\| + (1 + \omega_{prev}) \psi \left\| \bar{\mathbf{R}}^{-1} \right\| \\ &\quad + (1 + \omega_{prev}) \rho_{qr} \left\| \tilde{\mathbf{G}} \right\| \left\| \bar{\mathbf{R}}^{-1} \right\|, \end{aligned} \quad (15)$$

and furthermore,

$$\begin{aligned} \left\| I - \bar{\mathbf{Q}}_{new}^T \bar{\mathbf{Q}}_{new} \right\| &\leq \omega_{prev} + \omega_{qr} + 2 \left\| \bar{\mathbf{Q}}_{prev}^T \tilde{\mathbf{G}} \bar{\mathbf{R}}^{-1} \right\| \\ &\quad + 2(1 + \omega_{prev}) (\psi + \rho_{qr} \left\| \tilde{\mathbf{G}} \right\|) \left\| \bar{\mathbf{R}}^{-1} \right\|. \end{aligned}$$

Next, we estimate $\left\| \bar{\mathbf{R}}^{-1} \right\|$, which satisfies

$$\tilde{\mathbf{G}} + \Delta\mathbf{E}_{proj} + \Delta\mathbf{G} = \bar{\mathbf{Q}} \bar{\mathbf{R}}.$$

By Lemma 2, $\left\| \bar{\mathbf{R}}^{-1} \right\|$ can be bounded as

$$\begin{aligned} \left\| \bar{\mathbf{R}}^{-1} \right\| &\leq \frac{\left\| \bar{\mathbf{Q}} \right\|}{\sigma_{\min}(\tilde{\mathbf{G}}) - (\|\Delta\mathbf{E}_{proj}\| + \|\Delta\mathbf{G}\|)} \\ &\leq \frac{1 + \omega_{qr}}{\sigma_{\min}(\tilde{\mathbf{G}}) - (1 + \rho_{qr})\psi - \rho_{qr} \left\| \tilde{\mathbf{G}} \right\|}. \end{aligned} \quad (16)$$

The conclusion follows because

$$\begin{aligned} \|\tilde{\mathbf{G}}\| \|\bar{R}^{-1}\| &\leq \frac{(1 + \omega_{\text{qr}}) (\|\tilde{\mathbf{G}}\| + \psi)}{\sigma_{\min}(\tilde{\mathbf{G}}) - (1 + \rho_{\text{qr}})\psi - \rho_{\text{qr}} \|\tilde{\mathbf{G}}\|} \\ &\leq \frac{(1 + \omega_{\text{qr}}) (\kappa(\tilde{\mathbf{G}}) + \psi/\sigma_{\min}(\tilde{\mathbf{G}}))}{1 - (1 + \rho_{\text{qr}})\psi/\sigma_{\min}(\tilde{\mathbf{G}}) - \rho_{\text{qr}}\kappa(\tilde{\mathbf{G}})}. \end{aligned}$$

□

2.2 Loss of orthogonality of BCGS-A

According to Algorithm 1, the projection and intraortho stages can be written respectively as

$$\mathbf{G} = \text{Proj}(\mathbf{X}, \mathbf{Q}) := \mathbf{X} - \mathbf{Q}\mathbf{Q}^T\mathbf{X} \quad \text{and} \quad \text{QR}(\mathbf{G}) := \text{IO}(\mathbf{G}). \quad (17)$$

Specifically, for the k th inner loop of Algorithm 1,

$$\mathbf{V}_k = \text{Proj}(\mathbf{X}_k, \mathbf{Q}_{k-1}) = \mathbf{X}_k - \mathbf{Q}_{k-1}\mathbf{Q}_{k-1}^T\mathbf{X}_k, \quad \text{and} \quad (18)$$

$$[\mathbf{Q}_k, R_{kk}] = \text{QR}(\mathbf{V}_k) = \text{IO}(\mathbf{V}_k). \quad (19)$$

Then we define

$$\tilde{\mathbf{V}}_k = (I - \bar{\mathbf{Q}}_{k-1}\bar{\mathbf{Q}}_{k-1}^T)\mathbf{X}_k, \quad (20)$$

where $\bar{\mathbf{Q}}_{k-1}$ satisfies

$$\|I - \bar{\mathbf{Q}}_{k-1}^T\bar{\mathbf{Q}}_{k-1}\| \leq \omega_{k-1}. \quad (21)$$

Furthermore, $\tilde{\mathbf{V}}_k$ denotes the computed result of $\tilde{\mathbf{V}}_k$.

To use Lemma 1 to analyze the k th inner loop of Algorithm 1, we first estimate $\sigma_{\min}(\tilde{\mathbf{V}}_k)$ and $\kappa(\tilde{\mathbf{V}}_k)$ in the following lemma, and then analyze the specific $\psi := \psi_k^{(\text{BCGS-A})}$ satisfying $\|\tilde{\mathbf{V}}_k - \tilde{\mathbf{V}}_k\| \leq \psi_k^{(\text{BCGS-A})}$, as well as the quantity $\|\bar{\mathbf{Q}}_{k-1}^T\tilde{\mathbf{V}}_k\bar{R}_{kk}^{-1}\|$, which are related only to the projection stage in Lemma 4.

Lemma 3. *Let $\tilde{\mathbf{V}}_k$ and $\bar{\mathbf{Q}}_{k-1}$ satisfy (20) and (21). Assume that*

$$\mathbf{x}_{k-1} + \Delta\mathbf{x}_{k-1} = \bar{\mathbf{Q}}_{k-1}\bar{\mathcal{R}}_{k-1}, \quad \|\Delta\mathbf{x}_{k-1}\| \leq \rho_{k-1}\|\mathbf{x}_{k-1}\|, \quad (22)$$

with $\rho_{k-1}\kappa(\mathbf{x}_k) < 1$ and $\bar{\mathcal{R}}_{k-1}$ nonsingular. Then

$$\|\tilde{\mathbf{V}}_k\| \leq (1 + \omega_{k-1})\|\mathbf{x}_k\|, \quad (23)$$

$$\sigma_{\min}(\tilde{\mathbf{V}}_k) \geq \sigma_{\min}(\mathbf{x}_k) - \rho_{k-1}\|\mathbf{x}_{k-1}\|, \quad \text{and} \quad (24)$$

$$\kappa(\tilde{\mathbf{V}}_k) \leq \frac{(1 + \omega_{k-1})\kappa(\mathbf{x}_k)}{1 - \rho_{k-1}\kappa(\mathbf{x}_k)}. \quad (25)$$

Proof. Recalling the definition (20) of $\tilde{\mathbf{V}}_k$ and following [6, Equations (39)], it is easy to verify (24). Note that the two symmetric matrices $\bar{\mathbf{Q}}_{k-1}\bar{\mathbf{Q}}_{k-1}^T$ and $\bar{\mathbf{Q}}_{k-1}^T\bar{\mathbf{Q}}_{k-1}$ have the same nonzero eigenvalues. From the assumption (21),

$$\|I - \bar{\mathbf{Q}}_{k-1}\bar{\mathbf{Q}}_{k-1}^T\| = \max\{\|I - \bar{\mathbf{Q}}_{k-1}^T\bar{\mathbf{Q}}_{k-1}\|, 1\} \leq \max\{\omega_{k-1}, 1\} \leq 1 + \omega_{k-1}, \quad (26)$$

which, combined with the definition (20) of $\tilde{\mathbf{V}}_k$, gives (23). Combining (24) with (26), we have

$$\kappa(\tilde{\mathbf{V}}_k) = \frac{\|\tilde{\mathbf{V}}_k\|}{\sigma_{\min}(\tilde{\mathbf{V}}_k)} \leq \frac{(1 + \omega_{k-1})\|\mathbf{x}_k\|}{\sigma_{\min}(\mathbf{x}_k) - \rho_{k-1}\|\mathbf{x}_{k-1}\|} \leq \frac{(1 + \omega_{k-1})\kappa(\mathbf{x}_k)}{1 - \rho_{k-1}\kappa(\mathbf{x}_k)}, \quad (27)$$

giving (25). □

Lemma 4. Let $\tilde{\mathbf{V}}_k$ and $\tilde{\mathbf{Q}}_{k-1}$ satisfy (20) and (21). Then for the projection stage (18) computed by lines 3-4 in Algorithm 1, it holds that

$$\|\tilde{\mathbf{V}}_k - \tilde{\mathbf{V}}_k\| \leq \psi_k^{(\text{BCGS-A})} \leq \mathcal{O}(\varepsilon) \|\mathbf{X}_k\|, \quad (28)$$

$$\|\tilde{\mathbf{Q}}_{k-1}^T \tilde{\mathbf{V}}_k \tilde{\mathbf{R}}_{kk}^{-1}\| \leq (1 + \omega_{k-1}) \omega_{k-1} \|\mathbf{X}_k\| \|\tilde{\mathbf{R}}_{kk}^{-1}\|. \quad (29)$$

Proof. By (11) it follows that

$$\tilde{\mathbf{R}}_{1:k-1,k} = \tilde{\mathbf{Q}}_{k-1}^T \mathbf{X}_k + \Delta \tilde{\mathbf{R}}_{1:k-1,k}, \quad \|\Delta \tilde{\mathbf{R}}_{1:k-1,k}\| \leq \mathcal{O}(\varepsilon) \|\mathbf{X}_k\|. \quad (30)$$

Furthermore, we have

$$\tilde{\mathbf{V}}_k = \mathbf{X}_k - \tilde{\mathbf{Q}}_{k-1} \tilde{\mathbf{Q}}_{k-1}^T \mathbf{X}_k + \Delta \tilde{\mathbf{V}}_k = \tilde{\mathbf{V}}_k + \Delta \tilde{\mathbf{V}}_k, \quad \|\Delta \tilde{\mathbf{V}}_k\| \leq \mathcal{O}(\varepsilon) \|\mathbf{X}_k\|, \quad (31)$$

which gives (28). Then by the assumption (21), we find the bound (29) as follows:

$$\begin{aligned} \|\tilde{\mathbf{Q}}_{k-1}^T \tilde{\mathbf{V}}_k \tilde{\mathbf{R}}_{kk}^{-1}\| &= \|\tilde{\mathbf{Q}}_{k-1}^T (I - \tilde{\mathbf{Q}}_{k-1} \tilde{\mathbf{Q}}_{k-1}^T) \mathbf{X}_k \tilde{\mathbf{R}}_{kk}^{-1}\| \\ &\leq \|(I - \tilde{\mathbf{Q}}_{k-1}^T \tilde{\mathbf{Q}}_{k-1}) \tilde{\mathbf{Q}}_{k-1}^T \mathbf{X}_k \tilde{\mathbf{R}}_{kk}^{-1}\| \\ &\leq \|I - \tilde{\mathbf{Q}}_{k-1}^T \tilde{\mathbf{Q}}_{k-1}\| \|\tilde{\mathbf{Q}}_{k-1}\| \|\mathbf{X}_k\| \|\tilde{\mathbf{R}}_{kk}^{-1}\| \\ &\leq (1 + \omega_{k-1}) \omega_{k-1} \|\mathbf{X}_k\| \|\tilde{\mathbf{R}}_{kk}^{-1}\|. \end{aligned}$$

□

Lemma 1 indicates that we only need to estimate $\|\tilde{\mathbf{Q}}_{k-1}^T \tilde{\mathbf{V}}_k \tilde{\mathbf{R}}_{kk}^{-1}\|$, $\psi_k^{(\text{BCGS-A})}$, ρ_{qr} , $\sigma_{\min}(\tilde{\mathbf{V}}_k)$, and $\kappa(\tilde{\mathbf{V}}_k)$ to evaluate the LOO of $\tilde{\mathbf{Q}}_k$. Already, $\|\tilde{\mathbf{Q}}_{k-1}^T \tilde{\mathbf{V}}_k \tilde{\mathbf{R}}_{kk}^{-1}\|$ and $\psi_k^{(\text{BCGS-A})}$ have been determined in Lemma 4 together with the estimation of $\|\tilde{\mathbf{R}}_{kk}^{-1}\|$ shown in (16), while $\sigma_{\min}(\tilde{\mathbf{V}}_k)$ and $\kappa(\tilde{\mathbf{V}}_k)$ were addressed in Lemma 3. It is important to note that ρ_{qr} is dependent on IO_1 . Therefore, the subsequent lemma utilizes both Lemma 4 and Lemma 3 to describe the behavior of the k th inner loop of BCGS-A, guided by Lemma 1.

Lemma 5. Assume that $\tilde{\mathbf{Q}}_{k-1}$ satisfies (21), and that

$$\mathbf{x}_{k-1} + \Delta \mathbf{x}_{k-1} = \tilde{\mathbf{Q}}_{k-1} \tilde{\mathbf{R}}_{k-1}, \quad \|\Delta \mathbf{x}_{k-1}\| \leq \rho_{k-1} \|\mathbf{x}_{k-1}\|.$$

Suppose further that for all $\mathbf{X} \in \mathbb{R}^{m \times s}$ with $\kappa(\mathbf{X}) \leq \kappa(\mathbf{x})$, the following hold for $[\tilde{\mathbf{Q}}, \tilde{\mathbf{R}}] = \text{IO}_A(\mathbf{X})$:

$$\begin{aligned} \mathbf{X} + \Delta \mathbf{X} &= \tilde{\mathbf{Q}} \tilde{\mathbf{R}}, \quad \|\Delta \mathbf{X}\| \leq \mathcal{O}(\varepsilon) \|\mathbf{X}\|, \\ \|I - \tilde{\mathbf{Q}}^T \tilde{\mathbf{Q}}\| &\leq \mathcal{O}(\varepsilon) \kappa^{\alpha_A}(\mathbf{X}), \end{aligned}$$

and for $[\tilde{\mathbf{Q}}, \tilde{\mathbf{R}}] = \text{IO}(\mathbf{X})$:

$$\begin{aligned} \mathbf{X} + \Delta \mathbf{X} &= \tilde{\mathbf{Q}} \tilde{\mathbf{R}}, \quad \|\Delta \mathbf{X}\| \leq \mathcal{O}(\varepsilon) \|\mathbf{X}\|, \\ \|I - \tilde{\mathbf{Q}}^T \tilde{\mathbf{Q}}\| &\leq \mathcal{O}(\varepsilon) \kappa^\alpha(\mathbf{X}). \end{aligned}$$

Assume as well that $\mathcal{O}(\varepsilon) \kappa(\mathbf{x}_k) \leq \frac{1}{2}$ and $\rho_{k-1} \kappa(\mathbf{x}_k) < 1$. Then for the k th inner loop of Algorithm 1 with any $k \geq 2$,

$$\|I - \tilde{\mathbf{Q}}_k^T \tilde{\mathbf{Q}}_k\| \leq \omega_{k-1} + \frac{2\omega_{k-1}(1 + \omega_{k-1})(1 + \omega_{\text{qr}}) + \mathcal{O}(\varepsilon)}{1 - \mathcal{O}(\varepsilon) \kappa(\mathbf{x}_k)} \kappa(\mathbf{x}_k) + \omega_{\text{qr}}. \quad (32)$$

By induction on k , we obtain the following result on the LOO of BCGS-A.

Theorem 1. Let $\bar{\mathbf{Q}}$ and $\bar{\mathbf{R}}$ denote the computed results of Algorithm 1. Assume that for all $\mathbf{X} \in \mathbb{R}^{m \times s}$ with $\kappa(\mathbf{X}) \leq \kappa(\boldsymbol{\mathcal{X}})$, the following hold for $[\bar{\mathbf{Q}}, \bar{\mathbf{R}}] = \text{IO}_A(\mathbf{X})$:

$$\begin{aligned} \mathbf{X} + \Delta \mathbf{X} &= \bar{\mathbf{Q}} \bar{\mathbf{R}}, \quad \|\Delta \mathbf{X}\| \leq \mathcal{O}(\varepsilon) \|\mathbf{X}\|, \\ \|I - \bar{\mathbf{Q}}^T \bar{\mathbf{Q}}\| &\leq \mathcal{O}(\varepsilon) \kappa^{\alpha_A}(\mathbf{X}). \end{aligned}$$

Assume as well that for $[\bar{\mathbf{Q}}, \bar{\mathbf{R}}] = \text{IO}(\mathbf{X})$, it holds that

$$\begin{aligned} \mathbf{X} + \Delta \mathbf{X} &= \bar{\mathbf{Q}} \bar{\mathbf{R}}, \quad \|\Delta \mathbf{X}\| \leq \mathcal{O}(\varepsilon) \|\mathbf{X}\|, \\ \|I - \bar{\mathbf{Q}}^T \bar{\mathbf{Q}}\| &\leq \mathcal{O}(\varepsilon) \kappa^\alpha(\mathbf{X}). \end{aligned}$$

If $\mathcal{O}(\varepsilon) \kappa(\boldsymbol{\mathcal{X}}) \leq \frac{1}{2}$, then

$$\boldsymbol{\mathcal{X}} + \Delta \boldsymbol{\mathcal{X}} = \bar{\mathbf{Q}} \bar{\mathbf{R}}, \quad \|\Delta \boldsymbol{\mathcal{X}}\| \leq \mathcal{O}(\varepsilon) \|\boldsymbol{\mathcal{X}}\| \quad (33)$$

and

$$\|I - \bar{\mathbf{Q}}^T \bar{\mathbf{Q}}\| \leq \mathcal{O}(\varepsilon) (\kappa(\boldsymbol{\mathcal{X}}))^{p-2+\max\{\alpha_A+1, \alpha\}}. \quad (34)$$

Proof. First, we prove a bound on the residual of **BCGS** by an inductive approach on the block vectors of $\boldsymbol{\mathcal{X}}$. For the base case, the assumptions of IO_A directly give

$$\boldsymbol{\mathcal{X}}_1 + \Delta \boldsymbol{\mathcal{X}}_1 = \bar{\mathbf{Q}}_1 \bar{\mathbf{R}}_1, \quad \|\Delta \boldsymbol{\mathcal{X}}_1\| \leq \mathcal{O}(\varepsilon) \|\boldsymbol{\mathcal{X}}_1\|.$$

Then we prove that it holds for k provided it holds for $k-1$. Assume that $\boldsymbol{\mathcal{X}}_{k-1} + \Delta \boldsymbol{\mathcal{X}}_{k-1} = \bar{\mathbf{Q}}_{k-1} \bar{\mathbf{R}}_{k-1}$ with $\|\Delta \boldsymbol{\mathcal{X}}_{k-1}\| \leq \mathcal{O}(\varepsilon) \|\boldsymbol{\mathcal{X}}_{k-1}\|$. Then by (6), (30), (31), and Lemma 4,

$$\begin{aligned} \boldsymbol{\mathcal{X}}_k + \Delta \boldsymbol{\mathcal{X}}_k &= [\boldsymbol{\mathcal{X}}_{k-1} + \Delta \boldsymbol{\mathcal{X}}_{k-1} \quad \mathbf{X}_k + \Delta \mathbf{X}_k] \\ &= [\bar{\mathbf{Q}}_{k-1} \quad \bar{\mathbf{Q}}_k] \begin{bmatrix} \bar{\mathbf{R}}_{k-1} & \bar{\mathbf{R}}_{1:k-1,k} \\ 0 & \bar{\mathbf{R}}_{kk} \end{bmatrix} \\ &= [\bar{\mathbf{Q}}_{k-1} \bar{\mathbf{R}}_{k-1} \quad \bar{\mathbf{Q}}_{k-1} \bar{\mathbf{R}}_{1:k-1,k} + \bar{\mathbf{Q}}_k \bar{\mathbf{R}}_{kk}] \\ &= [\bar{\mathbf{Q}}_{k-1} \bar{\mathbf{R}}_{k-1} \quad \bar{\mathbf{Q}}_{k-1} (\bar{\mathbf{Q}}_{k-1}^T \mathbf{X}_k + \Delta \bar{\mathbf{R}}_{1:k-1,k}) + \mathbf{X}_k - \bar{\mathbf{Q}}_{k-1} \bar{\mathbf{Q}}_{k-1}^T \mathbf{X}_k + \Delta \tilde{\mathbf{V}}_k + \Delta \mathbf{G}_k] \\ &= [\bar{\mathbf{Q}}_{k-1} \bar{\mathbf{R}}_{k-1} \quad \mathbf{X}_k + \bar{\mathbf{Q}}_{k-1}^T \Delta \bar{\mathbf{R}}_{1:k-1,k} + \Delta \tilde{\mathbf{V}}_k + \Delta \mathbf{G}_k]. \end{aligned}$$

Thus, $\Delta \boldsymbol{\mathcal{X}}_k = \bar{\mathbf{Q}}_{k-1}^T \Delta \bar{\mathbf{R}}_{1:k-1,k} + \Delta \tilde{\mathbf{V}}_k + \Delta \mathbf{G}_k$ satisfies $\|\Delta \boldsymbol{\mathcal{X}}_k\| \leq \mathcal{O}(\varepsilon) \|\boldsymbol{\mathcal{X}}_k\|$ and further we have

$$\|\Delta \boldsymbol{\mathcal{X}}_k\| \leq \|\Delta \boldsymbol{\mathcal{X}}_{k-1}\| + \|\Delta \boldsymbol{\mathcal{X}}_k\| \leq \mathcal{O}(\varepsilon) \|\boldsymbol{\mathcal{X}}_k\|, \quad (35)$$

which proves (33) by induction.

Next it remains to prove the LOO (34) using Lemma 5 via induction. Note that from (33) we have already verified that the assumption of the residual in Lemma 5 is satisfied. The assumptions on IO_A directly give the base case for the LOO, i.e., $\omega_1 \leq \mathcal{O}(\varepsilon) \kappa^{\alpha_A}(\boldsymbol{\mathcal{X}}_1) \leq \mathcal{O}(\varepsilon) (\kappa(\boldsymbol{\mathcal{X}}_1))^{\max\{\alpha_A+1, \alpha\}-1}$. Now we assume that $\omega_{k-1} \leq \mathcal{O}(\varepsilon) (\kappa(\boldsymbol{\mathcal{X}}_{k-1}))^{\max\{\alpha_A+1, \alpha\}+k-3}$ and then bound ω_k . Using Lemma 5 and the assumption of IO we conclude the proof because

$$\begin{aligned} \|I - \bar{\mathbf{Q}}_k^T \bar{\mathbf{Q}}_k\| &\leq \mathcal{O}(\varepsilon) (\kappa(\boldsymbol{\mathcal{X}}_{k-1}))^{\max\{\alpha_A+1, \alpha\}+k-2} + \mathcal{O}(\varepsilon) \kappa^\alpha(\mathbf{X}_k) \\ &\leq \mathcal{O}(\varepsilon) (\kappa(\boldsymbol{\mathcal{X}}_k))^{\max\{\alpha_A+1, \alpha\}+k-2}. \end{aligned}$$

□

If $\omega_{k-1}, \omega_{\text{qr}} \leq \mathcal{O}(1)$ and $\omega_{\text{qr}} \leq \omega_{k-1}$ for some $k-1$, we can simplify (32) in Lemma 5 as

$$\|I - \bar{\mathbf{Q}}_k^T \bar{\mathbf{Q}}_k\| \leq \mathcal{O}(1) \|I - \bar{\mathbf{Q}}_{k-1}^T \bar{\mathbf{Q}}_{k-1}\| \kappa(\boldsymbol{\mathcal{X}}_k).$$

In other words, IO_A and IO have essentially no effect from one iteration to the next on the orthogonality of the basis. Theorem 1 makes this observation more precise. In particular, (34) shows that in the best of circumstances, $\kappa(\boldsymbol{\mathcal{X}})$ still has an exponent of at least $p-1$ in the bound, which is the same as what Kielbasiński and Schwetlick proved for column-wise CGS [18, pp 284] (i.e., for $s=1$). Table 2 compares provable LOO bounds for various choices of IO_A and IO . Although we have been unable to find numerical examples that attain this bound, Figure 1 clearly shows that $p > 2$, even when $\text{IO}_A = \text{IO} = \text{HouseQR}$.

IO _A	IO	$\ I - \bar{\mathbf{Q}}^T \bar{\mathbf{Q}}\ $
HouseQR	HouseQR or MGS	$\mathcal{O}(\varepsilon) (\kappa(\mathcal{X}))^{p-1}$
HouseQR or MGS	CholQR	$\mathcal{O}(\varepsilon) (\kappa(\mathcal{X}))^p$
CholQR	CholQR	$\mathcal{O}(\varepsilon) (\kappa(\mathcal{X}))^{p+1}$

Table 2: Upper bounds on the loss of orthogonality for **BCGS-A** with different IO analyzed in Theorem 1.

2.3 Loss of orthogonality of BCGSI+A

For Algorithm 2, the projection and intraortho stages can be written respectively as follows:

$$\mathbf{G} = \text{Proj}(\mathbf{X}, \mathbf{Q}) := (I - \mathbf{Q}\mathbf{Q}^T)(I - \mathbf{Q}\mathbf{Q}^T)\mathbf{X} \text{ and } \text{QR}(\mathbf{G}) := \text{IO}_2(\mathbf{G}). \quad (36)$$

Specifically, for the k th inner loop of Algorithm 2,

$$\mathbf{H}_k = \text{Proj}(\mathbf{X}_k S_{kk}^{-1}, \mathbf{Q}_{k-1}) = (I - \mathbf{Q}_{k-1} \mathbf{Q}_{k-1}^T)(I - \mathbf{Q}_{k-1} \mathbf{Q}_{k-1}^T) \mathbf{X}_k S_{kk}^{-1}, \quad (37)$$

$$[\mathbf{Q}_k, R_{kk}] = \text{QR}(\mathbf{H}_k) = \text{IO}_2(\mathbf{H}_k), \quad (38)$$

where $\mathbf{U}_k S_{kk} = \text{IO}_1((I - \mathbf{Q}_{k-1} \mathbf{Q}_{k-1}^T) \mathbf{X}_k)$.

Lemma 6. Let $\tilde{\mathbf{V}}_k = (I - \bar{\mathbf{Q}}_{k-1} \bar{\mathbf{Q}}_{k-1}^T) \mathbf{X}_k$ and $\tilde{\mathbf{H}}_k = (I - \bar{\mathbf{Q}}_{k-1} \bar{\mathbf{Q}}_{k-1}^T) \bar{\mathbf{U}}_k$, where $\bar{\mathbf{Q}}_{k-1}$ satisfies $\|I - \bar{\mathbf{Q}}_{k-1}^T \bar{\mathbf{Q}}_{k-1}\| \leq \omega_{k-1}$. Assume that for all $\mathbf{X} \in \mathbb{R}^{m \times s}$ with $\kappa(\mathbf{X}) \leq \kappa(\mathcal{X})$, the following hold for $[\bar{\mathbf{Q}}, \bar{\mathbf{R}}] = \text{IO}_1(\mathbf{X})$:

$$\begin{aligned} \mathbf{X} + \Delta \mathbf{X} &= \bar{\mathbf{Q}} \bar{\mathbf{R}}, \quad \|\Delta \mathbf{X}\| \leq \mathcal{O}(\varepsilon) \|\mathbf{X}\|, \\ \|I - \bar{\mathbf{Q}}^T \bar{\mathbf{Q}}\| &\leq \mathcal{O}(\varepsilon) \kappa^{\alpha_1}(\mathbf{X}). \end{aligned}$$

Similarly, assume the following hold for $[\bar{\mathbf{Q}}, \bar{\mathbf{R}}] = \text{IO}_2(\mathbf{X})$:

$$\begin{aligned} \mathbf{X} + \Delta \mathbf{X} &= \bar{\mathbf{Q}} \bar{\mathbf{R}}, \quad \|\Delta \mathbf{X}\| \leq \mathcal{O}(\varepsilon) \|\mathbf{X}\|, \\ \|I - \bar{\mathbf{Q}}^T \bar{\mathbf{Q}}\| &\leq \mathcal{O}(\varepsilon) \kappa^{\alpha_2}(\mathbf{X}). \end{aligned}$$

Furthermore, if

$$\mathbf{x}_{k-1} + \Delta \mathbf{x}_{k-1} = \bar{\mathbf{Q}}_{k-1} \bar{\mathbf{R}}_{k-1}, \quad \|\Delta \mathbf{x}_{k-1}\| \leq \rho_{k-1} \|\mathbf{x}_{k-1}\| \quad (39)$$

as well as

$$\mathcal{O}(\varepsilon) \kappa^{\alpha_1}(\mathbf{x}_k) + 2(\omega_{k-1} + \mathcal{O}(\varepsilon))(1 + \omega_{k-1})^2 \kappa(\mathbf{x}_k) + \rho_{k-1} \kappa(\mathbf{x}_k) \leq \frac{1}{2}, \quad (40)$$

then the quantities computed by Algorithm 2 satisfy the following, for any $k \geq 2$:

$$\bar{\mathbf{S}}_{1:k-1,k} = \bar{\mathbf{Q}}_{k-1}^T \mathbf{X}_k + \Delta \bar{\mathbf{S}}_{1:k-1,k}, \quad \|\Delta \bar{\mathbf{S}}_{1:k-1,k}\| \leq \mathcal{O}(\varepsilon) \|\mathbf{X}_k\|; \quad (41)$$

$$\bar{\mathbf{U}}_k \bar{\mathbf{S}}_{kk} = \tilde{\mathbf{V}}_k + \Delta \tilde{\mathbf{V}}_k, \quad \|\Delta \tilde{\mathbf{V}}_k\| \leq \mathcal{O}(\varepsilon) \|\mathbf{X}_k\|; \quad (42)$$

$$\|I - \bar{\mathbf{U}}_k^T \bar{\mathbf{U}}_k\| \leq \mathcal{O}(\varepsilon) \kappa^{\alpha_1}(\mathbf{x}_k), \quad \|\bar{\mathbf{U}}_k\| \leq 1 + \mathcal{O}(\varepsilon) \kappa^{\alpha_1}(\mathbf{x}_k); \quad (43)$$

$$\|\mathbf{X}_k\| \|\bar{\mathbf{S}}_{kk}^{-1}\| \leq 2\kappa(\mathbf{x}_k); \quad (44)$$

$$\bar{\mathbf{T}}_{1:k-1,k} = \bar{\mathbf{Q}}_{k-1}^T \bar{\mathbf{U}}_k + \Delta \bar{\mathbf{T}}_{1:k-1,k}, \quad (45)$$

$$\|\Delta \bar{\mathbf{T}}_{1:k-1,k}\| \leq \mathcal{O}(\varepsilon) (1 + \mathcal{O}(\varepsilon) \kappa^{\alpha_1}(\mathbf{x}_k));$$

$$\bar{\mathbf{Q}}_k \bar{\mathbf{T}}_{kk} = \tilde{\mathbf{H}}_k + \Delta \tilde{\mathbf{H}}_k, \quad \|\Delta \tilde{\mathbf{H}}_k\| \leq \mathcal{O}(\varepsilon) (1 + \mathcal{O}(\varepsilon) \kappa^{\alpha_1}(\mathbf{x}_k)); \quad (46)$$

$$\|I - \bar{\mathbf{Q}}_k^T \bar{\mathbf{Q}}_k\| \leq \mathcal{O}(\varepsilon), \quad \|\bar{\mathbf{Q}}_k\| \leq 1 + \mathcal{O}(\varepsilon); \quad (47)$$

$$\bar{\mathbf{R}}_{1:k-1,k} = \bar{\mathbf{S}}_{1:k-1,k} + \bar{\mathbf{T}}_{1:k-1,k} \bar{\mathbf{S}}_{kk} + \Delta \bar{\mathbf{R}}_{1:k-1,k}, \quad (48)$$

$$\|\Delta \bar{\mathbf{R}}_{1:k-1,k}\| \leq \mathcal{O}(\varepsilon) \|\mathbf{X}_k\|; \text{ and}$$

$$\bar{\mathbf{R}}_{kk} = \bar{\mathbf{T}}_{kk} \bar{\mathbf{S}}_{kk} + \Delta \bar{\mathbf{R}}_{kk}, \quad \|\Delta \bar{\mathbf{R}}_{kk}\| \leq \mathcal{O}(\varepsilon) \|\mathbf{X}_k\|. \quad (49)$$

Proof. Similarly to (30) and (31) in the proof of Lemma 4, it is easy to verify (41), (42), and

$$\bar{\mathcal{T}}_{1:k-1,k} = \bar{\mathcal{Q}}_{k-1}^T \bar{\mathcal{U}}_k + \Delta \bar{\mathcal{T}}_{1:k-1,k}, \quad \|\Delta \bar{\mathcal{T}}_{1:k-1,k}\| \leq \mathcal{O}(\varepsilon) \|\bar{\mathcal{U}}_k\|, \quad (50)$$

$$\bar{\mathcal{Q}}_k \bar{\mathcal{T}}_{kk} = \bar{\mathcal{H}}_k + \Delta \bar{\mathcal{H}}_k, \quad \|\Delta \bar{\mathcal{H}}_k\| \leq \mathcal{O}(\varepsilon) \|\bar{\mathcal{U}}_k\|. \quad (51)$$

By the assumption on IO_1 and by applying Lemma 3 and (31), we have

$$\|I - \bar{\mathcal{U}}_k^T \bar{\mathcal{U}}_k\| \leq \mathcal{O}(\varepsilon) \kappa^{\alpha_1}(\bar{\mathcal{V}}_k) \leq \mathcal{O}(\varepsilon) \kappa^{\alpha_1}(\tilde{\mathcal{V}}_k) \leq \mathcal{O}(\varepsilon) \kappa^{\alpha_1}(\mathcal{X}_k). \quad (52)$$

Furthermore, $\|\bar{\mathcal{U}}_k\| \leq 1 + \mathcal{O}(\varepsilon) \kappa^{\alpha_1}(\mathcal{X}_k)$ and $\sigma_{\min}(\bar{\mathcal{U}}_k) \geq 1 - \mathcal{O}(\varepsilon) \kappa^{\alpha_1}(\mathcal{X}_k)$. Combining this with (50) and (51), we bound $\|\Delta \bar{\mathcal{T}}_{1:k-1,k}\|$ and $\|\Delta \bar{\mathcal{H}}_k\|$ to obtain (45) and (46).

Next, we aim to bound $\|\mathcal{X}_k\| \|\bar{\mathcal{S}}_{kk}^{-1}\|$ and therefore need to analyze the relationship between $\|\bar{\mathcal{S}}_{kk}^{-1}\|$ and $\sigma_{\min}(\mathcal{X}_k)$. By (42) and Lemma 2, $\|\bar{\mathcal{S}}_{kk}^{-1}\|$ can be bounded as follows:

$$\|\bar{\mathcal{S}}_{kk}^{-1}\| \leq \frac{\|\bar{\mathcal{U}}_k\|}{\sigma_{\min}(\tilde{\mathcal{V}}_k) - \|\Delta \tilde{\mathcal{V}}_k\|} \leq \frac{1 + \mathcal{O}(\varepsilon) \kappa^{\alpha_1}(\mathcal{X}_k)}{\sigma_{\min}(\tilde{\mathcal{V}}_k) - \mathcal{O}(\varepsilon) \|\mathcal{X}_k\|}. \quad (53)$$

Together with the assumption (40) and the following implication of Lemma 3,

$$\sigma_{\min}(\tilde{\mathcal{V}}_k) \geq \sigma_{\min}(\mathcal{X}_k) - \rho_{k-1} \kappa(\mathcal{X}_k), \quad (54)$$

we bound $\|\mathcal{X}_k\| \|\bar{\mathcal{S}}_{kk}^{-1}\|$ as follows:

$$\begin{aligned} \|\mathcal{X}_k\| \|\bar{\mathcal{S}}_{kk}^{-1}\| &\leq \frac{\|\mathcal{X}_k\|}{\sigma_{\min}(\mathcal{X}_k) - \mathcal{O}(\varepsilon) \|\mathcal{X}_k\| - \rho_{k-1} \|\mathcal{X}_{k-1}\|} \\ &\leq \frac{\kappa(\mathcal{X}_k)}{1 - \mathcal{O}(\varepsilon) \kappa(\mathcal{X}_k) - \rho_{k-1} \kappa(\mathcal{X}_k)} \\ &\leq 2\kappa(\mathcal{X}_k). \end{aligned} \quad (55)$$

Now we seek a tighter bound on the LOO of $\bar{\mathcal{Q}}_k$. Recall the definition of $\bar{\mathcal{H}}_k$ (from this lemma's assumptions), and combine (43) with the assumption (40) to obtain

$$\begin{aligned} \bar{\mathcal{H}}_k &= (I - \bar{\mathcal{Q}}_{k-1} \bar{\mathcal{Q}}_{k-1}^T) \bar{\mathcal{U}}_k + \Delta \bar{\mathcal{H}}_k = \tilde{\mathcal{H}}_k + \Delta \bar{\mathcal{H}}_k, \\ \|\Delta \bar{\mathcal{H}}_k\| &\leq \mathcal{O}(\varepsilon) \|\bar{\mathcal{U}}_k\| \leq \mathcal{O}(\varepsilon). \end{aligned} \quad (56)$$

Combining (56) with the assumption on IO_2 , we have

$$\|I - \bar{\mathcal{Q}}_k^T \bar{\mathcal{Q}}_k\| \leq \mathcal{O}(\varepsilon) \kappa^{\alpha_2}(\bar{\mathcal{H}}_k) \leq \mathcal{O}(\varepsilon) \kappa^{\alpha_2}(\tilde{\mathcal{H}}_k). \quad (57)$$

By the definitions of $\tilde{\mathcal{V}}_k$ and $\tilde{\mathcal{H}}_k$, as well as (42), we find that

$$\begin{aligned} \sigma_{\min}(\tilde{\mathcal{H}}_k) &= \sigma_{\min} \left(\bar{\mathcal{U}}_k - \bar{\mathcal{Q}}_{k-1} \bar{\mathcal{Q}}_{k-1}^T (\tilde{\mathcal{V}}_k + \Delta \tilde{\mathcal{V}}_k) \bar{\mathcal{S}}_{kk}^{-1} \right) \\ &= \sigma_{\min} \left(\bar{\mathcal{U}}_k - \bar{\mathcal{Q}}_{k-1} (\bar{\mathcal{Q}}_{k-1}^T \bar{\mathcal{Q}}_{k-1} - I) \bar{\mathcal{Q}}_{k-1}^T \mathcal{X}_k \bar{\mathcal{S}}_{kk}^{-1} - \bar{\mathcal{Q}}_{k-1} \bar{\mathcal{Q}}_{k-1}^T \Delta \tilde{\mathcal{V}}_k \bar{\mathcal{S}}_{kk}^{-1} \right) \\ &\geq \sigma_{\min}(\bar{\mathcal{U}}_k) - \left\| \bar{\mathcal{Q}}_{k-1} (\bar{\mathcal{Q}}_{k-1}^T \bar{\mathcal{Q}}_{k-1} - I) \bar{\mathcal{Q}}_{k-1}^T \mathcal{X}_k \bar{\mathcal{S}}_{kk}^{-1} + \bar{\mathcal{Q}}_{k-1} \bar{\mathcal{Q}}_{k-1}^T \Delta \tilde{\mathcal{V}}_k \bar{\mathcal{S}}_{kk}^{-1} \right\| \\ &\geq \sigma_{\min}(\bar{\mathcal{U}}_k) - (\omega_{k-1} + \mathcal{O}(\varepsilon)) (1 + \omega_{k-1})^2 \|\mathcal{X}_k\| \|\bar{\mathcal{S}}_{kk}^{-1}\| \\ &\geq \sigma_{\min}(\bar{\mathcal{U}}_k) - 2(\omega_{k-1} + \mathcal{O}(\varepsilon)) (1 + \omega_{k-1})^2 \kappa(\mathcal{X}_k). \end{aligned} \quad (58)$$

Furthermore, together with

$$\|\tilde{\mathcal{H}}_k\| \leq \sqrt{m} (1 + \omega_{k-1}) \|\bar{\mathcal{U}}_k\| \leq \sqrt{m} (1 + \omega_{k-1}) (1 + \mathcal{O}(\varepsilon) \kappa^{\alpha_1}(\mathcal{X}_k)), \quad (59)$$

it follows that

$$\begin{aligned} \|I - \bar{\mathbf{Q}}_k^T \bar{\mathbf{Q}}_k\| &\leq \mathcal{O}(\varepsilon) \left(\frac{\sqrt{m}(1 + \omega_{k-1})(1 + \mathcal{O}(\varepsilon) \kappa^{\alpha_1}(\mathcal{X}_k))}{\sigma_{\min}(\bar{\mathbf{U}}_k) - 2(\omega_{k-1} + \mathcal{O}(\varepsilon))(1 + \omega_{k-1})^2 \kappa(\mathcal{X}_k)} \right)^{\alpha_2} \\ &\leq \mathcal{O}(\varepsilon) \left(\frac{\sqrt{m}(1 + \omega_{k-1})(1 + \mathcal{O}(\varepsilon) \kappa^{\alpha_1}(\mathcal{X}_k))}{1 - \mathcal{O}(\varepsilon) \kappa^{\alpha_1}(\mathcal{X}_k) - 2(\omega_{k-1} + \mathcal{O}(\varepsilon))(1 + \omega_{k-1})^2 \kappa(\mathcal{X}_k)} \right)^{\alpha_2} \\ &\leq \mathcal{O}(\varepsilon). \end{aligned} \quad (60)$$

A simple floating-point analysis on (41), (42), and (45) leads to (48). Similarly, the bound on $\|\Delta \bar{R}_{kk}\|$ can be obtained by combining (41) and (42) with (46) and (59). \square

We are now prepared to analyze the behavior of the k th inner loop of **BCGSI+A**.

Lemma 7. *Assume that $\bar{\mathbf{Q}}_{k-1}$ satisfies $\|I - \bar{\mathbf{Q}}_{k-1}^T \bar{\mathbf{Q}}_{k-1}\| \leq \omega_{k-1}$ and for all $\mathbf{X} \in \mathbb{R}^{m \times s}$ with $\kappa(\mathbf{X}) \leq \kappa(\mathcal{X})$, the following hold for $[\bar{\mathbf{Q}}, \bar{\mathbf{R}}] = \mathbf{IO}_1(\mathbf{X})$:*

$$\begin{aligned} \mathbf{X} + \Delta \mathbf{X} &= \bar{\mathbf{Q}} \bar{\mathbf{R}}, \quad \|\Delta \mathbf{X}\| \leq \mathcal{O}(\varepsilon) \|\mathbf{X}\|, \\ \|I - \bar{\mathbf{Q}}^T \bar{\mathbf{Q}}\| &\leq \mathcal{O}(\varepsilon) \kappa^{\alpha_1}(\mathbf{X}). \end{aligned}$$

Similarly, assume the following hold for $[\bar{\mathbf{Q}}, \bar{\mathbf{R}}] = \mathbf{IO}_2(\mathbf{X})$:

$$\begin{aligned} \mathbf{X} + \Delta \mathbf{X} &= \bar{\mathbf{Q}} \bar{\mathbf{R}}, \quad \|\Delta \mathbf{X}\| \leq \mathcal{O}(\varepsilon) \|\mathbf{X}\|, \\ \|I - \bar{\mathbf{Q}}^T \bar{\mathbf{Q}}\| &\leq \mathcal{O}(\varepsilon) \kappa^{\alpha_2}(\mathbf{X}). \end{aligned}$$

Furthermore, if

$$\mathbf{x}_{k-1} + \Delta \mathbf{x}_{k-1} = \bar{\mathbf{Q}}_{k-1} \bar{\mathbf{R}}_{k-1}, \quad \|\Delta \mathbf{x}_{k-1}\| \leq \rho_{k-1} \|\mathbf{x}_{k-1}\|, \quad (61)$$

as well as (40) holds, then for the k th inner loop of Algorithm 2 with any $k \geq 2$,

$$\|I - \bar{\mathbf{Q}}_k^T \bar{\mathbf{Q}}_k\| \leq \omega_{k-1} + 2\omega_{k-1}(1 + \omega_{k-1})(\omega_{k-1} + \mathcal{O}(\varepsilon)) \kappa(\mathcal{X}_k) + \mathcal{O}(\varepsilon).$$

Proof. We apply Lemma 6 to bound $\|\bar{\mathbf{Q}}_{k-1}^T \bar{\mathbf{Q}}_k\|$ as follows:

$$\begin{aligned} \|\bar{\mathbf{Q}}_{k-1}^T \bar{\mathbf{Q}}_k\| &\leq \|\bar{\mathbf{Q}}_{k-1}^T \tilde{\mathbf{H}}_k \bar{T}_{kk}^{-1}\| + \|\bar{\mathbf{Q}}_{k-1}^T \Delta \tilde{\mathbf{H}}_k \bar{T}_{kk}^{-1}\| \\ &\leq \|\bar{\mathbf{Q}}_{k-1}^T (I - \bar{\mathbf{Q}}_{k-1} \bar{\mathbf{Q}}_{k-1}^T) \bar{\mathbf{U}}_k \bar{T}_{kk}^{-1}\| + \|\bar{\mathbf{Q}}_{k-1}^T \Delta \tilde{\mathbf{H}}_k \bar{T}_{kk}^{-1}\| \\ &\leq \omega_{k-1} \|\bar{\mathbf{Q}}_{k-1}^T \bar{\mathbf{U}}_k \bar{T}_{kk}^{-1}\| + \|\bar{\mathbf{Q}}_{k-1}^T \Delta \tilde{\mathbf{H}}_k \bar{T}_{kk}^{-1}\| \\ &\leq \omega_{k-1} \left(\|\bar{\mathbf{Q}}_{k-1}^T \tilde{\mathbf{V}}_k \bar{S}_{kk}^{-1} \bar{T}_{kk}^{-1}\| + \|\bar{\mathbf{Q}}_{k-1}^T \Delta \tilde{\mathbf{V}}_k \bar{S}_{kk}^{-1} \bar{T}_{kk}^{-1}\| \right) \\ &\quad + \|\bar{\mathbf{Q}}_{k-1}^T \Delta \tilde{\mathbf{H}}_k \bar{T}_{kk}^{-1}\| \\ &\leq \omega_{k-1} \|\bar{\mathbf{Q}}_{k-1}^T (I - \bar{\mathbf{Q}}_{k-1} \bar{\mathbf{Q}}_{k-1}^T) \mathbf{X}_k \bar{S}_{kk}^{-1} \bar{T}_{kk}^{-1}\| \\ &\quad + \omega_{k-1} \|\bar{\mathbf{Q}}_{k-1}^T \Delta \tilde{\mathbf{V}}_k \bar{S}_{kk}^{-1} \bar{T}_{kk}^{-1}\| + \|\bar{\mathbf{Q}}_{k-1}^T \Delta \tilde{\mathbf{H}}_k \bar{T}_{kk}^{-1}\| \\ &\leq \omega_{k-1}^2 \|\bar{\mathbf{Q}}_{k-1}^T \mathbf{X}_k \bar{S}_{kk}^{-1} \bar{T}_{kk}^{-1}\| \\ &\quad + \omega_{k-1} \|\bar{\mathbf{Q}}_{k-1}^T \Delta \tilde{\mathbf{V}}_k \bar{S}_{kk}^{-1} \bar{T}_{kk}^{-1}\| + \|\bar{\mathbf{Q}}_{k-1}^T \Delta \tilde{\mathbf{H}}_k \bar{T}_{kk}^{-1}\| \\ &\leq \omega_{k-1} (1 + \omega_{k-1}) (\omega_{k-1} + \mathcal{O}(\varepsilon)) \|\mathbf{X}_k\| \|\bar{S}_{kk}^{-1}\| \|\bar{T}_{kk}^{-1}\| \\ &\quad + (1 + \omega_{k-1}) \mathcal{O}(\varepsilon) (1 + \mathcal{O}(\varepsilon) \kappa^{\alpha_1}(\mathcal{X}_k)) \|\bar{T}_{kk}^{-1}\|. \end{aligned} \quad (62)$$

By Lemma 2, (46), (47), and (58), we have

$$\begin{aligned} \|\bar{T}_{kk}^{-1}\| &\leq \frac{\|\bar{\mathbf{Q}}_k\|}{\sigma_{\min}(\bar{\mathbf{H}}_k) - \mathcal{O}(\varepsilon)(1 + \mathcal{O}(\varepsilon)\kappa^{\alpha_1}(\mathcal{X}_k))} \\ &\leq \frac{1 + \mathcal{O}(\varepsilon)}{1 - \mathcal{O}(\varepsilon)\kappa^{\alpha_1}(\mathcal{X}_k) - 2(\omega_{k-1} + \mathcal{O}(\varepsilon))(1 + \omega_{k-1})^2\kappa(\mathcal{X}_k)} \\ &\leq 2 + \mathcal{O}(\varepsilon). \end{aligned}$$

Combining this with (55) proved in Lemma 6, we bound $\|\bar{\mathbf{Q}}_{k-1}^T \bar{\mathbf{Q}}_k\|$. Finally, we conclude the proof because of

$$\|I - \bar{\mathbf{Q}}_k^T \bar{\mathbf{Q}}_k\| \leq \|I - \bar{\mathbf{Q}}_{k-1}^T \bar{\mathbf{Q}}_{k-1}\| + 2\|\bar{\mathbf{Q}}_{k-1}^T \bar{\mathbf{Q}}_k\| + \|I - \bar{\mathbf{Q}}_k^T \bar{\mathbf{Q}}_k\|.$$

and (47). \square

By induction on k , we achieve following theorem to show the LOO of **BCGSI+A**.

Theorem 2. Let $\bar{\mathbf{Q}}$ and $\bar{\mathbf{R}}$ denote the computed results of Algorithm 2. Assume that for all $\mathbf{X} \in \mathbb{R}^{m \times s}$ with $\kappa(\mathbf{X}) \leq \kappa(\mathcal{X})$, the following hold for $[\bar{\mathbf{Q}}, \bar{\mathbf{R}}] = \mathbf{IO}_A(\mathbf{X})$:

$$\begin{aligned} \mathbf{X} + \Delta\mathbf{X} &= \bar{\mathbf{Q}}\bar{\mathbf{R}}, \quad \|\Delta\mathbf{X}\| \leq \mathcal{O}(\varepsilon)\|\mathbf{X}\|, \\ \|I - \bar{\mathbf{Q}}^T \bar{\mathbf{Q}}\| &\leq \mathcal{O}(\varepsilon). \end{aligned}$$

Likewise, assume the following hold for $[\bar{\mathbf{Q}}, \bar{\mathbf{R}}] = \mathbf{IO}_1(\mathbf{X})$ and $[\bar{\mathbf{Q}}, \bar{\mathbf{R}}] = \mathbf{IO}_2(\mathbf{X})$, respectively:

$$\begin{aligned} \mathbf{X} + \Delta\mathbf{X} &= \bar{\mathbf{Q}}\bar{\mathbf{R}}, \quad \|\Delta\mathbf{X}\| \leq \mathcal{O}(\varepsilon)\|\mathbf{X}\|, \\ \|I - \bar{\mathbf{Q}}^T \bar{\mathbf{Q}}\| &\leq \mathcal{O}(\varepsilon)\kappa^{\alpha_1}(\mathbf{X}); \end{aligned}$$

and

$$\begin{aligned} \mathbf{X} + \Delta\mathbf{X} &= \bar{\mathbf{Q}}\bar{\mathbf{R}}, \quad \|\Delta\mathbf{X}\| \leq \mathcal{O}(\varepsilon)\|\mathbf{X}\|, \\ \|I - \bar{\mathbf{Q}}^T \bar{\mathbf{Q}}\| &\leq \mathcal{O}(\varepsilon)\kappa^{\alpha_2}(\mathbf{X}). \end{aligned}$$

If $\mathcal{O}(\varepsilon)\kappa^\theta(\mathcal{X}) < 1$ for $\theta := \max(\alpha_1, 1)$ is satisfied, then

$$\mathcal{X} + \Delta\mathcal{X} = \bar{\mathbf{Q}}\bar{\mathbf{R}}, \quad \|\Delta\mathcal{X}\| \leq \mathcal{O}(\varepsilon)\|\mathcal{X}\|, \quad (63)$$

and

$$\|I - \bar{\mathbf{Q}}^T \bar{\mathbf{Q}}\| \leq \mathcal{O}(\varepsilon). \quad (64)$$

Proof. By the assumption of \mathbf{IO}_A , we have $\|I - \bar{\mathbf{Q}}_1^T \bar{\mathbf{Q}}_1\| \leq \mathcal{O}(\varepsilon)$. Then we can draw the conclusion by induction on k followed by Lemma 7 if the residual bound (63) can be satisfied.

The assumptions of \mathbf{IO}_A directly give the base case. Assume that $\mathcal{X}_{k-1} + \Delta\mathcal{X}_{k-1} = \bar{\mathbf{Q}}_{k-1}\bar{\mathbf{R}}_{k-1}$ with $\|\Delta\mathcal{X}_{k-1}\| \leq \mathcal{O}(\varepsilon)\|\mathcal{X}_{k-1}\|$. Then our aim is to prove that it holds for k . By Lemma 6, we

have

$$\begin{aligned}
& \bar{\mathbf{Q}}_{k-1} \bar{\mathcal{R}}_{1:k-1,k} + \bar{\mathbf{Q}}_k \bar{R}_{kk} \\
&= \bar{\mathbf{Q}}_{k-1} \left(\bar{\mathbf{Q}}_{k-1}^T \mathbf{X}_k + \Delta \bar{\mathcal{S}}_{1:k-1,k} + (\bar{\mathbf{Q}}_{k-1}^T \bar{\mathbf{U}}_k + \Delta \bar{\mathcal{T}}_{1:k-1,k}) \bar{S}_{kk} + \Delta \bar{\mathcal{R}}_{1:k-1,k} \right) \\
&\quad + \bar{\mathbf{Q}}_k (\bar{T}_{kk} \bar{S}_{kk} + \Delta \bar{R}_{kk}) \\
&= \bar{\mathbf{Q}}_{k-1} \left(\bar{\mathbf{Q}}_{k-1}^T \mathbf{X}_k + \Delta \bar{\mathcal{S}}_{1:k-1,k} + (\bar{\mathbf{Q}}_{k-1}^T \bar{\mathbf{U}}_k + \Delta \bar{\mathcal{T}}_{1:k-1,k}) \bar{S}_{kk} + \Delta \bar{\mathcal{R}}_{1:k-1,k} \right) \\
&\quad + (\tilde{\mathbf{H}}_k + \Delta \tilde{\mathbf{H}}_k) \bar{S}_{kk} + \bar{\mathbf{Q}}_k \Delta \bar{R}_{kk} \\
&= \bar{\mathbf{Q}}_{k-1} \left(\bar{\mathbf{Q}}_{k-1}^T \mathbf{X}_k + \Delta \bar{\mathcal{S}}_{1:k-1,k} + (\bar{\mathbf{Q}}_{k-1}^T \bar{\mathbf{U}}_k + \Delta \bar{\mathcal{T}}_{1:k-1,k}) \bar{S}_{kk} + \Delta \bar{\mathcal{R}}_{1:k-1,k} \right) \\
&\quad + ((I - \bar{\mathbf{Q}}_{k-1} \bar{\mathbf{Q}}_{k-1}^T) \bar{\mathbf{U}}_k + \Delta \tilde{\mathbf{H}}_k) \bar{S}_{kk} + \bar{\mathbf{Q}}_k \Delta \bar{R}_{kk} \\
&= \bar{\mathbf{Q}}_{k-1} \left(\bar{\mathbf{Q}}_{k-1}^T \mathbf{X}_k + \Delta \bar{\mathcal{S}}_{1:k-1,k} + \Delta \bar{\mathcal{T}}_{1:k-1,k} \bar{S}_{kk} + \Delta \bar{\mathcal{R}}_{1:k-1,k} \right) + (\bar{\mathbf{U}}_k + \Delta \tilde{\mathbf{H}}_k) \bar{S}_{kk} \\
&\quad + \bar{\mathbf{Q}}_k \Delta \bar{R}_{kk} \\
&= \bar{\mathbf{Q}}_{k-1} \bar{\mathbf{Q}}_{k-1}^T \mathbf{X}_k + \tilde{\mathbf{V}}_k + \Delta \tilde{\mathbf{V}}_k + \Delta \tilde{\mathbf{H}}_k \bar{S}_{kk} + \bar{\mathbf{Q}}_k \Delta \bar{R}_{kk} + \bar{\mathbf{Q}}_{k-1} \Delta \bar{\mathcal{S}}_{1:k-1,k} \\
&\quad + \bar{\mathbf{Q}}_{k-1} \Delta \bar{\mathcal{T}}_{1:k-1,k} \bar{S}_{kk} + \bar{\mathbf{Q}}_{k-1} \Delta \bar{\mathcal{R}}_{1:k-1,k} \\
&= \mathbf{X}_k + \Delta \tilde{\mathbf{V}}_k + \Delta \tilde{\mathbf{H}}_k \bar{S}_{kk} + \bar{\mathbf{Q}}_k \Delta \bar{R}_{kk} + \bar{\mathbf{Q}}_{k-1} \Delta \bar{\mathcal{S}}_{1:k-1,k} + \bar{\mathbf{Q}}_{k-1} \Delta \bar{\mathcal{T}}_{1:k-1,k} \bar{S}_{kk} \\
&\quad + \bar{\mathbf{Q}}_{k-1} \Delta \bar{\mathcal{R}}_{1:k-1,k}.
\end{aligned} \tag{65}$$

Let

$$\begin{aligned}
\Delta \mathbf{X}_k &= \Delta \tilde{\mathbf{V}}_k + \Delta \tilde{\mathbf{H}}_k \bar{S}_{kk} + \bar{\mathbf{Q}}_k \Delta \bar{R}_{kk} + \bar{\mathbf{Q}}_{k-1} \Delta \bar{\mathcal{S}}_{1:k-1,k} \\
&\quad + \bar{\mathbf{Q}}_{k-1} \Delta \bar{\mathcal{T}}_{1:k-1,k} \bar{S}_{kk} + \bar{\mathbf{Q}}_{k-1} \Delta \bar{\mathcal{R}}_{1:k-1,k}.
\end{aligned}$$

Then can we conclude the proof of the residual because

$$\begin{aligned}
\boldsymbol{\mathcal{X}}_k + \Delta \boldsymbol{\mathcal{X}}_k &= [\boldsymbol{\mathcal{X}}_{k-1} + \Delta \boldsymbol{\mathcal{X}}_{k-1} \quad \mathbf{X}_k + \Delta \mathbf{X}_k] \\
&= [\bar{\mathbf{Q}}_{k-1} \bar{\mathcal{R}}_{k-1} \quad \bar{\mathbf{Q}}_{k-1} \bar{\mathcal{R}}_{1:k-1,k} + \bar{\mathbf{Q}}_k \bar{R}_{kk}]
\end{aligned}$$

with

$$\|\Delta \boldsymbol{\mathcal{X}}_k\| \leq \mathcal{O}(\varepsilon) \|\boldsymbol{\mathcal{X}}_{k-1}\| + \mathcal{O}(\varepsilon) \|\mathbf{X}_k\| \leq \mathcal{O}(\varepsilon) \|\boldsymbol{\mathcal{X}}_k\|.$$

Next we aim to prove the LOO using Lemma 7. The assumptions of IO_A directly give the base case for the LOO, i.e., $\omega_1 \leq \mathcal{O}(\varepsilon)$. Assume that $\omega_{k-1} \leq \mathcal{O}(\varepsilon)$. Then we obtain that (40) holds. Using Lemma 7 and the assumption of IO_1 and IO_2 we conclude the proof because

$$\left\| I - \bar{\mathbf{Q}}_k^T \bar{\mathbf{Q}}_k \right\| \leq \omega_{k-1} + \mathcal{O}(1) \omega_{k-1}^2 \kappa(\boldsymbol{\mathcal{X}}_k) + \mathcal{O}(\varepsilon) \leq \mathcal{O}(\varepsilon).$$

□

Theorem 2 reproduces the main result of [3], which analyzes **BCGSI+**, or equivalently **BCGSI+A** with $\text{IO}_A = \text{IO}_1 = \text{IO}_2$ in our nomenclature. Barlow and Smoktunowicz require that all IOs be as stable as **HouseQR**. In contrast, Theorem 2 shows that the choice of IO_2 has no effect on the LOO of **BCGSI+A**, while IO_1 only limits the conditioning of $\boldsymbol{\mathcal{X}}$ for which we can guarantee $\mathcal{O}(\varepsilon)$ LOO. Recently, Barlow proved a similar result for special cases of **BCGSI+A**, where $\text{IO}_A = \text{HouseQR}$, IO_1 is either **HouseQR** or a reorthogonalized **CholQR**, and $\text{IO}_2 = \text{CholQR}$ [2]. Indeed, Theorem 2 generalizes [2] and reveals additional possibilities that would further reduce the number of sync points. Consider, for example, **BCGSI+A** with $\text{IO}_A = \text{IO}_1 = \text{TSQR}$ and $\text{IO}_2 = \text{CholQR}$. Such an algorithm would only need 4 sync points per block column, as all IOs need only one global communication, and still achieve $\mathcal{O}(\varepsilon)$ LOO without any additional restriction on $\kappa(\boldsymbol{\mathcal{X}})$.

Unfortunately, Theorem 2 cannot guarantee stability for **BCGSI+A** \circ **CholQR** (i.e., $\text{IO}_1 = \text{IO}_2 = \text{CholQR}$) when $\kappa(\boldsymbol{\mathcal{X}}) > \frac{1}{\sqrt{\varepsilon}} \approx 10^8$, because then $\theta = 2$. Figure 3 shows **BCGSI+A** \circ **CholQR** deviating from $\mathcal{O}(\varepsilon)$ after $\kappa(\boldsymbol{\mathcal{X}}) > 10^8$ for a class of **piled**⁵ matrices, which are designed to highlight such

⁵Formed as $\boldsymbol{\mathcal{X}} = [\mathbf{X}_1 \quad \mathbf{X}_2 \quad \dots \quad \mathbf{X}_p]$, where \mathbf{X}_1 has small condition number and for $k \in \{2, \dots, p\}$, $\mathbf{X}_k = \mathbf{X}_{k-1} + \mathbf{Z}_k$, where each \mathbf{Z}_k has the same condition number for all k . Toggling the condition numbers of \mathbf{X}_1 and $\{\mathbf{Z}_k\}_{k=2}^p$ controls the overall conditioning of the test matrix.

edge-case behavior. At the same time, the LOO for $\text{BCGSI+} \circ \text{CholQR}$ is even more extreme; cf. Figure 2 as well. Practically speaking, if the application can tolerate $\kappa(\mathcal{X}) \leq 10^8$, $\text{BCGSI+A} \circ \text{CholQR}$ would be the superior algorithm here, as CholQR only requires one sync point per block vector.

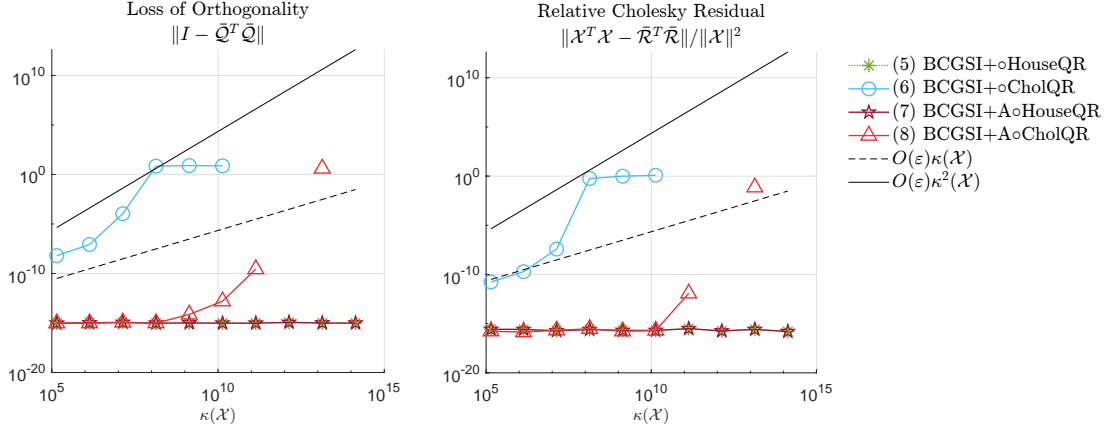


Figure 3: Comparison between BCGSI+ (i.e., Algorithm 2 with all IOs equal) and BCGSI+A ($\text{IO}_A = \text{HouseQR}$ and $\text{IO}_1 = \text{IO}_2$) on a class of piled matrices.

3 Derivation of a one-sync, reorthogonalized, block Gram-Schmidt method

BCGSI+ and its counterpart BCGSI+A both require 4 sync points per iteration, which is a disadvantage compared to BCGS/BCGS-A , which can have demonstrably worse LOO than $\mathcal{O}(\varepsilon) \kappa^2(\mathcal{X})$. Ideally, we would like to reduce the sync points to 2 or even 1 per iteration while keeping a small LOO. DCGS2 from [4] boasts both 1 sync point per column as well as $\mathcal{O}(\varepsilon)$ LOO, at least according to their numerical experiments. With an eye towards achieving 1 sync point per block column, we will generalize and adapt their derivation, starting from BCGSI+A . We note that BCGSI+A-3S and BCGSI+A-2S are considered to be intermediate steps towards the derivation of BCGSI+A-1S and its theory. This section aims to show how to achieve a one-sync algorithm using the four-sync approach and to illustrate the impact of reducing each sync point on stability. Unfortunately, BCGSI+A-1S has instability issues when $s > 1$, that is, its LOO is affected by the square of the condition number, as will be shown in Section 4. Consequently, this block variant (and thus the equivalent block variant proposed in [25, Figure 3]) is not the best choice for practical for use. We note that the deficiencies of this variant motivated the development of a stable one-sync variant in [9].

We can eliminate one sync point by skipping the first normalization step, denoted as $k.1.2$ in BCGSI+A ; consequently, we drop the distinction between IO_1 and IO_2 . This leads to BCGSI+A-3S , summarized as Algorithm 3; note again the three colors for each phase. Despite the small change—after all, BCGSI+A-3S still projects the basis twice and normalizes the projected block vector in step $k.2.2$ —the effect on the stability behavior is notable. Figure 4 demonstrates a small LOO when HouseQR is the IO and up to $\mathcal{O}(\varepsilon) \kappa^2(\mathcal{X})$ for when $\text{IO} = \text{CholQR}$. Furthermore, the relative Cholesky residual of BCGSI+A-3S begins to increase as well. $\text{BCGSI+A-3S} \circ \text{CholQR}$ in particular cannot handle $\kappa(\mathcal{X}) > \mathcal{O}\left(\frac{1}{\sqrt{\varepsilon}}\right)$, due to the Cholesky subroutine being applied to negative semidefinite matrices at some point.

BCGSI+A-3S can also be interpreted as a generalization of the “continuous projection” approach introduced in [26] as BCGS-CP . The only real difference is that we allow for `stable_qr` (i.e., the choice of IO) to differ between the first and subsequent steps, thus adding a little extra flexibility. Zou does not carry out a floating-point analysis of BCGS-CP , which we do in Section 4.1

By fixing the IO to be CholQR for iterations 2 through p and batching the inner products, we

Algorithm 3 $[\mathcal{Q}, \mathcal{R}] = \text{BCGSI+A-3S}(\mathcal{X}, \text{IO}_A, \text{IO})$

- 1: Allocate memory for \mathcal{Q}, \mathcal{R}
 - 2: $[\mathcal{Q}_1, R_{11}] = \text{IO}_A(\mathbf{X}_1)$
 - 3: **for** $k = 2, \dots, p$ **do**
 - 4: $\mathcal{S}_{1:k-1,k} = \mathcal{Q}_{k-1}^T \mathbf{X}_k$ ▷ step k.1.1 – first projection
 - 5: $\mathbf{V}_k = \mathbf{X}_k - \mathcal{Q}_{k-1} \mathcal{S}_{1:k-1,k}$ ▷ **step k.1.2' – skip normalization**
 - 6: $\mathcal{Y}_{1:k-1,k} = \mathcal{Q}_{k-1}^T \mathbf{V}_k$ ▷ step k.2.1 – second projection
 - 7: $[\mathcal{Q}_k, Y_{kk}] = \text{IO}(\mathbf{V}_k - \mathcal{Q}_{k-1} \mathcal{Y}_{1:k-1,k})$ ▷ step k.2.2 – second normalization
 - 8: $\mathcal{R}_{1:k-1,k} = \mathcal{S}_{1:k-1,k} + \mathcal{Y}_{1:k-1,k}$ ▷ step k.3.1 – form upper \mathcal{R} column
 - 9: $R_{kk} = Y_{kk}$ ▷ step k.3.2 – form \mathcal{R} diagonal entry
 - 10: **end for**
 - 11: **return** $\mathcal{Q} = [\mathcal{Q}_1, \dots, \mathcal{Q}_p], \mathcal{R} = (R_{ij})$
-

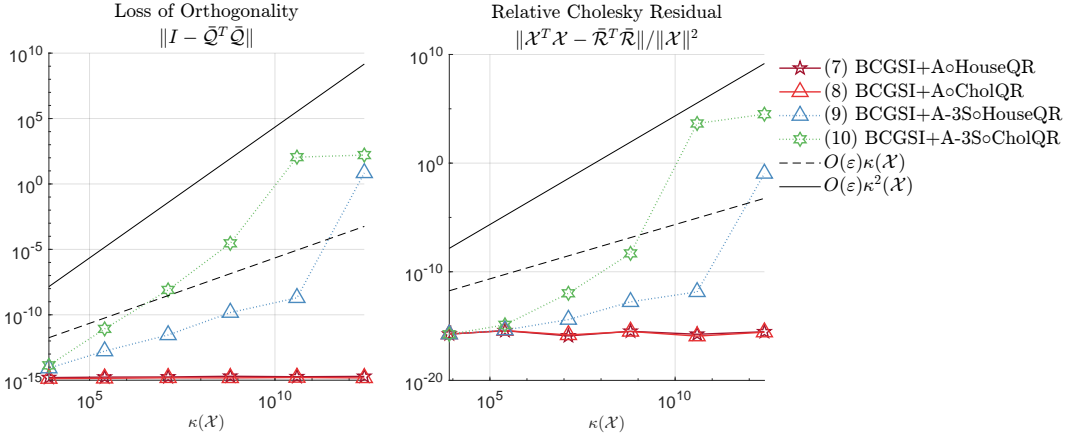


Figure 4: Comparison between **BCGSI+A** and **BCGSI+A-3S** on a class of monomial matrices. Note that IO_A is fixed as HouseQR, and $\text{IO} = \text{IO}_1 = \text{IO}_2$.

arrive at a 2-sync method, **BCGSI+A-2S**, displayed in Algorithm 4. The block Pythagorean theorem (cf. [7]) could also be used to derive this step, but we take a more straightforward approach here by just expanding the inner product implicit in $[\mathbf{Q}_k, Y_{kk}] = \text{CholQR}(\mathbf{V}_k - \mathbf{Q}_{k-1}\mathcal{Y}_{1:k-1,k})$ (and keeping in mind that we're still working in exact arithmetic for the derivation). In particular, we find that

$$\begin{aligned} Y_{kk} &= \mathbf{V}_k^T \mathbf{V}_k - \underbrace{\mathbf{V}_k^T \mathbf{Q}_{k-1}}_{=\mathcal{Y}_{1:k-1,k}^T} \mathcal{Y}_{1:k-1,k} - \mathcal{Y}_{1:k-1,k}^T \underbrace{\mathbf{Q}_{k-1}^T \mathbf{V}_k}_{=\mathcal{Y}_{1:k-1,k}} + \mathcal{Y}_{1:k-1,k}^T \underbrace{\mathbf{Q}_{k-1}^T \mathbf{Q}_{k-1}}_{=I} \mathcal{Y}_{1:k-1,k} \\ &= \underbrace{\mathbf{V}_k^T \mathbf{V}_k}_{=\Omega_k} - \mathcal{Y}_{1:k-1,k}^T \mathcal{Y}_{1:k-1,k} \end{aligned}$$

and $\mathbf{Q}_k = (\mathbf{V}_k - \mathbf{Q}_{k-1}\mathcal{Y}_{1:k-1,k}) Y_{kk}^{-1}$.

We assume that batching itself introduces only $\mathcal{O}(\varepsilon)$ errors for the matrix products, with the exact floating-point error depending on how the hardware and low-level libraries handle matrix-matrix multiplication. In which case, **BCGSI+A-2S** can be regarded as equivalent to **BCGSI+A-3S** \circ **CholQR** in floating-point error.

Algorithm 4 $[\mathbf{Q}, \mathcal{R}] = \text{BCGSI+A-2S}(\mathcal{X}, \text{IO}_A)$

```

1:  $[\mathbf{Q}_1, R_{11}] = \text{IO}_A(\mathbf{X}_1)$ 
2: for  $k = 2, \dots, p$  do
3:    $\mathcal{S}_{1:k-1,k} = \mathbf{Q}_{k-1}^T \mathbf{X}_k$  ▷ step k.1.1 – first projection
4:    $\mathbf{V}_k = \mathbf{X}_k - \mathbf{Q}_{k-1} \mathcal{S}_{1:k-1,k}$  ▷ step k.1.2' – skip normalization
5:    $\begin{bmatrix} \mathcal{Y}_{1:k-1,k} \\ \Omega_k \end{bmatrix} = [\mathbf{Q}_{k-1} \ \mathbf{V}_k]^T \mathbf{V}_k$  ▷ step k.2.1' – second projection, part of CholQR
6:    $Y_{kk} = \text{chol}(\Omega_k - \mathcal{Y}_{1:k-1,k}^T \mathcal{Y}_{1:k-1,k})$ 
7:    $\mathbf{Q}_k = (\mathbf{V}_k - \mathbf{Q}_{k-1} \mathcal{Y}_{1:k-1,k}) Y_{kk}^{-1}$  ▷ step k.2.2 – second normalization
8:    $\mathcal{R}_{1:k-1,k} = \mathcal{S}_{1:k-1,k} + \mathcal{Y}_{1:k-1,k}$  ▷ step k.3.1 – form upper  $\mathcal{R}$  column
9:    $R_{kk} = Y_{kk}$  ▷ step k.3.2 – form  $\mathcal{R}$  diagonal entry
10: end for
11: return  $\mathbf{Q} = [\mathbf{Q}_1, \dots, \mathbf{Q}_p], \mathcal{R} = (R_{ij})$ 

```

Deriving **BCGSI+A-1S** (Algorithm 5) from **BCGSI+A-2S** requires shifting the window over which the for-loop iterates. First, we bring out steps 2.1.1 and 2.1.2, which leaves \mathbf{V}_2 and \mathcal{S}_{12} to initialize the for-loop. We then batch all the inner products and define some intermediate quantities \mathbf{Z}_{k-1} and P_k . Consequently, we cannot compute $\mathcal{S}_{1:k,k+1}$ directly but rather have to reverse-engineer it from what has been computed in line 5:

$$\begin{aligned} \mathcal{S}_{1:k,k+1} &= \mathbf{Q}_k^T \mathbf{X}_{k+1} \\ &= [\mathbf{Q}_{k-1} \ \mathbf{Q}_k]^T \mathbf{X}_{k+1} \\ &= [\mathbf{Z}_{k-1} \ \mathbf{Q}_k^T \mathbf{X}_{k+1}] \end{aligned}$$

By line 7, we have \mathbf{Q}_k , but not its projection onto \mathbf{X}_{k+1} , which we cannot get until the next iteration. However, from the same line, we can compute $\mathbf{Q}_k^T \mathbf{X}_{k+1}$, as it is composed of pieces that can be pulled from line 5:

$$\mathbf{Q}_k^T \mathbf{X}_{k+1} = Y_{kk}^{-T} \left(\underbrace{\mathbf{V}_k^T \mathbf{X}_{k+1}}_{=P_k} - \mathcal{Y}_{1:k-1,k}^T \underbrace{\mathbf{Q}_{k-1}^T \mathbf{X}_{k+1}}_{=\mathbf{Z}_{k-1}} \right).$$

After the loop we have to complete the final step p . Interestingly, note that \mathcal{X} is no longer needed for the final inner product in line 13. We highlight again the colorful chaos of the pseudocode: it helps to illustrate what Bielich et al. [4] and Świrowdowicz et al. [22] called “lagging”, in the sense that “earlier” calculations in blue now take place after the “later” ones in red and purple within the for-loop.

A comparison of the 3-sync, 2-sync, and 1-sync variants is provided in Figure 5. **BCGSI+A-3S** remains under $\mathcal{O}(\varepsilon) \kappa^2(\mathcal{X})$, while both **BCGSI+A-2S** and **BCGSI+A-1S** explode dramatically once $\kappa(\mathcal{X}) > 10^9$.

Algorithm 5 $[\mathcal{Q}, \mathcal{R}] = \text{BCGSI+A-1S}(\mathcal{X}, \text{IO}_A)$

-
- 1: $[\mathcal{Q}_1, R_{11}] = \text{IO}_A(\mathbf{X}_1)$ ▷ Implicitly, initialize $S = I_{p_s}$
 - 2: $S_{12} = \mathcal{Q}_1^T \mathbf{X}_2$ ▷ step 2.1.1 – first projection
 - 3: $\mathbf{V}_2 = \mathbf{X}_2 - \mathcal{Q}_1 S_{12}$ ▷ step 2.1.2' – skip normalization
 - 4: **for** $k = 2, \dots, p-1$ **do**
 - 5: $\begin{bmatrix} \mathcal{Y}_{1:k-1,k} & \mathbf{Z}_{k-1} \\ \Omega_k & P_k \end{bmatrix} = [\mathcal{Q}_{k-1} \quad \mathbf{V}_k]^T [\mathbf{V}_k \quad \mathbf{X}_{k+1}]$ ▷ **step k.2.1', part of (k+1).1.1'**
 - 6: $Y_{kk} = \text{chol}(\Omega_k - \mathcal{Y}_{1:k-1,k}^T \mathcal{Y}_{1:k-1,k})$
 - 7: $\mathcal{Q}_k = (\mathbf{V}_k - \mathcal{Q}_{k-1} \mathcal{Y}_{1:k-1,k}) Y_{kk}^{-1}$ ▷ step k.2.2 – second normalization
 - 8: $\mathcal{R}_{1:k-1,k} = S_{1:k-1,k} + \mathcal{Y}_{1:k-1,k}$ ▷ step k.3.1 – form upper \mathcal{R} column
 - 9: $R_{kk} = Y_{kk}$ ▷ step k.3.2 – form \mathcal{R} diagonal entry
 - 10: $S_{1:k,k+1} = \begin{bmatrix} \mathbf{Z}_{k-1} \\ Y_{kk}^{-T} (P_k - \mathcal{Y}_{1:k-1,k}^T \mathbf{Z}_{k-1}) \end{bmatrix}$ ▷ **step (k+1).1.1' – reverse-engineer S**
 - 11: $\mathbf{V}_{k+1} = \mathbf{X}_{k+1} - \mathcal{Q}_k S_{1:k,k+1}$ ▷ step (k+1).1.2' – skip normalization
 - 12: **end for**
 - 13: $\begin{bmatrix} \mathcal{Y}_{1:p-1,p} \\ \Omega_p \end{bmatrix} = [\mathcal{Q}_{p-1} \quad \mathbf{V}_p]^T \mathbf{V}_p$ ▷ step p.2.1'
 - 14: $Y_{pp} = \text{chol}(\Omega_p - \mathcal{Y}_{1:p-1,p}^T \mathcal{Y}_{1:p-1,p})$
 - 15: $\mathcal{Q}_p = (\mathbf{V}_p - \mathcal{Q}_{p-1} \mathcal{Y}_{1:p-1,p}) Y_{pp}^{-1}$ ▷ step p.2.2 – second normalization
 - 16: $\mathcal{R}_{1:p-1,p} = S_{1:p-1,p} + \mathcal{Y}_{1:p-1,p}$ ▷ step p.3.1 – form upper \mathcal{R} column
 - 17: $R_{pp} = Y_{pp}$ ▷ step p.3.2 – form \mathcal{R} diagonal entry
 - 18: **return** $\mathcal{Q} = [\mathcal{Q}_1, \dots, \mathcal{Q}_p], \mathcal{R} = (R_{ij})$
-

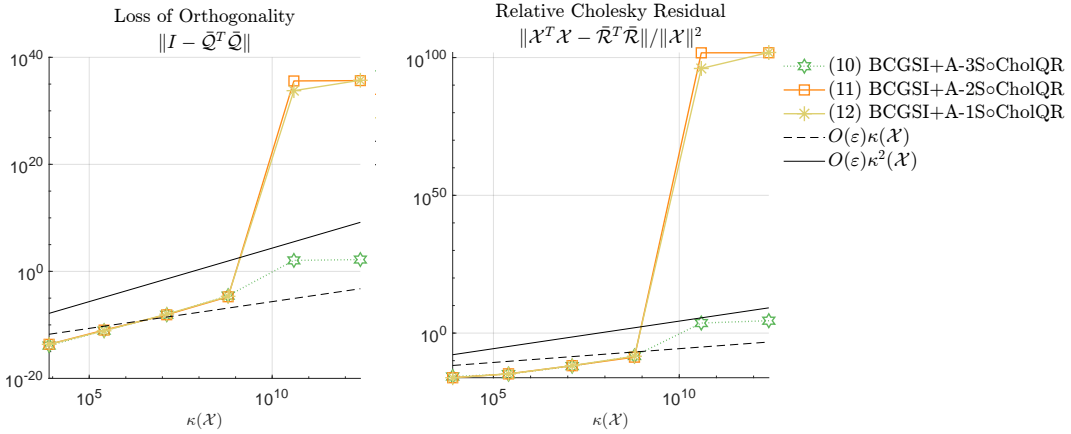


Figure 5: Comparison among low-sync versions of **BCGSI+A** on a class of monomial matrices. Note that IO_A is fixed as HouseQR.

This version of 1-sync **BCGSI+A** is aesthetically quite different from [8, Algorithm 7] or [25, Figure 3], as well as the column-wise versions of [4] and [22]. For one, a general IO_A is used in the first step. However, the core of the algorithm—i.e., everything in the for-loop—is fundamentally the same, up to $\mathcal{O}(\varepsilon)$ rounding errors. Our derivation for **BCGSI+A-1S** provides an alternative perspective from just writing out the first few steps of the for-loop, batching the inner products, and reverse-engineering the next column of \mathcal{S} from the most recently computed inner product.

The **monomial** example used in Figures 1-5— which are combined in Figure 6— paints a pessimistic picture for methods with reduced sync points. The **monomial** matrices are not especially extreme matrices; they are in fact designed to mimic s -step Krylov subspace methods and are built from powers of a well-conditioned operator. There are certainly cases where **BCGSI+A-1S** may be good enough; see Figure 7 for comparisons on the **default** matrices, which are built by explicitly defining a singular value decomposition from diagonal matrices with logarithmically spaced entries. Clearly all methods discussed so far appear more stable than **BCGS** on these simple matrices.

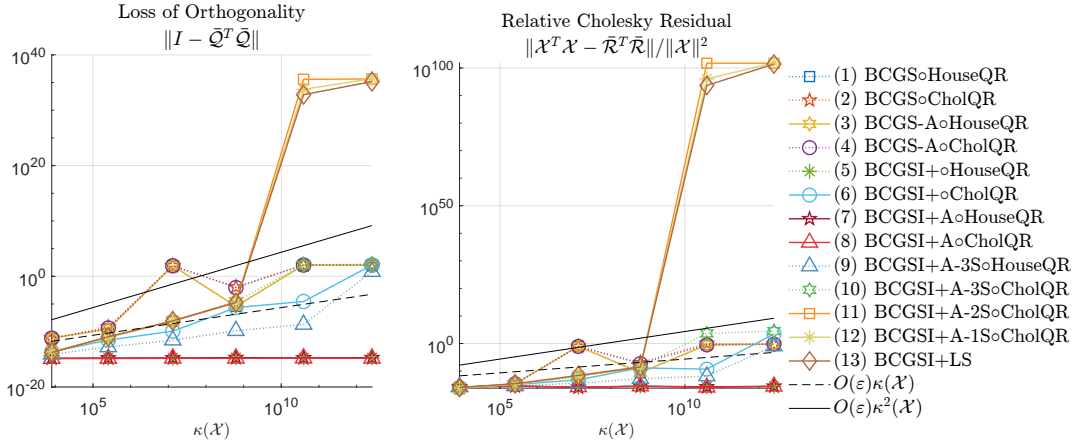


Figure 6: Comparison among **BCGS**, **BCGSI+**, **BCGSI+A**, and low-sync variants thereof on **monomial** matrices. **BCGSI+LS** is Algorithm 7 from [8]. Note that IO_A is fixed as **HouseQR** in **BlockStab**.

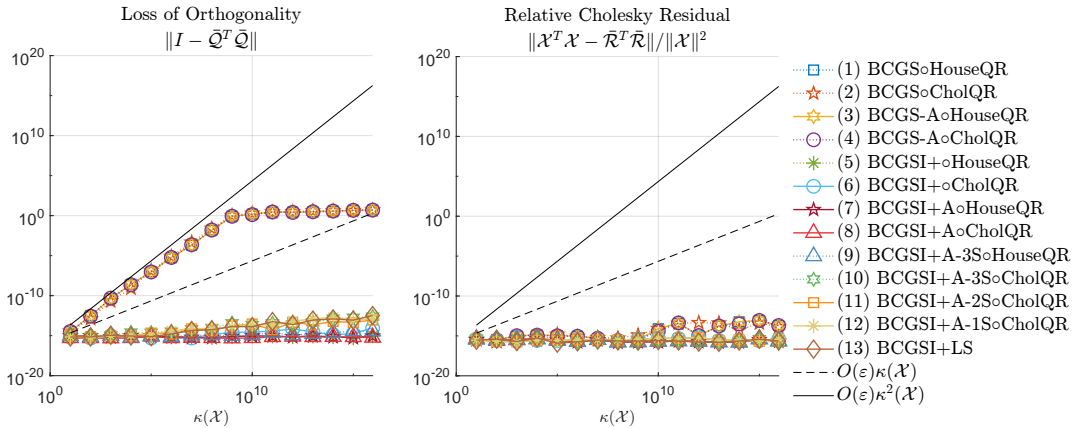


Figure 7: Comparison among **BCGS**, **BCGSI+**, **BCGSI+A**, and low-sync variants thereof on **default** matrices. **BCGSI+LS** is Algorithm 7 from [8]. Note that IO_A is fixed as **HouseQR** in **BlockStab**.

We remind the reader that Figures 1-7 are all generated by the MATLAB script `test_roadmap.m` in **BlockStab**, which we recommend downloading and interacting with for a better understanding of the nuances of these BGS variants.

4 Loss of orthogonality of low-sync versions of BCGSI+A

Figures 4-5 reinforce the challenges of proving tight upper bounds for the LOO of Algorithms 3-5. None of the variants has a small relative Cholesky residual, meaning that we cannot rely on the technique from [7], which inducts over the \mathcal{R} factor to obtain an LOO bound. We also know that the LOO can be worse than $\mathcal{O}(\varepsilon) \kappa^2(\mathcal{X})$, for $\mathcal{O}(\varepsilon) \kappa^2(\mathcal{X}) \leq 1$. However, we can still employ the general framework from Section 2.1 to prove some insightful bounds.

4.1 BCGSI+A-3S

For Algorithm 3, the projection and intraortho stage can be written respectively as

$$\mathbf{G} = \text{Proj}(\mathbf{X}, \mathbf{Q}) := (I - \mathbf{Q}\mathbf{Q}^T)(I - \mathbf{Q}\mathbf{Q}^T)\mathbf{X} \quad \text{and} \quad \text{QR}(\mathbf{G}) := \text{IO}(\mathbf{G}). \quad (66)$$

Specifically, for the k th inner loop of Algorithm 3,

$$\mathbf{W}_k = \text{Proj}(\mathbf{X}_k, \mathbf{Q}_{k-1}) = (I - \mathbf{Q}_{k-1}\mathbf{Q}_{k-1}^T)(I - \mathbf{Q}_{k-1}\mathbf{Q}_{k-1}^T)\mathbf{X}_k, \quad (67)$$

$$[\mathbf{Q}_k, \mathbf{R}_{kk}] = \text{QR}(\mathbf{W}_k) = \text{IO}(\mathbf{W}_k). \quad (68)$$

Then we define

$$\widetilde{\mathbf{W}}_k = (I - \bar{\mathbf{Q}}_{k-1}\bar{\mathbf{Q}}_{k-1}^T)(I - \bar{\mathbf{Q}}_{k-1}\bar{\mathbf{Q}}_{k-1}^T)\mathbf{X}_k, \quad (69)$$

where $\bar{\mathbf{Q}}_{k-1}$ satisfies (21). Furthermore, $\widetilde{\mathbf{W}}_k$ denotes the computed result of $\widetilde{\mathbf{W}}_k$.

In analogue to the analysis of BCGS-A, we first estimate $\sigma_{\min}(\widetilde{\mathbf{W}}_k)$ and $\kappa(\widetilde{\mathbf{W}}_k)$ in Lemma 8, and then analyze the specific $\psi := \psi_k^{(\text{BCGSI+A-3S})}$ satisfying $\|\widetilde{\mathbf{W}}_k - \bar{\mathbf{W}}_k\| \leq \psi_k^{(\text{BCGSI+A-3S})}$ for the k th inner loop and $\|\bar{\mathbf{Q}}_{k-1}^T \widetilde{\mathbf{W}}_k \bar{\mathbf{R}}_{kk}^{-1}\|$ that are related only to the projection stage in Lemma 9.

Lemma 8. *Let $\widetilde{\mathbf{W}}_k$ and $\bar{\mathbf{Q}}_{k-1}$ satisfy (69) and (21). Assume that*

$$\boldsymbol{\mathcal{X}}_{k-1} + \Delta\boldsymbol{\mathcal{X}}_{k-1} = \bar{\mathbf{Q}}_{k-1}\bar{\mathbf{R}}_{k-1}, \quad \|\Delta\boldsymbol{\mathcal{X}}_{k-1}\| \leq \rho_{k-1} \|\boldsymbol{\mathcal{X}}_{k-1}\| \quad (70)$$

with $\rho_{k-1}\kappa(\boldsymbol{\mathcal{X}}_k) < 1$ and $\bar{\mathbf{R}}_{k-1}$ nonsingular. Then for any $k \geq 2$

$$\|\widetilde{\mathbf{W}}_k\| \leq (1 + \omega_{k-1} + (1 + \omega_{k-1})^2\omega_{k-1}) \|\mathbf{X}_k\|, \quad (71)$$

$$\sigma_{\min}(\widetilde{\mathbf{W}}_k) \geq \sigma_{\min}(\boldsymbol{\mathcal{X}}_k) - \rho_{k-1} \|\boldsymbol{\mathcal{X}}_{k-1}\|, \quad \text{and} \quad (72)$$

$$\kappa(\widetilde{\mathbf{W}}_k) \leq \frac{(1 + \omega_{k-1} + (1 + \omega_{k-1})^2\omega_{k-1})\kappa(\boldsymbol{\mathcal{X}}_k)}{1 - \rho_{k-1}\kappa(\boldsymbol{\mathcal{X}}_k)}. \quad (73)$$

Proof. Similarly to the proof of Lemma 3, by the assumption (70) and

$$\begin{aligned} \widetilde{\mathbf{W}}_k &= \mathbf{X}_k - \bar{\mathbf{Q}}_{k-1}\bar{\mathbf{R}}_{k-1}\bar{\mathbf{R}}_{k-1}^{-1}(\bar{\mathbf{Q}}_{k-1}^T + \bar{\mathbf{Q}}_{k-1}^T(I - \bar{\mathbf{Q}}_{k-1}\bar{\mathbf{Q}}_{k-1}^T))\mathbf{X}_k \\ &= [\boldsymbol{\mathcal{X}}_{k-1} + \Delta\boldsymbol{\mathcal{X}}_{k-1} \quad \mathbf{X}_k] \mathbf{D}^T \end{aligned} \quad (74)$$

with $\mathbf{D} := \left[-\left(\bar{\mathbf{R}}_{k-1}^{-1}(\bar{\mathbf{Q}}_{k-1}^T + \bar{\mathbf{Q}}_{k-1}^T(I - \bar{\mathbf{Q}}_{k-1}\bar{\mathbf{Q}}_{k-1}^T))\mathbf{X}_k\right)^T \quad I \right]$, we obtain

$$\sigma_{\min}(\widetilde{\mathbf{W}}_k) \geq \sigma_{\min}(\boldsymbol{\mathcal{X}}_k) - \rho_{k-1} \|\boldsymbol{\mathcal{X}}_{k-1}\| \geq \sigma_{\min}(\boldsymbol{\mathcal{X}}_k) - \rho_{k-1} \|\boldsymbol{\mathcal{X}}_k\|. \quad (75)$$

Combining (75) with (26) and

$$\begin{aligned} \|\widetilde{\mathbf{W}}_k\| &\leq \left(\|I - \bar{\mathbf{Q}}_{k-1}\bar{\mathbf{Q}}_{k-1}^T\| + \|\bar{\mathbf{Q}}_{k-1}\|^2 \|I - \bar{\mathbf{Q}}_{k-1}\bar{\mathbf{Q}}_{k-1}^T\| \right) \|\mathbf{X}_k\| \\ &\leq (1 + \omega_{k-1} + (1 + \omega_{k-1})^2\omega_{k-1}) \|\mathbf{X}_k\|, \end{aligned} \quad (76)$$

we have

$$\kappa(\widetilde{\mathbf{W}}_k) \leq \frac{(1 + \omega_{k-1} + (1 + \omega_{k-1})^2\omega_{k-1})\kappa(\boldsymbol{\mathcal{X}}_k)}{1 - \rho_{k-1}\kappa(\boldsymbol{\mathcal{X}}_k)}. \quad (77)$$

□

Lemma 9. Let $\widetilde{\mathbf{W}}_k$ and $\widetilde{\mathbf{Q}}_{k-1}$ satisfy (69) and (21), and $\widetilde{\mathbf{W}}_k$ be the computed result of $\widetilde{\mathbf{W}}_k$. For the projection stage (67) computed by lines 4–6 in Algorithm 3, with any $k \geq 2$, it holds that

$$\begin{aligned} \left\| \widetilde{\mathbf{W}}_k - \widetilde{\mathbf{W}}_k \right\| &\leq \psi_k^{(\text{BCGSI+A-3S})} \leq \mathcal{O}(\varepsilon) \left\| \widetilde{\mathbf{W}}_k \right\| + \mathcal{O}(\varepsilon^2) \|\mathbf{X}_k\| + \mathcal{O}(\varepsilon) \omega_{k-1} \|\mathbf{X}_k\|, \\ \left\| \widetilde{\mathbf{Q}}_{k-1}^T \widetilde{\mathbf{W}}_k \bar{R}_{kk}^{-1} \right\| &\leq (1 + \omega_{k-1}) \omega_{k-1}^2 \|\mathbf{X}_k\| \left\| \bar{R}_{kk}^{-1} \right\|. \end{aligned}$$

Proof. By Lemma 4, we have

$$\begin{aligned} \bar{\mathbf{V}}_k &= \widetilde{\mathbf{V}}_k + \Delta \widetilde{\mathbf{V}}_k, \quad \left\| \Delta \widetilde{\mathbf{V}}_k \right\| \leq \mathcal{O}(\varepsilon) \|\mathbf{X}_k\|, \\ \bar{\mathbf{W}}_k &= \widetilde{\mathbf{W}}_k + \Delta \widetilde{\mathbf{W}}_k, \quad \left\| \Delta \widetilde{\mathbf{W}}_k \right\| \leq \mathcal{O}(\varepsilon) \|\bar{\mathbf{V}}_k\| \leq \mathcal{O}(\varepsilon) \left\| \widetilde{\mathbf{V}}_k \right\| + \mathcal{O}(\varepsilon^2) \|\mathbf{X}_k\| \end{aligned} \quad (78)$$

with the definition (20) of $\widetilde{\mathbf{V}}_k$. Noticing that with

$$\widetilde{\mathbf{W}}_k = \widetilde{\mathbf{V}}_k - \widetilde{\mathbf{Q}}_{k-1} (I - \widetilde{\mathbf{Q}}_{k-1}^T \widetilde{\mathbf{Q}}_{k-1}) \widetilde{\mathbf{Q}}_{k-1}^T \mathbf{X}_k,$$

we bound $\psi_k^{(\text{BCGSI+A-3S})}$ because

$$\left\| \widetilde{\mathbf{V}}_k \right\| \leq \left\| \widetilde{\mathbf{W}}_k \right\| + (1 + \omega_{k-1})^2 \omega_{k-1} \|\mathbf{X}_k\|.$$

Then by (69), $\left\| \widetilde{\mathbf{Q}}_{k-1}^T \widetilde{\mathbf{W}}_k \bar{R}_{kk}^{-1} \right\|$ is bounded as follows:

$$\begin{aligned} \left\| \widetilde{\mathbf{Q}}_{k-1}^T \widetilde{\mathbf{W}}_k \bar{R}_{kk}^{-1} \right\| &= \left\| \widetilde{\mathbf{Q}}_{k-1}^T (I - \widetilde{\mathbf{Q}}_{k-1} \widetilde{\mathbf{Q}}_{k-1}^T) (I - \widetilde{\mathbf{Q}}_{k-1} \widetilde{\mathbf{Q}}_{k-1}^T) \mathbf{X}_k \bar{R}_{kk}^{-1} \right\| \\ &\leq \left\| (I - \widetilde{\mathbf{Q}}_{k-1}^T \widetilde{\mathbf{Q}}_{k-1}) (I - \widetilde{\mathbf{Q}}_{k-1} \widetilde{\mathbf{Q}}_{k-1}^T) \widetilde{\mathbf{Q}}_{k-1}^T \mathbf{X}_k \bar{R}_{kk}^{-1} \right\| \\ &\leq \left\| I - \widetilde{\mathbf{Q}}_{k-1}^T \widetilde{\mathbf{Q}}_{k-1} \right\|^2 \left\| \widetilde{\mathbf{Q}}_{k-1} \right\| \|\mathbf{X}_k\| \left\| \bar{R}_{kk}^{-1} \right\| \\ &\leq (1 + \omega_{k-1}) \omega_{k-1}^2 \|\mathbf{X}_k\| \left\| \bar{R}_{kk}^{-1} \right\|. \end{aligned}$$

□

The following lemma analyzes the behavior of the k th inner loop of **BCGSI+A-3S**.

Lemma 10. Assume that $\mathcal{O}(\varepsilon) \kappa(\mathbf{X}_k) \leq \frac{1}{2}$, $\widetilde{\mathbf{Q}}_{k-1}$ satisfies (21), and

$$\mathbf{x}_{k-1} + \Delta \mathbf{x}_{k-1} = \widetilde{\mathbf{Q}}_{k-1} \bar{\mathbf{R}}_{k-1,k-1}, \quad \left\| \Delta \mathbf{x}_{k-1} \right\| \leq \mathcal{O}(\varepsilon) \|\mathbf{x}_{k-1}\|.$$

Then for the k th inner loop of Algorithm 3 with any $k \geq 2$:

$$\left\| I - \widetilde{\mathbf{Q}}_k^T \widetilde{\mathbf{Q}}_k \right\| \leq \omega_{k-1} + \mathcal{O}(\varepsilon) \kappa(\mathbf{X}_k) + 4(1 + \omega_{k-1}) \omega_{k-1}^2 (1 + \omega_{\text{qr}}) \kappa(\mathbf{X}_k) + \omega_{\text{qr}}.$$

Proof. By Lemma 1 and Lemma 9, we have

$$\begin{aligned} \left\| I - \widetilde{\mathbf{Q}}_k^T \widetilde{\mathbf{Q}}_k \right\| &\leq \omega_{k-1} + \frac{\mathcal{O}(\varepsilon) \kappa(\widetilde{\mathbf{W}}_k) + (\mathcal{O}(\varepsilon^2) + \mathcal{O}(\varepsilon) \omega_{k-1}) \|\mathbf{X}_k\| / \sigma_{\min}(\widetilde{\mathbf{W}}_k)}{1 - \mathcal{O}(\varepsilon) \|\mathbf{X}_k\| / \sigma_{\min}(\widetilde{\mathbf{W}}_k) - \mathcal{O}(\varepsilon) \kappa(\widetilde{\mathbf{W}}_k)} \\ &\quad + \frac{2(1 + \omega_{k-1}) \omega_{k-1}^2 (1 + \omega_{\text{qr}}) \|\mathbf{X}_k\|}{\sigma_{\min}(\widetilde{\mathbf{W}}_k) - \mathcal{O}(\varepsilon) \|\mathbf{X}_k\| - \mathcal{O}(\varepsilon) \left\| \widetilde{\mathbf{W}}_k \right\|} + \omega_{\text{qr}}. \end{aligned} \quad (79)$$

Combining (79) with Lemma 8 and the assumption $\mathcal{O}(\varepsilon) \kappa(\mathbf{X}_k) \leq \frac{1}{2}$, we conclude the proof because

$$\begin{aligned} \left\| I - \widetilde{\mathbf{Q}}_k^T \widetilde{\mathbf{Q}}_k \right\| &\leq \omega_{k-1} + \frac{\mathcal{O}(\varepsilon) \kappa(\widetilde{\mathbf{W}}_k) + (\mathcal{O}(\varepsilon^2) + \mathcal{O}(\varepsilon) \omega_{k-1}) \kappa(\mathbf{X}_k)}{1 - \mathcal{O}(\varepsilon) \kappa(\mathbf{X}_k)} \\ &\quad + \frac{2(1 + \omega_{k-1}) \omega_{k-1}^2 (1 + \omega_{\text{qr}}) \kappa(\mathbf{X}_k)}{1 - \mathcal{O}(\varepsilon) \kappa(\mathbf{X}_k)} + \omega_{\text{qr}}. \end{aligned} \quad (80)$$

□

By induction on k , we obtain the following theorem to show the loss of orthogonality of **BCGSI+A-3S**.

Theorem 3. *Let $\bar{\mathbf{Q}}$ and $\bar{\mathbf{R}}$ denote the computed results of Algorithm 3. Assume that for all $\mathbf{X} \in \mathbb{R}^{m \times s}$ with $\kappa(\mathbf{X}) \leq \kappa(\boldsymbol{\mathcal{X}})$, the following hold for $[\bar{\mathbf{Q}}, \bar{\mathbf{R}}] = \text{IO}_A(\mathbf{X})$:*

$$\begin{aligned} \mathbf{X} + \Delta \mathbf{X} &= \bar{\mathbf{Q}} \bar{\mathbf{R}}, \quad \|\Delta \mathbf{X}\| \leq \mathcal{O}(\varepsilon) \|\mathbf{X}\|, \\ \|I - \bar{\mathbf{Q}}^T \bar{\mathbf{Q}}\| &\leq \mathcal{O}(\varepsilon) \kappa^{\alpha_A}(\mathbf{X}), \end{aligned}$$

and for $[\bar{\mathbf{Q}}, \bar{\mathbf{R}}] = \text{IO}(\mathbf{X})$, it holds that

$$\begin{aligned} \mathbf{X} + \Delta \mathbf{X} &= \bar{\mathbf{Q}} \bar{\mathbf{R}}, \quad \|\Delta \mathbf{X}\| \leq \mathcal{O}(\varepsilon) \|\mathbf{X}\|, \\ \|I - \bar{\mathbf{Q}}^T \bar{\mathbf{Q}}\| &\leq \mathcal{O}(\varepsilon) \kappa^\alpha(\mathbf{X}). \end{aligned}$$

If $\alpha_A \leq \alpha$ and $\mathcal{O}(\varepsilon) \kappa^\theta(\boldsymbol{\mathcal{X}}) \leq \frac{1}{2}$ with $\theta := \max(\alpha + 1, 2)$, is satisfied, then

$$\boldsymbol{\mathcal{X}} + \Delta \boldsymbol{\mathcal{X}} = \bar{\mathbf{Q}} \bar{\mathbf{R}}, \quad \|\Delta \boldsymbol{\mathcal{X}}\| \leq \mathcal{O}(\varepsilon) \|\boldsymbol{\mathcal{X}}\|$$

and

$$\|I - \bar{\mathbf{Q}}^T \bar{\mathbf{Q}}\| \leq \mathcal{O}(\varepsilon) (\kappa(\boldsymbol{\mathcal{X}}))^{\max\{\alpha, 1\}}. \quad (81)$$

Proof. We only need to verify the assumptions of Lemma 10, which are guaranteed by the assumption $\mathcal{O}(\varepsilon) \kappa^\theta(\boldsymbol{\mathcal{X}}) \leq \frac{1}{2}$ and the residual bound that we establish in the rest of the proof.

The assumptions on IO_A directly give the base case of the residual bound. Assume that $\boldsymbol{\mathcal{X}}_{k-1} + \Delta \boldsymbol{\mathcal{X}}_{k-1} = \bar{\mathbf{Q}}_{k-1} \bar{\mathbf{R}}_{k-1, k-1}$ with $\|\Delta \boldsymbol{\mathcal{X}}_{k-1}\| \leq \mathcal{O}(\varepsilon) \|\boldsymbol{\mathcal{X}}_{k-1}\|$. By [16] and the assumption on IO_A and IO , we obtain

$$\begin{aligned} \bar{\mathbf{R}}_{1:k-1, k} &= \bar{\mathbf{S}}_{1:k-1, k} + \bar{\mathbf{Y}}_{1:k-1, k} + \Delta \bar{\mathbf{R}}_{1:k-1, k} \\ &= (\bar{\mathbf{Q}}_{k-1}^T \mathbf{X}_k + \Delta \bar{\mathbf{S}}_{1:k-1, k}) + (\bar{\mathbf{Q}}_{k-1}^T \bar{\mathbf{V}}_k + \Delta \bar{\mathbf{Y}}_{1:k-1, k}) + \Delta \bar{\mathbf{R}}_{1:k-1, k} \\ &= \bar{\mathbf{Q}}_{k-1}^T \mathbf{X}_k + \bar{\mathbf{Q}}_{k-1}^T \bar{\mathbf{V}}_k + \Delta \mathbf{E}_{\mathcal{R}}, \end{aligned} \quad (82)$$

where $\Delta \mathbf{E}_{\mathcal{R}} = \Delta \bar{\mathbf{S}}_{1:k-1, k} + \Delta \bar{\mathbf{Y}}_{1:k-1, k} + \Delta \bar{\mathbf{R}}_{1:k-1, k}$ satisfies

$$\|\Delta \mathbf{E}_{\mathcal{R}}\| \leq \mathcal{O}(\varepsilon) \|\mathbf{X}_k\|. \quad (83)$$

Then recalling the definitions (20) and (69), we have

$$\begin{aligned} \bar{\mathbf{Q}}_{k-1} \bar{\mathbf{R}}_{1:k-1, k} + \bar{\mathbf{Q}}_k \bar{\mathbf{R}}_{kk} &= \bar{\mathbf{Q}}_{k-1} \left(\bar{\mathbf{Q}}_{k-1}^T (\mathbf{X}_k + \tilde{\mathbf{V}}_k + \Delta \tilde{\mathbf{V}}_k) + \Delta \mathbf{E}_{\mathcal{R}} \right) + \tilde{\mathbf{W}}_k \\ &\quad + \Delta \mathbf{E}_{\text{proj}} + \Delta \mathbf{G}_k \\ &= \mathbf{X}_k + \bar{\mathbf{Q}}_{k-1} \bar{\mathbf{Q}}_{k-1}^T \Delta \tilde{\mathbf{V}}_k + \bar{\mathbf{Q}}_{k-1} \Delta \mathbf{E}_{\mathcal{R}} \\ &\quad + \Delta \mathbf{E}_{\text{proj}} + \Delta \mathbf{G}_k, \end{aligned} \quad (84)$$

where $\Delta \mathbf{E}_{\text{proj}} = \bar{\mathbf{W}}_k - \tilde{\mathbf{W}}_k$ and $\Delta \mathbf{G}_k$ satisfies $\bar{\mathbf{W}}_k + \Delta \mathbf{G}_k = \bar{\mathbf{Q}}_k \bar{\mathbf{R}}_{kk}$. Combining (84) with (5), (6), (83), and Lemma 9, we draw the conclusion followed by the proof of Theorem 1 because

$$\begin{aligned} \boldsymbol{\mathcal{X}}_k + \Delta \boldsymbol{\mathcal{X}}_k &= [\boldsymbol{\mathcal{X}}_{k-1} + \Delta \boldsymbol{\mathcal{X}}_{k-1} \quad \mathbf{X}_k + \Delta \mathbf{X}_k] \\ &= [\bar{\mathbf{Q}}_{k-1} \bar{\mathbf{R}}_{k-1, k-1} \quad \bar{\mathbf{Q}}_{k-1} \bar{\mathbf{R}}_{1:k-1, k} + \bar{\mathbf{Q}}_k \bar{\mathbf{R}}_{kk}], \end{aligned}$$

and

$$\bar{\mathbf{Q}}_{k-1} \bar{\mathbf{R}}_{1:k-1, k} + \bar{\mathbf{Q}}_k \bar{\mathbf{R}}_{kk} = \mathbf{X}_k + \bar{\mathbf{Q}}_{k-1} \bar{\mathbf{Q}}_{k-1}^T \Delta \tilde{\mathbf{V}}_k + \bar{\mathbf{Q}}_{k-1} \Delta \mathbf{E}_{\mathcal{R}} + \Delta \mathbf{E}_{\text{proj}} + \Delta \mathbf{G}_k,$$

where $\Delta \boldsymbol{\mathcal{X}}_k = \bar{\mathbf{Q}}_{k-1} \bar{\mathbf{Q}}_{k-1}^T \Delta \tilde{\mathbf{V}}_k + \bar{\mathbf{Q}}_{k-1} \Delta \mathbf{E}_{\mathcal{R}} + \Delta \mathbf{E}_{\text{proj}} + \Delta \mathbf{G}_k$ satisfies $\|\Delta \boldsymbol{\mathcal{X}}_k\| \leq \mathcal{O}(\varepsilon) \|\boldsymbol{\mathcal{X}}_k\|$. By induction on k , the residual bound has been proved.

Next we aim to prove the LOO using Lemma 10. The assumptions on IO_A directly give the base case for the LOO, i.e.,

$$\omega_1 \leq \mathcal{O}(\varepsilon) (\kappa(\boldsymbol{\mathcal{X}}))^{\alpha_A} \leq \mathcal{O}(\varepsilon) (\kappa(\boldsymbol{\mathcal{X}}))^{\max\{\alpha, 1\}}.$$

Now we assume that $\omega_{k-1} \leq \mathcal{O}(\varepsilon) (\kappa(\mathcal{X}))^{\max\{\alpha, 1\}}$. Using Lemma 10 and the assumption on IO, we conclude that

$$\begin{aligned} \left\| I - \bar{\mathcal{Q}}_k^T \bar{\mathcal{Q}}_k \right\| &\leq \omega_{k-1} (4(1 + \omega_{k-1})(1 + \mathcal{O}(\varepsilon))\omega_{k-1}\kappa(\mathcal{X}_k) + 1) + \mathcal{O}(\varepsilon) \kappa(\mathcal{X}_k) \\ &\leq \mathcal{O}(\varepsilon) (\kappa(\mathcal{X}_k))^{\max\{\alpha, 1\}}. \end{aligned}$$

Note that $4(1 + \omega_{k-1})(1 + \mathcal{O}(\varepsilon))\omega_{k-1}\kappa(\mathcal{X}_k) \leq 1$ requires $\mathcal{O}(\varepsilon) \kappa^{\alpha+1}(\mathcal{X}_k) \leq 1$, which is guaranteed by the assumption $\mathcal{O}(\varepsilon) \kappa^\theta(\mathcal{X}) \leq \frac{1}{2}$. \square

With Theorem 3 we have proven our observations from Figure 4 in Section 3. By removing the first IO in the inner loop, we implicitly impose a restriction on $\kappa(\mathcal{X})$ dictated by the remaining IO. In particular, for **BCGSI+A-3S** \circ **HouseQR**, $\theta = 2$, and for **BCGSI+A-3S** \circ **CholQR**, $\theta = 3$. Practically speaking, in double precision, the first translates to the requirement that $\kappa(\mathcal{X}) \leq 10^8$, and the latter to $\kappa(\mathcal{X}) \leq 10^{5.3}$.

4.2 BCGSI+A-2S

For the k th inner loop of Algorithm 4, the projection stage also satisfies (67). Comparing **BCGSI+A-2S** and **BCGSI+A-3S** \circ **CholQR**, the only difference is that for the intraortho stage, **BCGSI+A-2S** applies a Cholesky factorization (implicitly via line 6) to

$$\mathbf{V}_k^T \mathbf{V}_k - (\bar{\mathcal{Q}}_{k-1}^T \mathbf{V}_k)^T (\bar{\mathcal{Q}}_{k-1}^T \mathbf{V}_k),$$

with $\mathbf{V}_k = (I - \bar{\mathcal{Q}}_{k-1} \bar{\mathcal{Q}}_{k-1}^T) \mathbf{X}_k$. This means that we need to estimate the terms related to the intraortho stage, namely ω_{qr} , in Lemma 10 and then we derive the loss of orthogonality of **BCGSI+A-2S** directly by applying Lemma 10 in a manner similar to the proof of Theorem 3. In the following lemma, we give a bound on ω_{qr} .

Lemma 11. *Let $\tilde{\mathbf{V}}_k$, $\tilde{\mathbf{W}}_k$, and $\bar{\mathcal{Q}}_{k-1}$ satisfy (20), (69), and (21), and $\bar{\mathbf{V}}_k$ and $\bar{\mathbf{W}}_k$ be the computed results of $\tilde{\mathbf{V}}_k$ and $\tilde{\mathbf{W}}_k$. Assume that (70) is satisfied with*

$$2((1 + \omega_{k-1})^2 \omega_{k-1}^3 + \mathcal{O}(\varepsilon)) \kappa^2(\mathcal{X}_k) + (\mathcal{O}(\varepsilon) (1 + \omega_{k-1}) + \rho_{k-1}) \kappa(\mathcal{X}_k) \leq \frac{1}{2}. \quad (85)$$

Then for $\bar{\mathcal{Q}}_k$ and \bar{Y}_{kk} with any $k \geq 2$ computed by lines 5–7 in Algorithm 4,

$$\begin{aligned} \bar{\mathbf{W}}_k + \Delta \mathbf{W}_k &= \bar{\mathcal{Q}}_k \bar{Y}_{kk} = \bar{\mathcal{Q}}_k \bar{R}_{kk}, \quad \|\Delta \mathbf{W}_k\| \leq \mathcal{O}(\varepsilon) \|\bar{\mathbf{W}}_k\|, \\ \|\bar{\mathcal{Q}}_k^T \bar{\mathcal{Q}}_k - I\| &\leq (2 \cdot (1 + \omega_{k-1})^2 \omega_{k-1}^3 + \mathcal{O}(\varepsilon)) \kappa(\mathcal{X}_k). \end{aligned}$$

Proof. By [16, Theorem 8.5 and Lemma 6.6], there exists ΔR_i such that

$$(\bar{Y}_{kk}^T + \Delta R_i^T) \bar{\mathcal{Q}}(i, :)^T = \bar{\mathbf{W}}_k(i, :)^T, \quad \|\Delta R_i\| \leq \mathcal{O}(\varepsilon) \|\bar{Y}_{kk}\|, \quad (86)$$

for $i = 1, 2, \dots, m$, where we have used MATLAB notation to access rows. Then we obtain

$$\bar{\mathbf{W}}_k + \Delta \mathbf{W}_k = \bar{\mathcal{Q}}_k \bar{Y}_{kk}, \quad \Delta \mathbf{W}_k(i, :)^T = \Delta R_i^T \bar{\mathcal{Q}}_k(i, :)^T, \quad (87)$$

where $\Delta \mathbf{W}_k$ satisfies

$$\|\Delta \mathbf{W}_k\| \leq \mathcal{O}(\varepsilon) \|\bar{\mathcal{Q}}_k\| \|\bar{Y}_{kk}\|. \quad (88)$$

We therefore need to estimate $\|\bar{Y}_{kk}\|$ and $\|\bar{\mathcal{Q}}_k\|$.

By standard rounding-error bounds and (11),

$$\bar{Y}_{1:k-1,k} = \bar{\mathcal{Q}}_{k-1}^T \bar{\mathbf{V}}_k + \Delta \mathcal{Y}_k, \quad \|\Delta \mathcal{Y}_k\| \leq \mathcal{O}(\varepsilon) \|\bar{\mathbf{V}}_k\|, \quad (89)$$

$$\bar{\Omega}_k = \bar{\mathbf{V}}_k^T \bar{\mathbf{V}}_k + \Delta \Omega_k, \quad \|\Delta \Omega_k\| \leq \mathcal{O}(\varepsilon) \|\bar{\mathbf{V}}_k\|^2, \quad (90)$$

$$\bar{\mathbf{W}}_k = (I - \bar{\mathcal{Q}}_{k-1} \bar{\mathcal{Q}}_{k-1}^T) \bar{\mathbf{V}}_k + \Delta \mathbf{E}_W, \quad \|\Delta \mathbf{E}_W\| \leq \mathcal{O}(\varepsilon) \|\bar{\mathbf{V}}_k\|. \quad (91)$$

Applying [16, Theorem 10.3] to line 6 of Algorithm 4 leads to

$$\bar{Y}_{kk}^T \bar{Y}_{kk} = \bar{\Omega}_k - \bar{Y}_{1:k-1,k}^T \bar{Y}_{1:k-1,k} + \Delta F_k + \Delta C_k, \quad (92)$$

where ΔF_k is the floating-point error from the computations $\bar{\Omega}_k - \bar{Y}_{1:k-1,k}^T \bar{Y}_{1:k-1,k}$, while ΔC_k denotes the Cholesky error. Furthermore, the following bounds hold:

$$\|\Delta F_k\| \leq \mathcal{O}(\varepsilon) \|\bar{\mathbf{V}}_k\|^2 \quad \text{and} \quad \|\Delta C_k\| \leq \mathcal{O}(\varepsilon) \|\bar{\mathbf{V}}_k\|^2. \quad (93)$$

Combining (93) with (89) and (90), we have

$$\bar{Y}_{kk}^T \bar{Y}_{kk} = \bar{\mathbf{V}}_k^T \bar{\mathbf{V}}_k - \bar{\mathbf{V}}_k^T \bar{\mathbf{Q}}_{k-1} \bar{\mathbf{Q}}_{k-1}^T \bar{\mathbf{V}}_k + \Delta \mathbf{Y}_k, \quad \|\Delta \mathbf{Y}_k\| \leq \mathcal{O}(\varepsilon) \|\bar{\mathbf{V}}_k\|^2. \quad (94)$$

Let

$$\begin{aligned} \mathbf{M}_k^{(1)} &= \bar{\mathbf{V}}_k^T (I - \bar{\mathbf{Q}}_{k-1} \bar{\mathbf{Q}}_{k-1}^T) \bar{\mathbf{V}}_k, \quad \text{and} \\ \mathbf{M}_k^{(2)} &= \bar{\mathbf{V}}_k^T (I - \bar{\mathbf{Q}}_{k-1} \bar{\mathbf{Q}}_{k-1}^T) (I - \bar{\mathbf{Q}}_{k-1} \bar{\mathbf{Q}}_{k-1}^T) \bar{\mathbf{V}}_k. \end{aligned}$$

Notice that

$$\begin{aligned} \mathbf{M}_k^{(1)} &= \mathbf{M}_k^{(2)} + \bar{\mathbf{V}}_k^T \bar{\mathbf{Q}}_{k-1} (I - \bar{\mathbf{Q}}_{k-1}^T \bar{\mathbf{Q}}_{k-1}) \bar{\mathbf{Q}}_{k-1}^T \bar{\mathbf{V}}_k, \quad \text{and} \\ \mathbf{M}_k^{(2)} &= \bar{\mathbf{W}}_k^T \bar{\mathbf{W}}_k - \Delta \mathbf{E}_W^T \bar{\mathbf{W}}_k - \bar{\mathbf{W}}_k^T \Delta \mathbf{E}_W + \Delta \mathbf{E}_W^T \Delta \mathbf{E}_W. \end{aligned}$$

Then

$$\bar{Y}_{kk}^T \bar{Y}_{kk} = \mathbf{M}_k^{(2)} + \bar{\mathbf{V}}_k^T \bar{\mathbf{Q}}_{k-1} (I - \bar{\mathbf{Q}}_{k-1}^T \bar{\mathbf{Q}}_{k-1}) \bar{\mathbf{Q}}_{k-1}^T \bar{\mathbf{V}}_k + \Delta \mathbf{Y}_k = \bar{\mathbf{W}}_k^T \bar{\mathbf{W}}_k + \Delta \mathbf{M}, \quad (95)$$

where

$$\begin{aligned} \Delta \mathbf{M} &= -\Delta \mathbf{E}_W^T \bar{\mathbf{W}}_k - \bar{\mathbf{W}}_k^T \Delta \mathbf{E}_W + \Delta \mathbf{E}_W^T \Delta \mathbf{E}_W \\ &\quad + \bar{\mathbf{V}}_k^T \bar{\mathbf{Q}}_{k-1} (I - \bar{\mathbf{Q}}_{k-1}^T \bar{\mathbf{Q}}_{k-1}) \bar{\mathbf{Q}}_{k-1}^T \bar{\mathbf{V}}_k + \Delta \mathbf{Y}_k. \end{aligned}$$

From Lemmas 3, 4, 8, and 9, $\left\| \bar{\mathbf{V}}_k^T \bar{\mathbf{Q}}_{k-1} (I - \bar{\mathbf{Q}}_{k-1}^T \bar{\mathbf{Q}}_{k-1}) \bar{\mathbf{Q}}_{k-1}^T \bar{\mathbf{V}}_k \right\|$ can be bounded by

$$\begin{aligned} &\left\| \bar{\mathbf{V}}_k^T \bar{\mathbf{Q}}_{k-1} (I - \bar{\mathbf{Q}}_{k-1}^T \bar{\mathbf{Q}}_{k-1}) \bar{\mathbf{Q}}_{k-1}^T \bar{\mathbf{V}}_k \right\| \\ &\leq \left\| \tilde{\mathbf{V}}_k^T \bar{\mathbf{Q}}_{k-1} (I - \bar{\mathbf{Q}}_{k-1}^T \bar{\mathbf{Q}}_{k-1}) \bar{\mathbf{Q}}_{k-1}^T \tilde{\mathbf{V}}_k \right\| + \mathcal{O}(\varepsilon) \|\mathbf{X}_k\|^2 \\ &\leq \left\| \mathbf{X}_k^T \bar{\mathbf{Q}}_{k-1} (I - \bar{\mathbf{Q}}_{k-1}^T \bar{\mathbf{Q}}_{k-1})^3 \bar{\mathbf{Q}}_{k-1}^T \mathbf{X}_k \right\| + \mathcal{O}(\varepsilon) \|\mathbf{X}_k\|^2 \\ &\leq ((1 + \omega_{k-1})^2 \omega_{k-1}^3 + \mathcal{O}(\varepsilon)) \|\mathbf{X}_k\|^2, \end{aligned} \quad (96)$$

and further together with (26) and (92),

$$\begin{aligned} \|\Delta \mathbf{M}\| &\leq ((1 + \omega_{k-1})^2 \omega_{k-1}^3 + \mathcal{O}(\varepsilon)) \|\mathbf{X}_k\|^2 + \mathcal{O}(\varepsilon) \|\bar{\mathbf{V}}_k\|^2 \\ &\leq ((1 + \omega_{k-1})^2 \omega_{k-1}^3 + \mathcal{O}(\varepsilon)) \|\mathbf{X}_k\|^2. \end{aligned} \quad (97)$$

Note that also from Lemmas 8, 9, and (26), we have

$$\begin{aligned} &\frac{((1 + \omega_{k-1})^2 \omega_{k-1}^3 + \mathcal{O}(\varepsilon)) \|\mathbf{X}_k\|^2}{\sigma_{\min}^2(\bar{\mathbf{W}}_k)} \\ &\leq \frac{((1 + \omega_{k-1})^2 \omega_{k-1}^3 + \mathcal{O}(\varepsilon)) \|\mathbf{X}_k\|^2}{\sigma_{\min}^2(\bar{\mathbf{W}}_k) - \mathcal{O}(\varepsilon) \|\mathbf{X}_k\| - \mathcal{O}(\varepsilon) \omega_{k-1} \|\mathbf{X}_k\|} \\ &\leq \frac{((1 + \omega_{k-1})^2 \omega_{k-1}^3 + \mathcal{O}(\varepsilon)) \|\mathbf{X}_k\|^2}{\sigma_{\min}(\mathbf{X}_k) - \rho_{k-1} \|\mathbf{X}_{k-1}\| - \mathcal{O}(\varepsilon) \|\mathbf{X}_k\| - \mathcal{O}(\varepsilon) \omega_{k-1} \|\mathbf{X}_k\|} \\ &\leq \frac{((1 + \omega_{k-1})^2 \omega_{k-1}^3 + \mathcal{O}(\varepsilon)) \kappa^2(\mathbf{X}_k)}{1 - \rho_{k-1} \kappa(\mathbf{X}_k) - \mathcal{O}(\varepsilon) (1 + \omega_{k-1}) \kappa(\mathbf{X}_k)} \\ &\leq \frac{1}{2} \end{aligned} \quad (98)$$

by the assumption (85). From (95) and (97), it then follows that

$$\begin{aligned} \|\bar{Y}_{kk}\|^2 &\leq \|\bar{\mathbf{W}}_k\|^2 + ((1 + \omega_{k-1})^2 \omega_{k-1}^3 + \mathcal{O}(\varepsilon)) \|\mathbf{X}_k\|^2 \\ &\leq \|\bar{\mathbf{W}}_k\|^2 \left(1 + \frac{((1 + \omega_{k-1})^2 \omega_{k-1}^3 + \mathcal{O}(\varepsilon)) \|\mathbf{X}_k\|^2}{\sigma_{\min}^2(\bar{\mathbf{W}}_k)} \right) \\ &\leq 2 \|\bar{\mathbf{W}}_k\|^2 \end{aligned} \quad (99)$$

and

$$\sigma_{\min}^2(\bar{Y}_{kk}) \geq \sigma_{\min}^2(\bar{\mathbf{W}}_k) - ((1 + \omega_{k-1})^2 \omega_{k-1}^3 + \mathcal{O}(\varepsilon)) \|\mathbf{X}_k\|^2. \quad (100)$$

Furthermore, we then have

$$\begin{aligned} \kappa(\bar{Y}_{kk}) &\leq \sqrt{\frac{2 \|\bar{\mathbf{W}}_k\|^2}{\sigma_{\min}^2(\bar{\mathbf{W}}_k) - ((1 + \omega_{k-1})^2 \omega_{k-1}^3 + \mathcal{O}(\varepsilon)) \|\mathbf{X}_k\|^2}} \\ &= \sqrt{\frac{2\kappa(\bar{\mathbf{W}}_k)^2}{1 - ((1 + \omega_{k-1})^2 \omega_{k-1}^3 + \mathcal{O}(\varepsilon)) \|\mathbf{X}_k\|^2 / \sigma_{\min}^2(\bar{\mathbf{W}}_k)}} \\ &\leq 2\kappa(\bar{\mathbf{W}}_k). \end{aligned} \quad (101)$$

From (87), it follows that

$$\begin{aligned} \bar{\mathbf{Q}}_k^T \bar{\mathbf{Q}}_k &= \bar{Y}_{kk}^{-T} \bar{\mathbf{W}}_k^T \bar{\mathbf{W}}_k \bar{Y}_{kk}^{-1} + \bar{Y}_{kk}^{-T} \Delta \mathbf{W}_k^T \bar{\mathbf{W}}_k \bar{Y}_{kk}^{-1} \\ &\quad + \bar{Y}_{kk}^{-T} \bar{\mathbf{W}}_k^T \Delta \mathbf{W}_k \bar{Y}_{kk}^{-1} + \bar{Y}_{kk}^{-T} \Delta \mathbf{W}_k^T \Delta \mathbf{W}_k \bar{Y}_{kk}^{-1}. \end{aligned} \quad (102)$$

Combining (102) with (88), (95), (98), (100), and (101), it holds that

$$\begin{aligned} \|\bar{Y}_{kk}^{-T} \bar{\mathbf{W}}_k^T \bar{\mathbf{W}}_k \bar{Y}_{kk}^{-1}\| &\leq 1 + \frac{((1 + \omega_{k-1})^2 \omega_{k-1}^3 + \mathcal{O}(\varepsilon)) \|\mathbf{X}_k\|^2}{\sigma_{\min}(\bar{\mathbf{W}}_k)^2 - ((1 + \omega_{k-1})^2 \omega_{k-1}^3 + \mathcal{O}(\varepsilon)) \|\mathbf{X}_k\|^2} \leq 2, \\ \|\bar{\mathbf{W}}_k \bar{Y}_{kk}^{-1}\| &\leq \|\bar{\mathbf{Q}}_k\| + \mathcal{O}(\varepsilon) \|\bar{\mathbf{Q}}_k\| \kappa(\bar{\mathbf{W}}_k), \text{ and} \\ \|\Delta \mathbf{W}_k \bar{Y}_{kk}^{-1}\| &\leq \mathcal{O}(\varepsilon) \|\bar{\mathbf{Q}}_k\| \kappa(\bar{Y}_{kk}) \leq \mathcal{O}(\varepsilon) \|\bar{\mathbf{Q}}_k\| \kappa(\bar{\mathbf{W}}_k), \end{aligned}$$

which implies that

$$\begin{aligned} \|\bar{\mathbf{Q}}_k\|^2 &\leq \|\bar{Y}_{kk}^{-T} \bar{\mathbf{W}}_k^T \bar{\mathbf{W}}_k \bar{Y}_{kk}^{-1}\| + \mathcal{O}(\varepsilon) \|\bar{\mathbf{Q}}_k\|^2 \kappa(\bar{\mathbf{W}}_k) + (\mathcal{O}(\varepsilon) \kappa(\bar{\mathbf{W}}_k))^2 \|\bar{\mathbf{Q}}_k\|^2 \\ &\leq 2 + \mathcal{O}(\varepsilon) \kappa(\bar{\mathbf{W}}_k) \|\bar{\mathbf{Q}}_k\|^2. \end{aligned}$$

Thus we have

$$\|\bar{\mathbf{Q}}_k\| \leq \sqrt{\frac{2}{1 - \mathcal{O}(\varepsilon) \kappa(\bar{\mathbf{W}}_k)}} \leq 2.$$

Together with (88) and (99), we bound $\Delta \mathbf{W}_k$ by $\mathcal{O}(\varepsilon) \|\bar{\mathbf{W}}_k\|$. From (88) and (102), we conclude

$$\|I - \bar{\mathbf{Q}}_k^T \bar{\mathbf{Q}}_k\| \leq \frac{((1 + \omega_{k-1})^2 \omega_{k-1}^3 + \mathcal{O}(\varepsilon)) \|\mathbf{X}_k\|^2}{\sigma_{\min}(\bar{\mathbf{W}}_k)^2 - ((1 + \omega_{k-1})^2 \omega_{k-1}^3 + \mathcal{O}(\varepsilon)) \|\mathbf{X}_k\|^2} + \mathcal{O}(\varepsilon) \kappa(\bar{\mathbf{W}}_k). \quad (103)$$

□

Assuming that $\omega_{k-1} \leq \mathcal{O}(\varepsilon) \kappa^2(\mathbf{X}_{k-1})$, the assumption (85) of Lemma 11 can be guaranteed by $\mathcal{O}(\varepsilon) \kappa^{8/3}(\mathbf{X}_k) \leq \frac{1}{2}$. It further follows that

$$\|I - \bar{\mathbf{Q}}_k^T \bar{\mathbf{Q}}_k\| \leq \mathcal{O}(\varepsilon) \omega_{k-1}^3 \kappa(\mathbf{X}_k) + \mathcal{O}(\varepsilon) \kappa(\mathbf{X}_k) \leq \mathcal{O}(\varepsilon) \kappa^2(\mathbf{X}_k),$$

because the requirement $\mathcal{O}(\varepsilon) \kappa^{8/3}(\mathbf{X}_k) \leq \frac{1}{2}$ can imply $\omega_{k-1}^2 \kappa(\mathbf{X}_k) \leq 1$. Theorem 4 summarizes the results for BCGSI+A-2S using Theorem 3 with Lemmas 10 and 11.

Theorem 4. Let $\bar{\mathbf{Q}}$ and $\bar{\mathbf{R}}$ denote the computed result of Algorithm 4. Assume that for all $\mathbf{X} \in \mathbb{R}^{m \times s}$ with $\kappa(\mathbf{X}) \leq \kappa(\boldsymbol{\mathcal{X}})$, the following hold for $[\bar{\mathbf{Q}}, \bar{\mathbf{R}}] = \text{IO}_A(\mathbf{X})$:

$$\begin{aligned} \mathbf{X} + \Delta\mathbf{X} &= \bar{\mathbf{Q}}\bar{\mathbf{R}}, \quad \|\Delta\mathbf{X}\| \leq \mathcal{O}(\varepsilon) \|\mathbf{X}\|, \\ \|I - \bar{\mathbf{Q}}^T \bar{\mathbf{Q}}\| &\leq \mathcal{O}(\varepsilon) \kappa^{\alpha_A}(\mathbf{X}). \end{aligned}$$

If $\alpha_A \leq 2$ and $\mathcal{O}(\varepsilon) \kappa^3(\boldsymbol{\mathcal{X}}) \leq \frac{1}{2}$ is satisfied, then

$$\boldsymbol{\mathcal{X}} + \Delta\boldsymbol{\mathcal{X}} = \bar{\mathbf{Q}}\bar{\mathbf{R}}, \quad \|\Delta\boldsymbol{\mathcal{X}}\| \leq \mathcal{O}(\varepsilon) \|\boldsymbol{\mathcal{X}}\|$$

and

$$\|I - \bar{\mathbf{Q}}^T \bar{\mathbf{Q}}\| \leq \mathcal{O}(\varepsilon) \kappa^2(\boldsymbol{\mathcal{X}}). \quad (104)$$

Similarly to Theorem 3, Theorem 4 reifies observations from Figure 5, most notably the common behavior between $\text{BCGSI+A-3S} \circ \text{CholQR}$ and $\text{BCGSI+A-2S} \circ \text{CholQR}$. In particular, one cannot expect the two-sync variant to be better than $\text{BCGSI+A-3S} \circ \text{CholQR}$, and indeed, the exponent on $\kappa(\boldsymbol{\mathcal{X}})$ is fixed to 3 now, meaning that in double precision, we cannot prove stability when $\kappa(\boldsymbol{\mathcal{X}}) > 10^{5.3}$.

4.3 BCGSI+A-1S

The main difference between BCGSI+A-1S and BCGSI+A-2S is how \mathbf{W}_k defined in (67) is computed, particularly \mathbf{V}_k . Thus, just as in the proof of BCGSI+A-2S , we only need to estimate the specific ψ for the k th inner loop of Algorithm 5, i.e., $\psi_k^{(\text{BCGSI+A-1S})}$, and then we can derive the LOO for BCGSI+A-1S using the same logic as in Theorem 4.

Lemma 12. Let $\tilde{\mathbf{V}}_k$, $\tilde{\mathbf{W}}_k$, and $\bar{\mathbf{Q}}_{k-1}$ satisfy (20), (69), and (21), and $\bar{\mathbf{V}}_k$ and $\bar{\mathbf{W}}_k$ be the computed results of $\tilde{\mathbf{V}}_k$ and $\tilde{\mathbf{W}}_k$ by Algorithm 5. Assume that (70) is satisfied with

$$\begin{aligned} &2((1 + \omega_{k-1})^2 \omega_{k-1}^3 \kappa^2(\boldsymbol{\mathcal{X}}_k) + \mathcal{O}(\varepsilon) \kappa^3(\boldsymbol{\mathcal{X}}_k)) \\ &+ (\mathcal{O}(\varepsilon) (1 + \omega_{k-1}) + \rho_{k-1}) \kappa(\boldsymbol{\mathcal{X}}_k) \leq \frac{1}{2}. \end{aligned} \quad (105)$$

Then for the projection stage (67) with any $k \geq 2$ computed by lines 8–11 and 5 in Algorithm 5,

$$\|\bar{\mathbf{W}}_k - \tilde{\mathbf{W}}_k\| \leq \psi_k^{(\text{BCGSI+A-1S})} \leq \mathcal{O}(\varepsilon) \kappa(\boldsymbol{\mathcal{X}}_{k-1}) \|\mathbf{X}_k\|.$$

Proof. We estimate $\psi_k^{(\text{BCGSI+A-1S})}$ satisfying $\|\bar{\mathbf{W}}_k - \tilde{\mathbf{W}}_k\| \leq \psi_k^{(\text{BCGSI+A-1S})}$ by analyzing the rounding error of computing $\bar{\mathbf{S}}_{k,k+1}$, i.e., $\|\bar{\mathbf{S}}_{k,k+1} - \bar{\mathbf{Q}}_k^T \mathbf{X}_{k+1}\|$. Then our aim is to prove

$$\begin{aligned} \bar{\mathbf{S}}_{k,k+1} &= \bar{\mathbf{Q}}_k \mathbf{X}_{k+1} + \Delta\mathbf{S}_{k,k+1}, \quad \|\Delta\mathbf{S}_{k,k+1}\| \leq \mathcal{O}(\varepsilon) \kappa(\boldsymbol{\mathcal{X}}_k) \|\mathbf{X}_{k+1}\|; \\ \bar{\mathbf{V}}_{k+1} &= \tilde{\mathbf{V}}_{k+1} + \Delta\tilde{\mathbf{V}}_{k+1}, \quad \|\Delta\tilde{\mathbf{V}}_{k+1}\| \leq \mathcal{O}(\varepsilon) \kappa(\boldsymbol{\mathcal{X}}_k) \|\mathbf{X}_{k+1}\|; \text{ and} \\ \bar{\mathbf{W}}_{k+1} &= \tilde{\mathbf{W}}_{k+1} + \Delta\tilde{\mathbf{W}}_{k+1}, \quad \|\Delta\tilde{\mathbf{W}}_{k+1}\| \leq \mathcal{O}(\varepsilon) \kappa(\boldsymbol{\mathcal{X}}_k) \|\mathbf{X}_{k+1}\| \end{aligned}$$

by induction. Standard rounding-error analysis and Lemma 9 give the base case. Now we assume that the following $i-1$ case with $3 \leq i \leq k$ hold:

$$\begin{aligned} \bar{\mathbf{S}}_{i-1,i} &= \bar{\mathbf{Q}}_{i-1} \mathbf{X}_i + \Delta\mathbf{S}_{i-1,i}, \quad \|\Delta\mathbf{S}_{i-1,i}\| \leq \mathcal{O}(\varepsilon) \kappa(\boldsymbol{\mathcal{X}}_{i-1}) \|\mathbf{X}_i\|; \\ \bar{\mathbf{V}}_i &= \tilde{\mathbf{V}}_i + \Delta\tilde{\mathbf{V}}_i, \quad \|\Delta\tilde{\mathbf{V}}_i\| \leq \mathcal{O}(\varepsilon) \kappa(\boldsymbol{\mathcal{X}}_{i-1}) \|\mathbf{X}_i\|; \text{ and} \\ \bar{\mathbf{W}}_i &= \tilde{\mathbf{W}}_i + \Delta\tilde{\mathbf{W}}_i, \quad \|\Delta\tilde{\mathbf{W}}_i\| \leq \mathcal{O}(\varepsilon) \kappa(\boldsymbol{\mathcal{X}}_{i-1}) \|\mathbf{X}_i\|, \end{aligned} \quad (106)$$

and then aim to prove the above also hold for i . Note that the base case $i=2$ has already been proved. A straightforward rounding-error analysis gives

$$\bar{\mathbf{Z}}_{i-1} = \bar{\mathbf{Q}}_{i-1}^T \mathbf{X}_{i+1} + \Delta\mathbf{Z}_{i-1}, \quad \|\Delta\mathbf{Z}_{i-1}\| \leq \mathcal{O}(\varepsilon) \|\mathbf{X}_{i+1}\|, \quad (107)$$

$$\bar{\mathbf{P}}_i = \bar{\mathbf{V}}_i^T \mathbf{X}_{i+1} + \Delta\mathbf{P}_i, \quad \|\Delta\mathbf{P}_i\| \leq \mathcal{O}(\varepsilon) \|\bar{\mathbf{V}}_i\| \|\mathbf{X}_{i+1}\|, \text{ and} \quad (108)$$

$$\bar{\mathcal{Y}}_{1:i-1,i} = \bar{\mathbf{Q}}_{i-1}^T \bar{\mathbf{V}}_i + \Delta\mathcal{Y}_{1:i-1,i}, \quad \|\Delta\mathcal{Y}_{1:i-1,i}\| \leq \mathcal{O}(\varepsilon) \|\bar{\mathbf{V}}_i\|. \quad (109)$$

Furthermore, similarly to (87), we obtain

$$\begin{aligned}
\bar{Y}_{ii}^T \bar{\mathcal{S}}_{i,i+1} &= \bar{P}_i - \bar{Y}_{1:i-1,i}^T \bar{\mathcal{Z}}_{i-1} + \Delta E_i + \Delta \mathcal{S}_{i,i+1}, \\
&= \bar{V}_i^T \mathbf{X}_{i+1} + \Delta P_i - \bar{Y}_{1:i-1,i}^T (\bar{\mathcal{Q}}_{i-1}^T \mathbf{X}_{i+1} + \Delta \mathcal{Z}_{i-1}) \\
&\quad + \Delta E_i + \Delta \mathcal{S}_{i,i+1} \\
&= \bar{V}_i^T \mathbf{X}_{i+1} - \bar{Y}_{1:i-1,i}^T \bar{\mathcal{Q}}_{i-1}^T \mathbf{X}_{i+1} + \Delta P_i - \bar{V}_i^T \bar{\mathcal{Q}}_{i-1} \Delta \mathcal{Z}_{i-1} \\
&\quad + \Delta E_i + \Delta \mathcal{S}_{i,i+1},
\end{aligned} \tag{110}$$

where ΔE_i is the floating-point error from the sum and product of $\bar{P}_i - \bar{Y}_{1:i-1,i}^T \bar{\mathcal{Z}}_{i-1}$ and $\Delta \mathcal{S}_{i,i+1}$ is from solving the triangular system $\bar{Y}_{ii}^{-T} (\bar{P}_i - \bar{Y}_{1:i-1,i}^T \bar{\mathcal{Z}}_{i-1} + \Delta E_i)$. Thus, the following bounds hold:

$$\|\Delta F_i\| \leq \mathcal{O}(\varepsilon) \|\bar{V}_i\| \|\mathbf{X}_{i+1}\| \quad \text{and} \quad \|\Delta \mathcal{S}_{i,i+1}\| \leq \mathcal{O}(\varepsilon) \|\bar{\mathcal{S}}_{i,i+1}\| \|\bar{Y}_{ii}\| \tag{111}$$

with $\Delta F_i := \Delta P_i - \bar{V}_i^T \bar{\mathcal{Q}}_{i-1} \Delta \mathcal{Z}_{i-1} + \Delta E_i$. Similarly to (95) and (97), we have

$$\begin{aligned}
\bar{Y}_{ii}^T \bar{Y}_{ii} &= \bar{W}_i^T \bar{W}_i + \Delta M, \quad \text{with} \\
\|\Delta M\| &\leq ((1 + \omega_{i-1})^2 \omega_{i-1}^3 + \mathcal{O}(\varepsilon) \kappa(\mathcal{X}_{i-1})) \|\mathbf{X}_i\|^2.
\end{aligned} \tag{112}$$

Furthermore, in analogy to (100) and (101), it holds that

$$\begin{aligned}
\|\bar{Y}_{ii}\|^2 &\leq 2 \|\bar{W}_i\|, \\
\sigma_{\min}^2(\bar{Y}_{ii}) &\geq \sigma_{\min}^2(\bar{W}_i) - ((1 + \omega_{i-1})^2 \omega_{i-1}^3 + \mathcal{O}(\varepsilon) \kappa(\mathcal{X}_{i-1})) \|\mathbf{X}_i\|^2, \quad \text{and} \\
\kappa(\bar{Y}_{ii}) &\leq 2\kappa(\bar{W}_i) \leq 2\kappa(\bar{W}_i) + \mathcal{O}(\varepsilon) \kappa(\mathcal{X}_{i-1}) \|\mathbf{X}_i\|,
\end{aligned} \tag{113}$$

which relies on the assumption (105). Combining (110) with (113), we obtain

$$\bar{\mathcal{S}}_{i,i+1} = \bar{Y}_{ii}^{-T} \left(\bar{V}_i^T \mathbf{X}_{i+1} - \bar{Y}_{1:i-1,i}^T \bar{\mathcal{Q}}_{i-1}^T \mathbf{X}_{i+1} \right) + \bar{Y}_{ii}^{-T} \Delta F_i + \bar{Y}_{ii}^{-T} \Delta \mathcal{S}_{i,i+1}, \tag{114}$$

with

$$\begin{aligned}
\|\bar{Y}_{ii}^{-T} \Delta F_i\| &\leq \mathcal{O}(\varepsilon) \|\bar{V}_i\| \|\mathbf{X}_{i+1}\| \|\bar{Y}_{ii}^{-1}\|, \quad \text{and} \\
\|\bar{Y}_{ii}^{-T} \Delta \mathcal{S}_{i,i+1}\| &\leq \mathcal{O}(\varepsilon) \|\bar{\mathcal{S}}_{i,i+1}\| (2\kappa(\bar{W}_i) + \mathcal{O}(\varepsilon) \kappa(\mathcal{X}_{i-1}) \|\mathbf{X}_i\|).
\end{aligned} \tag{115}$$

Now we bound the distance between $\bar{\mathcal{S}}_{i,i+1}$ and $\bar{Q}_i^T \mathbf{X}_{i+1}$. Following the same logic as with (110), we have

$$\bar{V}_i - \bar{\mathcal{Q}}_{i-1} \bar{Y}_{1:i-1,i} + \Delta C_i = \bar{Q}_i \bar{Y}_{ii}, \quad \|\Delta C_i\| \leq \mathcal{O}(\varepsilon) \|\bar{V}_i\| + \mathcal{O}(\varepsilon) \|\bar{Y}_{ii}\|.$$

Furthermore, by (113) and the assumption (105), it follows that

$$(\bar{V}_i - \bar{\mathcal{Q}}_{i-1} \bar{Y}_{1:i-1,i}) \bar{Y}_{ii}^{-1} + \Delta D_i = \bar{Q}_i \tag{116}$$

with $\Delta D_i = \Delta C_i \bar{Y}_{ii}^{-1}$ satisfying

$$\|\Delta D_i\| \leq \frac{\mathcal{O}(\varepsilon) \|\bar{V}_i\|}{\sigma_{\min}(\bar{W}_i)} + \mathcal{O}(\varepsilon) \kappa(\bar{Y}_{ii}) \leq \mathcal{O}(\varepsilon) \kappa(\mathcal{X}_i). \tag{117}$$

Together with (114) and (115), we arrive at

$$\begin{aligned}
\bar{\mathcal{S}}_{i,i+1} &= \bar{Q}_i^T \mathbf{X}_{i+1} - \Delta D_i^T \mathbf{X}_{i+1} + \bar{Y}_{ii}^{-T} \Delta F_i + \bar{Y}_{ii}^{-T} \Delta \mathcal{S}_{i,i+1} \\
&= \bar{Q}_i^T \mathbf{X}_{i+1} + \Delta \bar{\mathcal{S}}_{i,i+1},
\end{aligned}$$

where $\Delta \bar{\mathcal{S}}_{i,i+1} = -\Delta D_i^T \mathbf{X}_{i+1} + \bar{Y}_{ii}^{-T} \Delta F_i + \bar{Y}_{ii}^{-T} \Delta \mathcal{S}_{i,i+1}$ satisfies

$$\|\Delta \bar{\mathcal{S}}_{i,i+1}\| \leq \mathcal{O}(\varepsilon) \kappa(\mathcal{X}_i) \|\mathbf{X}_{i+1}\|.$$

Then standard floating-point analysis yields

$$\tilde{\mathbf{V}}_{i+1} = \tilde{\mathbf{V}}_{i+1} + \Delta \tilde{\mathbf{V}}_{i+1}, \quad \|\Delta \tilde{\mathbf{V}}_{i+1}\| \leq \mathcal{O}(\varepsilon) \kappa(\mathbf{x}_i) \|\mathbf{x}_{i+1}\|, \quad (118)$$

and further,

$$\tilde{\mathbf{W}}_{i+1} = \tilde{\mathbf{W}}_{i+1} + \Delta \tilde{\mathbf{W}}_{i+1}, \quad \|\Delta \tilde{\mathbf{W}}_{i+1}\| \leq \mathcal{O}(\varepsilon) \kappa(\mathbf{x}_i) \|\mathbf{x}_{i+1}\|, \quad (119)$$

which gives the bound on $\psi_k^{(\text{BCGSI+A-1S})}$ by induction on i and noticing $\|\tilde{\mathbf{W}}_k - \tilde{\mathbf{W}}_k\| \leq \psi_k^{(\text{BCGSI+A-1S})}$. \square

By imitating the proof of [BCGSI+A-3S](#), Lemma 1 leads to the following result on the LOO of [BCGSI+A-1S](#).

Theorem 5. *Let $\bar{\mathbf{Q}}$ and $\bar{\mathbf{R}}$ denote the computed results of Algorithm 5. Assume that for all $\mathbf{X} \in \mathbb{R}^{m \times s}$ with $\kappa(\mathbf{X}) \leq \kappa(\mathbf{X})$, the following hold for $[\bar{\mathbf{Q}}, \bar{\mathbf{R}}] = \text{IO}_A(\mathbf{X})$:*

$$\begin{aligned} \mathbf{X} + \Delta \mathbf{X} &= \bar{\mathbf{Q}} \bar{\mathbf{R}}, \quad \|\Delta \mathbf{X}\| \leq \mathcal{O}(\varepsilon) \|\mathbf{X}\|, \\ \|I - \bar{\mathbf{Q}}^T \bar{\mathbf{Q}}\| &\leq \mathcal{O}(\varepsilon) \kappa^{\alpha_A}(\mathbf{X}). \end{aligned}$$

If $\alpha_A \leq 2$ and $\mathcal{O}(\varepsilon) \kappa^3(\mathbf{X}) \leq \frac{1}{2}$ are satisfied, then

$$\mathbf{x} + \Delta \mathbf{x} = \bar{\mathbf{Q}} \bar{\mathbf{R}}, \quad \|\Delta \mathbf{x}\| \leq \mathcal{O}(\varepsilon) \|\mathbf{x}\|$$

and

$$\|I - \bar{\mathbf{Q}}^T \bar{\mathbf{Q}}\| \leq \mathcal{O}(\varepsilon) \kappa^2(\mathbf{x}). \quad (120)$$

Theorem 5 concludes the journey through sync-point reductions and, much like Theorems 3 and 4, confirms the observations from Figure 5 in Section 3. It is clear that shifting the window of the for-loop is not to blame for any LOO; the problem stems already from the eliminated IO in [BCGSI+A-3S](#) and fixing `CholQR` as the remaining IO in [BCGSI+A-2S](#).

5 Summary and consequences of bounds

Table 3 summarizes the key assumptions and conclusions of the main theorems from Sections 2 and 4. A key feature of our results is the range of $\kappa(\mathbf{X})$ for which LOO bounds are provable (and attainable). All bounds require at least that \mathbf{X} is numerically full rank; as we reduce the number of sync points, that restriction becomes tighter. [BCGSI+A-3S](#) requires $\kappa(\mathbf{X}) \lesssim 10^8$ in double precision (or worse if $\alpha > 1$), while [BCGSI+A-2S](#) and [BCGSI+A-1S](#) need $\kappa(\mathbf{X}) \lesssim 10^{5.3}$. Figure 8 demonstrates [BCGSI+A-3S](#) \circ `HouseQR` ($\alpha = 0, \theta = 2$) deviating from $\mathcal{O}(\varepsilon) \kappa^2(\mathbf{X})$ after $\kappa(\mathbf{X})$ exceeds 10^9 and [BCGSI+A-3S](#) \circ `CholQR` ($\alpha = 2, \theta = 3$) deviating much earlier, once $\kappa(\mathbf{X})$ exceeds 10^6 . Figure 9 tells a similar story for [BCGSI+A-2S](#) and [BCGSI+A-1S](#): both begin to deviate after $\kappa(\mathbf{X}) = 10^6$.

Table 3: Summary of all major theorems, their assumptions, and their LOO bounds for [BCGSI+A](#) and lower sync variants thereof. For the column IO_A , we state only the exponent such that IO_A has LOO bounded by $\mathcal{O}(\varepsilon) \kappa^{\alpha_A}(\mathbf{X})$ for block vectors \mathbf{X} . See Table 1 for examples of α_* .

Variant	Theorem	IO_A	$\mathcal{O}(\varepsilon) \kappa^\theta(\mathbf{X}) \leq \frac{1}{2}$	$\ I - \bar{\mathbf{Q}}^T \bar{\mathbf{Q}}\ $
BCGSI+A	2	$\alpha_A = 0$	$\theta = \max(\alpha_1, 1)$	$\mathcal{O}(\varepsilon)$
BCGSI+A-3S	3	$\alpha_A \leq \alpha$	$\theta = \max(\alpha + 1, 2)$	$\mathcal{O}(\varepsilon) \kappa^{\max(\alpha, 1)}(\mathbf{X})$
BCGSI+A-2S	4	$\alpha_A \leq 2$	$\theta = 3$	$\mathcal{O}(\varepsilon) \kappa^2(\mathbf{X})$
BCGSI+A-1S	5	$\alpha_A \leq 2$	$\theta = 3$	$\mathcal{O}(\varepsilon) \kappa^2(\mathbf{X})$

For completeness, we also provide Figure 10, which aggregates plots for all methods discussed on the `piled` matrices. Compare with Figures 6 and 7. In particular, the `piled` matrices are quite tough for [BCGS](#) and [BCGS-A](#).

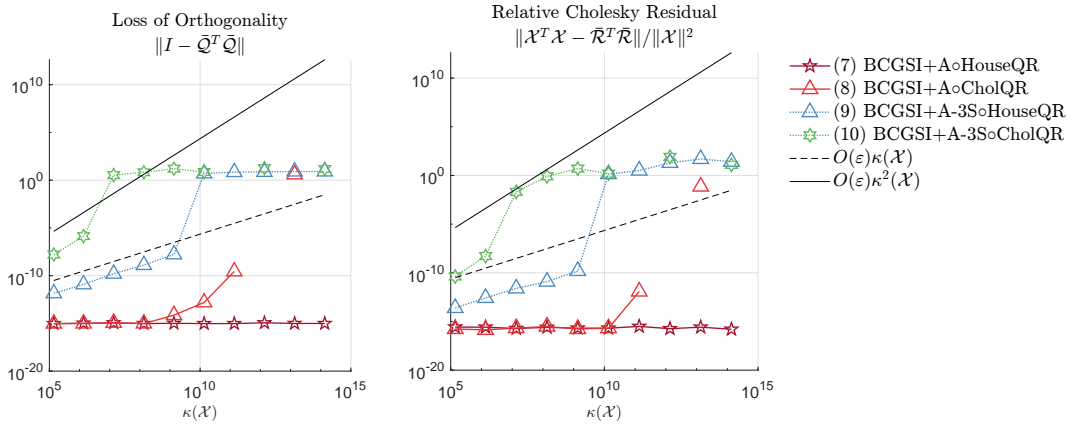


Figure 8: Comparison between **BCGSI+A** and **BCGSI+A-3S** on a class of piled matrices. Note that IO_A is fixed as **HouseQR**, and $\text{IO} = \text{IO}_1 = \text{IO}_2$.

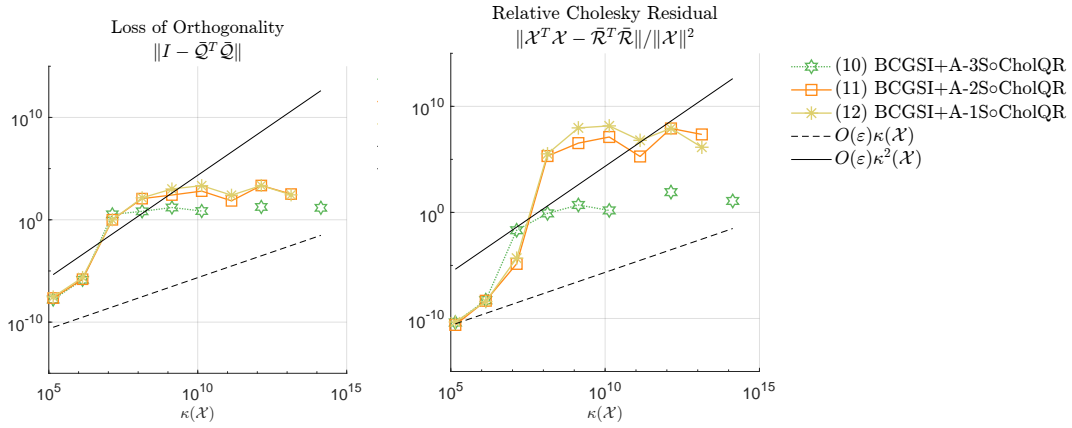


Figure 9: Comparison among low-sync versions of **BCGSI+A** on a class of piled matrices. Note that IO_A is fixed as **HouseQR**.

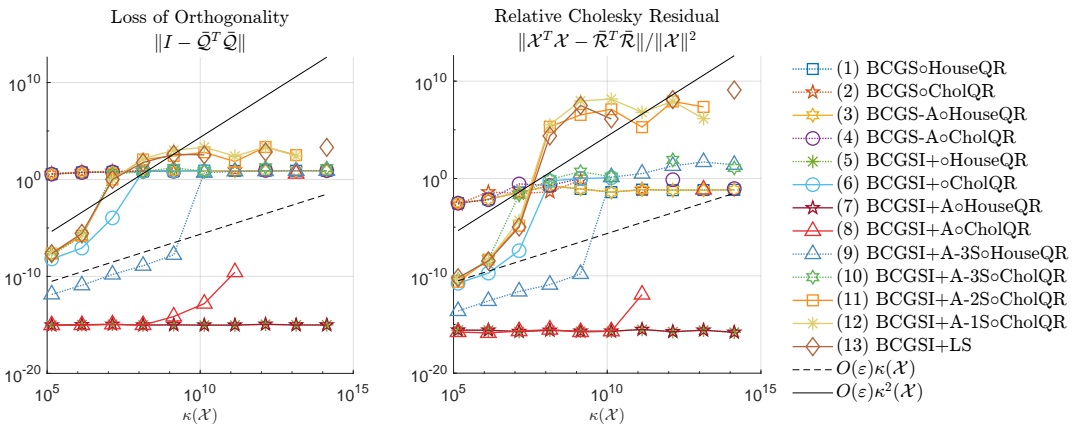


Figure 10: Comparison among **BCGS**, **BCGSI+**, **BCGSI+A**, and low-sync variants thereof on piled matrices. **BCGSI+LS** is Algorithm 7 from [8]. Note that IO_A is fixed as **HouseQR** in **BlockStab**.

Despite the rather pessimistic behavior for block variants we have observed, there is yet good news for the column version of **BCGSI+A-1S**, i.e., when $s = 1$. Our results apply trivially to the column version and in fact address the open issue of the stability of a one-sync, reorthogonalized CGS, first introduced as [22, Algorithm 3] and revisited as DCGS2 in [4].

Corollary 1. *Let $\bar{\mathcal{Q}}$ and $\bar{\mathcal{R}}$ denote the computed result of Algorithm 3, 4, or 5 with $s = 1$. If $\mathcal{O}(\varepsilon)\kappa(\mathcal{X}) \leq \frac{1}{2}$ is satisfied, then*

$$\mathcal{X} + \Delta\mathcal{X} = \bar{\mathcal{Q}}\bar{\mathcal{R}}, \quad \|\Delta\mathcal{X}\| \leq \mathcal{O}(\varepsilon)\|\mathcal{X}\| \quad (121)$$

and

$$\|I - \bar{\mathcal{Q}}^T \bar{\mathcal{Q}}\| \leq \mathcal{O}(\varepsilon). \quad (122)$$

Proof. First note that the proof of Theorem 3 is based on Lemma 10. Now we aim to derive a new version of Lemma 10 for $s = 1$. Notice that for $s = 1$, \mathcal{X}_k has only one column and furthermore $\widetilde{\mathcal{W}}_k$ defined by (69) also has only one column, which trivially implies that $\kappa(\widetilde{\mathcal{W}}_k) = 1$. Combining this realization with (80), we obtain

$$\begin{aligned} \|I - \bar{\mathcal{Q}}_k^T \bar{\mathcal{Q}}_k\| &\leq \omega_{k-1} + \mathcal{O}(\varepsilon) + \mathcal{O}(\varepsilon)\omega_{k-1}\kappa(\mathcal{X}_k) \\ &\quad + 4(1 + \omega_{k-1})\omega_{k-1}^2(1 + \omega_{\text{qr}})\kappa(\mathcal{X}_k) + \omega_{\text{qr}} \end{aligned} \quad (123)$$

with the assumption $\mathcal{O}(\varepsilon)\kappa(\mathcal{X}_k) \leq \frac{1}{2}$. Then we use (123) instead of Lemma 10, similarly to the proof of Theorem 3, to conclude that (121) and (122) hold for **BCGSI+A-3S** with $s = 1$.

Recalling Section 4.2, the only difference between **BCGSI+A-2S** and **BCGSI+A-3S** \circ **CholQR** is the estimation of ω_{qr} , i.e., $\|I - \bar{\mathcal{Q}}_k^T \bar{\mathcal{Q}}_k\|$, which has been bounded in Lemma 11. When $s = 1$, $\kappa(\widetilde{\mathcal{W}}_k) = 1$, and by (103),

$$\sigma_{\min}(\bar{\mathcal{W}}_k) = \|\bar{\mathcal{W}}_k\| \geq \|I - \bar{\mathcal{Q}}_{k-1}^T \bar{\mathcal{Q}}_{k-1}\|^2 \sigma_{\min}(\mathcal{X}_k) \geq \sigma_{\min}(\mathcal{X}_k) = \|\mathcal{X}_k\|.$$

We then have

$$\|I - \bar{\mathcal{Q}}_k^T \bar{\mathcal{Q}}_k\| \leq 2 \cdot (1 + \omega_{k-1})^2 \omega_{k-1}^3 + \mathcal{O}(\varepsilon).$$

Similarly to the proof of Theorem 4, we can prove that (121) and (122) hold for **BCGSI+A-2S** with $s = 1$.

For **BCGSI+A-1S**, we only need to rewrite Lemma 12 for $s = 1$. Since $\kappa(\mathcal{X}_1) = \kappa(\mathcal{X}_1) = 1$, $\kappa(\mathcal{X}_1)$ can be eliminated from the upper bounds of $\Delta\mathcal{S}_{1,2}$, $\Delta\widetilde{\mathcal{V}}_2$, and $\Delta\widetilde{\mathcal{W}}_2$ for the base case, i.e., (106) with $i = 2$. Furthermore, $\kappa(\mathcal{X}_{i-1})$ can be eliminated from the upper bounds of $\Delta\mathcal{S}_{i-1,i}$, $\Delta\widetilde{\mathcal{V}}_i$, and $\Delta\widetilde{\mathcal{W}}_i$ in (106). Then following the same process of Lemma 12, it holds that

$$\|\bar{\mathcal{W}}_k - \widetilde{\mathcal{W}}_k\| \leq \psi_k^{(\text{BCGSI+A-1S})} \leq \mathcal{O}(\varepsilon)\|\mathcal{X}_k\|.$$

In analogue to the proof of Theorem 5, we can conclude the proof for **BCGSI+A-1S** with $s = 1$. \square

Figure 11 shows a comparison among column versions of the methods discussed here. Note that for all methods $\text{IO}_A = \text{IO}_1 = \text{IO}_2$, as all QR subroutines reduce to scaling a column vector by its norm. Consequently, all versions of **BCGS** and **BCGS-A** are equivalent, as well as **BCGSI+** and **BCGSI+A**, etc. Such redundancies have been removed to make the figure more legible. Clearly all variants except **BCGS/BCGS-A** achieve $\mathcal{O}(\varepsilon)$ LOO and relative Cholesky residual.

6 Conclusions

In this work, we provide a number of new results on the loss of orthogonality in variants of block Gram-Schmidt. To enable a uniform approach to our analyses, we introduce an abstract framework which considers the effects of the projection and intraorthogonalization stages of a **BCGS** method.

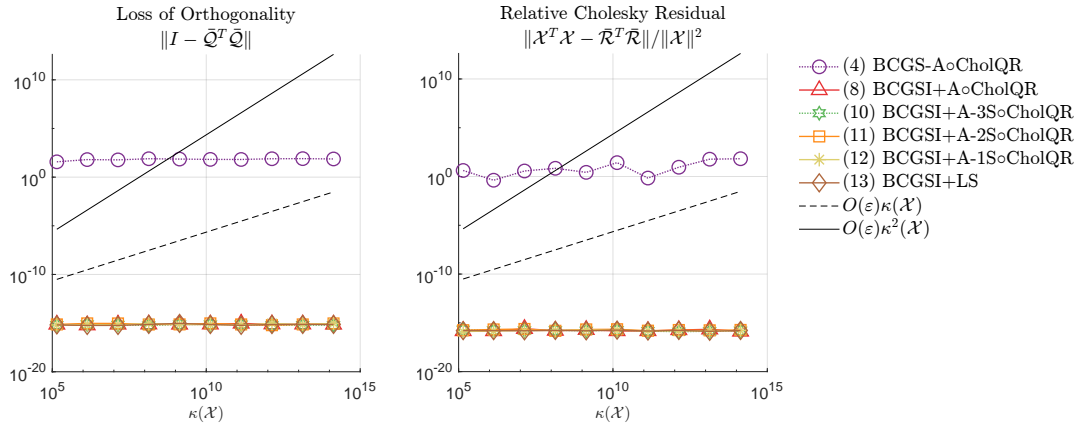


Figure 11: Comparison among column variants ($s = 1$) for piled matrices. BCGSI+LS is Algorithm 7 from [8]. Note that IO_A is fixed as HouseQR in BlockStab.

We first introduce a modification of the basic BCGS method, called BCGS-A, in which the IO used for the first block vector can be different than that used for subsequent blocks. We prove a bound on the resulting LOO. As a side effect, this gives the first known bound on the LOO for BCGS in the literature.

We then introduce a reorthogonalized variant of BCGS-A, BCGSI+A, and prove a bound on its LOO. Our results reproduce the bound given by Barlow and Smoktunowicz for the case that a single IO is used throughout [3]. Further, our analysis provides a valuable insight: we only need a “strong” IO on the very first block. After this, less expensive and less stable IOs can be used. The first IO used in the main loop determines the constraint on the condition number of \mathcal{X} . The second IO, used for the reorthogonalization, has no effect.

The resulting BCGSI+A has four synchronization points. We then demonstrate, through a series of steps, how each sequential removal of a synchronization point affects the LOO and constraints on the condition number for which the bound holds. We eventually reach a low-sync version with only a single synchronization point, equivalent to methods previously proposed in the literature, and we show that unfortunately, the LOO depends on the square of the condition number, which has been conjectured previously in [8].

Despite the unsatisfactory results for the block variant, our analysis also gives bounds for column (non-block) one-sync variants which have been proposed in the literature [4, 22], and it is shown that these attain a LOO on the level of the unit roundoff.

Acknowledgments

The second author would like to thank the Computational Methods in Systems and Control Theory group at the Max Planck Institute for Dynamics of Complex Technical Systems for funding the fourth author’s visit in March 2023. The fourth author would like to thank the Chemnitz University of Technology for funding the second author’s visit in July 2023.

The first, third, and fourth authors are supported by the European Union (ERC, inEXASCALE, 101075632). Views and opinions expressed are those of the authors only and do not necessarily reflect those of the European Union or the European Research Council. Neither the European Union nor the granting authority can be held responsible for them. The first and the fourth authors acknowledge support from the Charles University GAUK project No. 202722 and the Exascale Computing Project (17-SC-20-SC), a collaborative effort of the U.S. Department of Energy Office of Science and the National Nuclear Security Administration. The first author acknowledges support from the Charles University Research Centre program No. UNCE/24/SCI/005.

References

- [1] G. Ballard, E. Carson, J. Demmel, M. Hoemmen, N. Knight, and O. Schwartz. Communication lower bounds and optimal algorithms for numerical linear algebra. *Acta Numerica 2011, Vol 20*, 23(2014):1–155, 2014. doi:[10.1017/S0962492914000038](https://doi.org/10.1017/S0962492914000038).
- [2] J. L. Barlow. Reorthogonalized block classical Gram-Schmidt using two Cholesky-based TSQR algorithms. *SIAM J. Matrix Anal. Appl.*, 45(3):1487–1517, 2024. doi:[10.1137/23M1605387](https://doi.org/10.1137/23M1605387).
- [3] J. L. Barlow and A. Smoktunowicz. Reorthogonalized block classical Gram-Schmidt. *Numerische Mathematik*, 123:395–423, 2013. doi:[10.1007/s00211-012-0496-2](https://doi.org/10.1007/s00211-012-0496-2).
- [4] D. Bielich, J. Langou, S. Thomas, K. Świrydowicz, I. Yamazaki, and E. G. Boman. Low-synch Gram-Schmidt with delayed reorthogonalization for Krylov solvers. *Parallel Computing*, 112:102940, 2022. doi:[10.1016/j.parco.2022.102940](https://doi.org/10.1016/j.parco.2022.102940).
- [5] A. Buttari, N. J. Higham, T. Mary, and B. Vieu. A modular framework for the backward error analysis of GMRES. Technical Report hal-04525918, HAL science ouverte, 2024. URL: <https://hal.science/hal-04525918>.
- [6] E. Carson, K. Lund, Y. Ma, and E. Oktay. Reorthogonalized Pythagorean variants of block classical Gram-Schmidt. E-Print 2405.01298v1, arXiv, 2024. doi:[10.48550/arXiv.2405.01298](https://doi.org/10.48550/arXiv.2405.01298).
- [7] E. Carson, K. Lund, and M. Rozložník. The stability of block variants of classical Gram-Schmidt. *SIAM J. Matrix Anal. Appl.*, 42(3):1365–1380, 2021. doi:[10.1137/21M1394424](https://doi.org/10.1137/21M1394424).
- [8] E. Carson, K. Lund, M. Rozložník, and S. Thomas. Block Gram-Schmidt algorithms and their stability properties. *Linear Algebra Appl.*, 638(20):150–195, 2022. doi:[10.1016/j.laa.2021.12.017](https://doi.org/10.1016/j.laa.2021.12.017).
- [9] E. Carson and Y. Ma. A stable one-synchronization variant of reorthogonalized block classical Gram-Schmidt. *SIAM Journal on Scientific Computing*, 47(4):A2353–A2377, 2025.
- [10] E. C. Carson. *Communication-Avoiding Krylov Subspace Methods in Theory and Practice*. PhD thesis, Department of Computer Science, University of California, Berkeley, 2015. URL: <http://escholarship.org/uc/item/6r91c407>.
- [11] J. Demmel, L. Grigori, M. Hoemmen, and J. Langou. Communication-optimal parallel and sequential QR and LU factorizations. *SIAM J. Sci. Comput.*, 34(1):A206–A239, 2012. doi:[10.1137/080731992](https://doi.org/10.1137/080731992).
- [12] J. W. Demmel, L. Grigori, M. Gu, and H. Xiang. Communication avoiding rank revealing QR factorization with column pivoting. *SIAM Journal on Matrix Analysis and Applications*, 36(1):55–89, 2015. doi:[10.1137/13092157X](https://doi.org/10.1137/13092157X).
- [13] L. Giraud, J. Langou, M. Rozložník, and J. Van Den Eshof. Rounding error analysis of the classical Gram-Schmidt orthogonalization process. *Numerische Mathematik*, 101:87–100, 2005. doi:[10.1007/s00211-005-0615-4](https://doi.org/10.1007/s00211-005-0615-4).
- [14] G. H. Golub and C. F. Van Loan. *Matrix Computations*. Johns Hopkins Studies in the Mathematical Sciences. Johns Hopkins University Press, Baltimore, 4 edition, 2013.
- [15] A. Greenbaum, M. Rozložník, and Z. Strakoš. Numerical behaviour of the modified Gram-Schmidt GMRES implementation. *BIT Numerical Mathematics*, 37(3):706–719, 1997. doi:[10.1007/BF02510248](https://doi.org/10.1007/BF02510248).
- [16] N. J. Higham. *Accuracy and Stability of Numerical Algorithms*. Society for Industrial and Applied Mathematics, Philadelphia, 2nd ed edition, 2002.
- [17] M. Hoemmen. *Communication-Avoiding Krylov Subspace Methods*. PhD thesis, Department of Computer Science, University of California at Berkeley, 2010. URL: <http://www2.eecs.berkeley.edu/Pubs/TechRpts/2010/EECS-2010-37.pdf>.

- [18] A. Kielbasiński and H. Schwetlick. *Numerische Lineare Algebra: Eine Computerorientierte Einführung*. Mathematik für Naturwissenschaft und Technik 18. Deutscher Verlag der Wissenschaften, Berlin, 1988.
- [19] K. Lund. Adaptively restarted block Krylov subspace methods with low-synchronization skeletons. *Numerical Algorithms*, 93(2):731–764, 2023. doi:10.1007/s11075-022-01437-1.
- [20] D. Mori, Y. Yamamoto, and S. L. Zhang. Backward error analysis of the AllReduce algorithm for householder QR decomposition. *Japan Journal of Industrial and Applied Mathematics*, 29(1):111–130, 2012. doi:10.1007/s13160-011-0053-x.
- [21] E. Oktay and E. Carson. Using Mixed Precision in Low-Synchronization Reorthogonalized Block Classical Gram-Schmidt. *PAMM*, 23(1):e202200060, 2023. doi:10.1002/pamm.202200060.
- [22] K. Świrydowicz, J. Langou, S. Ananthan, U. Yang, and S. Thomas. Low synchronization Gram-Schmidt and generalized minimal residual algorithms. *Numerical Linear Algebra with Applications*, 28(2):e2343, 2021. doi:10.1002/nla.2343.
- [23] Y. Yamamoto, Y. Nakatsukasa, Y. Yanagisawa, and T. Fukaya. Roundoff error analysis of the Cholesky QR2 algorithm. *Electronic Transactions on Numerical Analysis*, 44:306–326, 2015. URL: <http://www.emis.de/journals/ETNA/vol.44.2015/pp306-326.dir/pp306-326.pdf>.
- [24] I. Yamazaki, A. J. Higgins, E. G. Boman, and D. B. Szyld. Two-Stage Block Orthogonalization to Improve Performance of s-step GMRES. In *2024 IEEE International Parallel and Distributed Processing Symposium (IPDPS)*, pages 26–37, San Francisco, CA, USA, 2024. doi:10.1109/IPDPS57955.2024.00012.
- [25] I. Yamazaki, S. Thomas, M. Hoemmen, E. G. Boman, K. Świrydowicz, and J. J. Elliot. Low-synchronization orthogonalization schemes for s-step and pipelined Krylov solvers in Trilinos. In *Proceedings of the 2020 SIAM Conference on Parallel Processing for Scientific Computing (PP)*, pages 118–128, 2020. doi:10.1137/1.9781611976137.11.
- [26] Q. Zou. A flexible block classical Gram-Schmidt skeleton with reorthogonalization. *Numerical Linear Algebra with Applications*, 30(5):e2491, 2023. doi:10.1002/nla.2491.